

AN ABSTRACT OF THE THESIS OF

William Walter Hauswirth for the Doctor of Philosophy  
(Name) (Degree)  
in Chemistry presented on Oct. 16, 1970  
(Major) (Date)

Title: FLUORESCENCE STUDIES ON THE BASES OF THE NUCLEIC  
ACIDS IN SOLUTION AT ROOM TEMPERATURE

Redacted for privacy

Abstract approved:

Malcolm Daniels

Fluorescence of adenine, guanine, thymine, cytosine, and uracil has been detected at room temperature in neutral aqueous solution using a digital signal accumulation technique and right angle fluorescence detection from solutions with absorbances between 0.4 and 0.7. The quantum yields are respectively  $2.6 \times 10^{-4}$ ,  $3.0 \times 10^{-4}$ ,  $1 \times 10^{-4}$ ,  $0.8 \times 10^{-4}$ , and  $0.5 \times 10^{-4}$  when excited at their low energy absorption maxima. Singlet lifetimes calculated from these yields may mean a recalculation of excited state processes occurring in DNA which were previously based on low temperature data. Corrected relative emission spectra are presented and compared with reported low temperature data. The corrected relative excitation spectra all show significant differences from the absorption spectrum when both are determined under identical conditions of concentration and spectral bandwidth on the same instrument. This behavior is discussed in terms

of a)  $n-\pi^*$  and  $\pi-\pi^*$  states, b) emission from a minor tautomer and c) kinetics of competing deactivation processes. From a development of c), rate constants for processes occurring from the  $0'$  level are calculated for intersystem crossing, internal conversion, and (singlet) photochemical reaction in thymine and uracil.

From solvent induced shifts of absorption and fluorescence spectra, the excited state dipole moment of thymine ( $\mu_e = 8.0 \pm 2.20$ ) and the  $\pi-\pi^*$  nature of the transitions responsible for fluorescence are deduced. Consideration of the singlet lifetime of thymine in relation to the rates of excited state process implies that fluorescence may occur from a Franck-Condon excited state and this is discussed in terms of possible solute-solvent interactions.

A study of the pH effects on the spectral shape, magnitude, and polarization of thymine emission concludes that the emitting states of ionized thymine are of a  $\pi-\pi^*$  nature, that fluorescence may arise within the # 1, 2, 4, 5, and 6  $\pi$ -conjugated system in the thymine molecule, and that excited state ionizations do not occur in the fluorescent forms of thymine. These deductions are discussed in relation to DNA excited state processes.

Fluorescence Studies on the Bases  
of the Nucleic Acids in Solution  
at Room Temperature

by

William Walter Hauswirth

A THESIS

submitted to

Oregon State University

in partial fulfillment of  
the requirements for the  
degree of

Doctor of Philosophy

June 1971

APPROVED:

Redacted for privacy

---

Associate Professor of Chemistry

in charge of major

Redacted for privacy

---

Chairman of Department of Chemistry

Redacted for privacy

---

Dean of Graduate School

Date thesis is presented October 16, 1970

Typed by Barbara Eby for William Walter Hauswirth

## ACKNOWLEDGMENT

The author wishes to express his sincere thanks to Dr. Malcolm Daniels for his guidance, constant interest and innumerable lively discussions during the preparation of this thesis. The emission polarization measurements run by Drs. Irvin Isenberg and Raymond McKenzie are gratefully appreciated, as is the use of the Turner spectrofluorimeter by the Pacific Northwest Water Laboratory.

Special thanks are due my wife, Judith, for her good spirits and hard work, and not least to Cory E. for her smile.

## DEDICATION

To my mother and in the memory of my father.

## TABLE OF CONTENTS

GENERAL INTRODUCTION	1
PART A. Excitation and Emission Properties of Excited States	1
Absorption	1
Emission	5
Ground and Excited State Processes	7
Properties of Excited States	13
Excited State Acid-Base Equilibria	22
Excited State Interactions	24
PART B. Aspects of DNA Excited States and its Constituents	26
PART C. Thesis Aim and Organization	34
Need for Room Temperature Data	34
Thesis Organization	37
I. FLUORESCENCE OF THE PURINE AND PYRIMIDINE BASES OF THE NUCLEIC ACIDS IN NEUTRAL AQUEOUS SOLUTION AT 300° K	38
Introduction	38
Materials and Methods	39
Results	42
Discussion	56
Pyrimidines	56
Purines	68
Quantum Yields and Lifetimes	72
0-0' Energies	74
II. SOLVENT EFFECTS ON THYMINE FLUORESCENCE	77
Introduction	77
Materials and Methods	78
Results and Discussion	78
Spectral Shifts and Shape	79
Quantum Yields	92
III. pH EFFECTS ON THYMINE FLUORESCENCE AT 300° K	100
Introduction	100
Materials and Methods	103
Results	103
Discussion	116
Emission Spectra	116
Emission Polarization	119
pH Effects	121

BIBLIOGRAPHY	128
APPENDIX I.	140
APPENDIX II.	166
APPENDIX III.	172

## LIST OF FIGURES

<u>Figure</u>		<u>Page</u>
I. 1	Some schematic ground and excited state processes in an organic molecule.	9
I. 2	Schematic representation of possible Franck-Condon excited and ground states.	15
I. 3	Energy levels of acidic and basic forms of an organic molecule.	23
I. 4	Structure and numbering system of thymine, its nucleoside, nucleotide, and the major thymine dimer isolated from irradiated DNA.	29
1. 1	Corrected fluorescence excitation, emission spectra and absorption spectrum for adenine.	43
1. 2	Corrected fluorescence excitation, emission spectra and absorption spectrum for guanine.	44
1. 3	Corrected fluorescence excitation, emission spectra and absorption spectrum for cytosine.	45
1. 4	Corrected fluorescence excitation, emission spectra and absorption spectrum for uracil.	46
1. 5	Corrected fluorescence excitation, emission spectra and absorption spectrum for thymine.	47
1. 6	Relative fluorescence excitation intensity vs. energy.	54
1. 7	Relative absorption spectrum, relative corrected fluorescence excitation intensities and relative emission spectrum for $5 \times 10^{-5}$ M 2,4-diethoxy thymine.	59
1. 8	Grottrian diagram of possible deactivation pathways following excitation into the first vibronic manifold.	60

<u>Figure</u>		<u>Page</u>
1. 9	Variation in fluorescence quantum yield with excitation energy.	62
1. 10	$1/\phi_f$ vs. excitation energy.	64
1. 11	$1/\phi_f$ vs. excitation energy.	70
1. 12	Comparison of the 0-0' energies for the purines and pyrimidines and their nucleotides as a function of temperature.	75
2. 1	Absorption spectra and fluorescence emission spectra for thymine in hydrogen bonding solvents.	84
2. 2	Absorption spectra and fluorescence emission spectra for thymine in non-hydrogen-bonding solvents.	85
2. 3	Plot of the difference between absorption and fluorescence spectral maxima of thymine vs. $\Delta f$ .	88
2. 4	Schematic diagram of the effect of various solvents on the absorption and fluorescence energy at thymine.	98
3. 1	Nomenclature of the neutral and ionized forms of thymine from neutral pH to 10M NaOH.	101
3. 2	Fluorescence excitation and emission spectra and absorption spectrum of $5 \times 10^{-5}$ M thymine in 0. 01 M NaOH.	105
3. 3	Fluorescence excitation and emission spectra and absorption spectrum of $5 \times 10^{-5}$ M thymine in 1 M NaOH.	106
3. 4	Fluorescence excitation and emission spectra and absorption spectrum of $5 \times 10^{-5}$ thymine in 10 M NaOH.	107
3. 5	Concentration of absorbing species of thymine as a function of pH.	108

<u>Figure</u>		<u>Page</u>
3.6	Absorption spectra of $10^{-4}$ M thymine taken on a Cary 15 in 0.025 M borax buffers between pH 6.54 and 10.4.	109
3.7	Absorption spectra of $10^{-4}$ M thymine as a function of [NaOH].	110
3.8	pH effect on some fluorescence properties of thymine.	114
3.9	Solution viscosity as a function of NaOH concentration.	122
A. 1. 1	Relative absorption and emission spectra and uncorrected spectra for anthracene in cyclohexane.	153
A. 1. 2	Corrected emission spectrum of PPO in cyclohexane normalized to unity at $2.80 \mu\text{m}^{-1}$ .	156
A. 1. 3	Relative absorption and uncorrected fluorescence excitation spectra of quinine.	159
A. 2. 1	Adenine excitation spectrum, Turner Model 210 output.	167
A. 2. 2	Adenine emission, Turner Model 210 output.	168
A. 2. 3	Adenine excitation spectrum, multichannel analyzer output.	169
A. 2. 4	Adenine emission spectrum, multichannel analyzer output.	170

## LIST OF TABLES

<u>Table</u>	<u>Page</u>	
I. 1	Survey of previous measured and estimated excited state properties of nucleic and constituents in a room temperature aqueous environment.	33
1. 1	Comparison of absorption spectra ratios for several brands of thymine taken on a Turner Model 210 and a Cary Model 15.	49
1. 2	Fluorescent properties of the bases at room temperature.	51
1. 3	Comparison of the shift in low energy maxima from circular dichroism (CD) spectra of the pyrimidine nucleosides and fluorescence excitation spectra of the corresponding free bases with the low energy absorption maxima of each nucleoside or base.	57
1. 4	Calculated rate constants for some excited state processes.	67
2. 1	Properties of solvents.	83
2. 2	Absorption and fluorescence properties of $5 \times 10^{-5}$ M thymine in various solvents.	87
2. 3	Comparison of the quantum yield for hydrate and dimer formation in $H_2O$ and $D_2O$ for UMP and thymine.	94
3. 1	Ground and excited state pK's of thymine.	115
3. 2	Room temperature fluorescence of thymine derivatives.	125
A. 1. 1	Relative absorbance and corrected fluorescence excitation spectrum intensities for several concentrations of anthracene in cyclohexane.	152
A. 1. 2	Relative fluorescence emission spectrum intensities for several concentrations of anthracene in cyclohexane.	154

<u>Table</u>	<u>Page</u>	
A. 1. 3	Relative absorbance and corrected excitation spectrum intensities for several concentrations of PPO in cyclohexane.	155
A. 1. 4	Relative absorbance and corrected fluorescence excitation spectrum intensities for several concentrations of quinine bisulfate in 0. 1 N H <sub>2</sub> SO <sub>4</sub> .	158
A. 1. 5	Relative absorbance and corrected excitation spectrum intensities for 8 x 10 <sup>-5</sup> M thymine in 0. 01 N NaOH.	160
A. 1. 6	Fluorescence quantum yields as a function of absorbance at the excitation wave number.	162
A. 1. 7	Ratio of fluorescence quantum yields for solutions of 0. 40 absorbance to those at 0. 20 absorbance.	163
A. 2. 1	Data used for calculating adenine fluorescence excitation and emission spectra.	171
A. 3. 1	PPO; 6 x 10 <sup>-7</sup> M in nitrogen flushed cyclohexane at 300° K.	172
A. 3. 2	Anthracene; 5 x 10 <sup>-6</sup> M in nitrogen flushed cyclohexane at 300° K.	173
A. 3. 3	Quinine bisulfate; 5 x 10 <sup>-6</sup> M in 0. 1 N H <sub>2</sub> SO <sub>4</sub> at 300° K.	174
A. 3. 4	Thymine in 0. 01 N NaOH, 10 <sup>-4</sup> M at 300° K.	175

# FLUORESCENCE STUDIES ON THE BASES OF THE NUCLEIC ACIDS IN SOLUTION AT ROOM TEMPERATURE

## GENERAL INTRODUCTION

An introduction which is merely a summary of textbook information is neither desirable nor useful and therefore this section has been divided into three parts each with a specific purpose. Part A deals with general excited state processes and properties, particularly emphasizing those investigated by means of fluorescence. Equations are stated or developed only when they are of the most fundamental importance or if they are to be used later. Part B summarizes the present state of our knowledge concerning the excited states of the nucleic acids and their constituents, and their relevance to the photochemistry and photobiology of DNA. Particular attention is paid to the free bases and their nucleotides. Part C presents the need for and aims of this work in light of the information in Parts A and B.

## PART A

### Excitation and Emission Properties of Excited States

#### Absorption

The primary physical process in the production of excited states and subsequent photochemistry in molecules is the act of photon

absorption (Other modes of excitation including thermal population, chemical reaction, electrical discharge and ionizing radiation will not be considered. ).

For absorption to have any finite probability, the energy of the impinging photon ( $h\nu$ ) must be equal to or exceed the energy difference between initial and final states, thus

$$h\nu \sim E_{\ell} - E_m$$

is a necessary condition of absorption. From a microscopic point of view, in a two level system the probability of absorption over a unit time is  $\rho B_{\ell \rightarrow m}$  where  $\rho$  is the electromagnetic radiation density of energy  $h\nu_{\ell \rightarrow m}$ , and  $B_{\ell \rightarrow m}$  is the Einstein absorption coefficient. From time-dependent perturbation theory, assuming only electric dipole interaction,

$$B_{\ell \rightarrow m} = \frac{8\pi^3}{3h^2} D_{\ell \rightarrow m}^2 \quad (I. 1)$$

The probability of absorption between two states is therefore governed by the magnitude of the dipole strength defined as,

$$D_{\ell \rightarrow m}^2 = \left| \frac{m}{\hbar} \langle \ell | \underline{M} | m \rangle \right|^2 = \left| \int \Psi_{\ell} \underline{M} \Psi_m d\tau \right|^2 \quad (I. 2)$$

where  $\Psi_{\ell}$  and  $\Psi_m$  are the total electronic wave function for the initial and final states, respectively. The dipole moment operator  $\underline{M}$  is the product of the electron charge  $e$  and the distance  $r_j$  to the center of

positive charge, summed over all electrons  $j$  in the molecule,

$$\underline{M} = \sum_j e r_j.$$

A more explicit view of electronic states in organic molecules includes a series of vibrational states associated with each electronic level. From the Born-Oppenheimer approximation the wave function of each vibronic state can be written as the product of a vibrational function  $\phi$  and an electronic function  $\theta$ . (Additional indices  $a$  and  $b$  are introduced to label the vibrational level within the electronic manifold.) Thus

$$\Psi_{l a} \cong \theta_l \phi_{l a} \quad \text{and} \quad \Psi_{m b} \cong \theta_m \phi_{m b} \quad (\text{I. 3})$$

and (I.3) can replace the purely electronic states in (I.2), yielding a transition moment  $\underline{m}_{l a \rightarrow m b}$  and a dipole strength  $D_{l a \rightarrow m b}$  for vibronic transitions.

The size of the transition moment integral in  $D_{l a \rightarrow m b}$  then governs the efficiency of absorption. If it is zero the absorption is said to be "forbidden".  $|\underline{m}_{l a \rightarrow m b}|^2$  will vanish if a transition between states of different spin multiplicity (eg. singlet  $\rightarrow$  triplet) is considered and these processes are said to be "spin forbidden". In reality, however, "pure" states in molecules do not exist and the interaction of spin and orbital angular momenta (augmented by local heavy atoms) allows some amount of different multiplicity in any state of a

given spin, thus there is a small but finite transition moment for singlet-triplet absorptions and weak S→T absorptions are observed (eg. McGlynn et al., 1964).

Other requirements which may lead to "forbidden" transitions involve symmetry selection rules, where the integral of  $\Psi_{\ell a} M \Psi_{mb}$  will vanish unless it is totally symmetric; and the overlap of  $\Psi_{\ell a}$  and  $\Psi_{mb}$  due to a change in position of electronic charge. For example  $\pi-\pi^*$  transitions (absorption by a bonding  $\pi$  electron resulting in its promotion to a  $\pi^*$  non-bonding state) normally have a large overlap and are therefore intense, while  $n-\pi^*$  transitions, although at lower energy, have a small  $\Psi_{\ell a}(n) - \Psi_{mb}(\pi^*)$  overlap and even if otherwise "allowed" are usually of low intensity. This is of particular interest for the singlet-singlet transitions of the purines and pyrimidines where both  $\pi-\pi^*$  and  $n-\pi^*$  transitions may occur in the first absorption band (see Section I).

The experimentally determined parameter used in measuring absorption probability is the molar extinction coefficient  $\epsilon(\bar{\nu})$  and is defined as

$$\ln\left(\frac{I_0^{\bar{\nu}}}{I^{\bar{\nu}}}\right) = 2.3 \epsilon(\bar{\nu}) c l. \quad (I.4)$$

$I_0^{\bar{\nu}}$  and  $I^{\bar{\nu}}$  are the intensities of the incident and transmitted light of energy  $\bar{\nu}$ , respectively,  $c$  is the molar concentration and  $l$  is the optical pathlength. In terms of  $\epsilon(\bar{\nu})$  the Einstein absorption

coefficient for a molecule can be expressed

$$B_{l o \rightarrow m b} = \frac{2303c}{hNn_{l o \rightarrow m b}} \int \epsilon(\bar{\nu}) \frac{d\bar{\nu}}{\bar{\nu}} \quad (I.5)$$

(Strickler and Berg, 1962).  $n_{l o \rightarrow m b}$  is the refractive index over the absorption band and is usually approximated by the average refractive index over absorption,  $n_a$ . The integral is over the  $l o \rightarrow m b$  vibronic absorption band where absorption is assumed to originate from the ground vibration state  $a = 0$  (as long as vibrational levels are not spaced close to the ground state  $a = 0$ , which is usually the case, thermal energies will not excite many molecules above the  $a = 0$  state at room temperatures, according to the Boltzman Law.)

### Emission

It was assumed above that the Einstein development for a two level system could be extended to a molecular system where the transition is still between single vibronic states (Strickler and Berg, 1962). If it is also assumed that the ground and excited states have similar vibronic wave functions ( $\Psi_{l a} \approx \Psi_{m b}$ ) and similar nuclear configurations ( $\underline{M} \approx \underline{M}$  excited), it can be shown that

$$B_{l o \rightarrow m b} = B_{m o \rightarrow l a} \quad (I.6)$$

Equation (I.6) implies a similar shape between absorption and emission, but with emission shifted to lower energies (Stoke's shift), since all

$m_o \rightarrow l_a$  energies are lower than  $l_o \rightarrow m_b$  except  $E_{m_o \rightarrow l_o} = E_{l_o \rightarrow m_o}$  (which is the 0-0' energy, see Figure 1). This is the basis for the mirror image relationship between absorption and fluorescence first found empirically by Levschin (1931) (more fully discussed later).

As for absorption, the probability of emission (or any vibrational or electronic transition) is proportional to the dipole strength as defined in Equation (I.2). In the absence of an external field spontaneous emission will still occur, generally from the state  $m_o$ , and its probability is given by the Einstein equation (Einstein, 1917)

$$A_{m_o \rightarrow l_a} = \frac{8\pi h \bar{\nu}^3 n_f^3}{c^3} B_{m_o \rightarrow l_a} \quad (I.7)$$

where  $n_f$  is the mean index of refraction over the emission spectrum (its inclusion is a later refinement by Perrin (1926) and Lewis and Kasha (1945)). Since the magnitude of  $A_{m_o \rightarrow l_b}$  is proportional to  $(\bar{\nu})^3$ , spontaneous emission usually dominates induced emission in organic molecules, even in an external electromagnetic field (except for very high intensity fields such as those encountered in lasers).

From Equations (I.5) and (I.7) the relationship between  $A_{m_o \rightarrow l_a}$  and the experimentally determined absorption spectrum  $\epsilon(\nu)$ , is derived (Strickler and Berg, 1962; Birks and Dyson, 1963).

$$A_{m_o \rightarrow l_a} = \frac{8(2303)\pi}{c^2 N} \frac{n_f^3}{n_a} \langle \bar{\nu}_f^3 \rangle_{ave} \int \epsilon(\bar{\nu}) \frac{d\bar{\nu}}{\bar{\nu}} \quad (I.8)$$

where  $\langle \bar{\nu}_f^3 \rangle_{\text{ave}}$  is the mean value of  $(\bar{\nu}_f)^3$  in the emission spectrum and  $n_f$  is the average index of refraction over the emission wave-numbers.

Being primarily concerned with excited singlet states in this work, the emission process of interest is fluorescence (specifically singlet  $\rightarrow$  singlet emission). In the absence of exciting light, the molecules in state  $mo$  at time  $t$  ( $N_{mo}$ ) are related to those initially present ( $N_{mo}^0$ ) by

$$N_{mo} = N_{mo}^0 \exp(-A_{mo \rightarrow la} t) \quad (\text{I.9})$$

and a radiative lifetime of the first excited singlet can be defined as

$\tau_0 = \frac{1}{A_{mo \rightarrow la}}$ .  $\tau_0$  is then calculated by combining Equation (1.8) and a definition of the classical dipole oscillator strength for absorption,

$$f_{lm} = \left( \frac{m_e hc^2 \bar{\nu}_{l \rightarrow m}}{\pi e^2} \right) B_{l \rightarrow m} = \frac{2303 m_e c^2}{\pi e^2 N} \int \epsilon(\bar{\nu}) d\bar{\nu}. \quad (\text{I.10})$$

Thus,

$$\frac{1}{\tau_0} = A_{mo \rightarrow la} = \frac{f_{lm} n_f^2}{1.34} \left( \frac{\bar{\nu}_f}{\bar{\nu}_a} \right)^3. \quad (\text{I.11})$$

### Ground and Excited State Processes

Singlet-singlet absorption and radiative transitions between states of like multiplicity (fluorescence) have already been partially discussed. A number of other ground and excited state processes also

commonly occur and are schematically summarized in Figure I. 1.

Observed excitation processes include singlet-singlet absorption ( $S \rightarrow S$ ) to any higher singlet state (dependent of course on the incident energy), triplet-triplet ( $T \rightarrow T$ ) absorption (usually accomplished with high intensity flash population of the  $T_1$  state closely followed by a second flash for the absorption) and spin forbidden singlet-triplet ( $S-T$ ) absorption.

Radiationless excited state processes include internal conversion ( $ic$ ) and intersystem crossing ( $isc$ ). Internal conversions are of two general sorts. i) Relaxations ( $ic_v$ ) to the lowest vibrational state within a vibronic manifold. At room temperature this process is commonly considered to be rapid with  $k_{ic_v} \sim 10^{12} \text{ sec}^{-1}$ . (Rentzepis (1968) finds a value of  $\sim 7 \times 10^{12}$  for azulene by pulse laser techniques). Compared to other processes  $ic_v$  is usually fast and accounts for the fact that other excited state fates generally begin from the  $0'$  vibronic level. ii) Isoenergetic transitions between vibronic manifolds of the same multiplicity ( $ic_i$ ), also rapid at room temperature. Coupled with  $ic_v$ , this is a major singlet depopulation mode competing with fluorescence (henceforth these two internal conversions will be considered as one and labelled  $ic$ ).

Intersystem crossing ( $isc$ ) is an isoenergetic transition between states of different multiplicity. Although "spin forbidden",  $isc$  can at times compete quite efficiently with "allowed" transitions from the  $S_1$

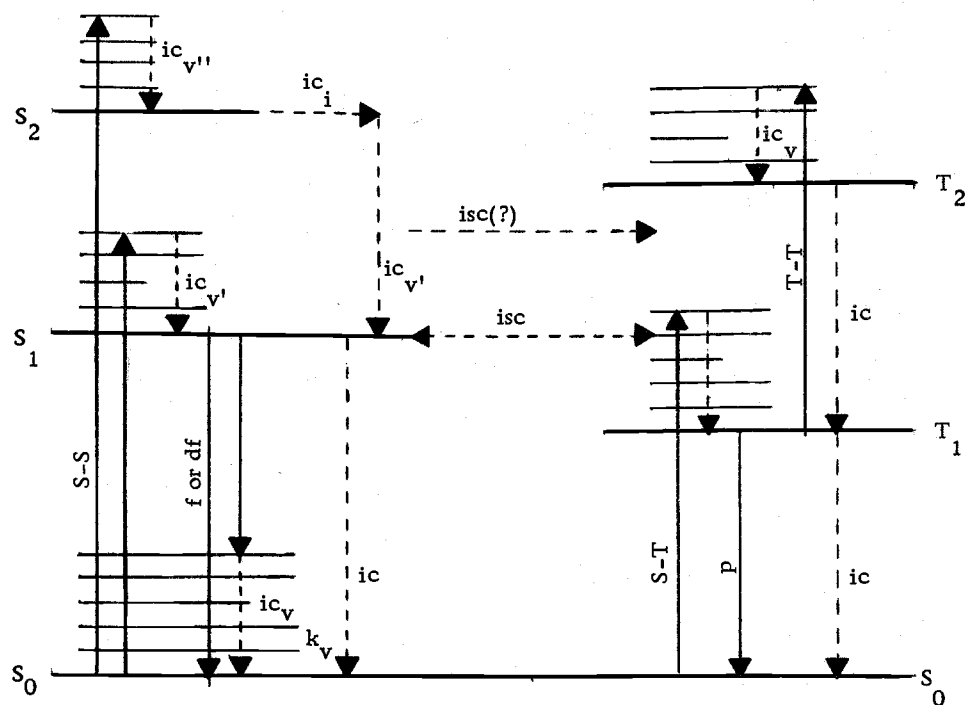


Figure I. 1. Some schematic ground and excited state processes in an organic molecule. Solid lines are radiative transitions and dashed lines are non-radiative transitions. Symbols are explained in the text; ' and '' refer to vibrational levels in the first and second excited states respectively.

state.  $k_{isc} \approx 10^8 \text{ sec}^{-1}$  for  $S \rightarrow T$  transitions in  $\pi-\pi^*$  states and possibly even higher for  $n-\pi^*$  states (Wilkinson and Dubois, 1963).

Radiative processes include fluorescence  $f$ , phosphorescence  $p$  and delayed fluorescence  $df$ . From the Franck-Condon principle, electronic transitions occur so quickly ( $\sim 10^{-15}$  sec) that the internuclear distance can be assumed fixed during the transition and can be represented as vertical lines in diagrams such as Figure I.1. For the fluorescence spectrum ( $F(\bar{\nu})$ ), the spontaneous and induced Einstein coefficients are

$$A_{S_1 0 \rightarrow S_0 a} \propto \int F(\bar{\nu}) d\bar{\nu}$$

and

(I.12)

$$B_{S_1 0 \rightarrow S_0 a} \propto \frac{1}{n_f^3} \int \frac{F(\bar{\nu})}{\bar{\nu}^3} d\bar{\nu}$$

If the condition of similar  $S_0$  and  $S_1$  vibrational spacings holds, Equation (I.6), then from Equations (I.5), (I.6) and (I.12) a test of the mirror image relationship between fluorescence and absorption spectra can be made by plotting  $\frac{\epsilon(\bar{\nu})}{\bar{\nu}}$  and  $\frac{F(\bar{\nu})}{\bar{\nu}^3}$  vs  $\bar{\nu}$  and reflecting the spectra around  $\bar{\nu}_{00}$  (Forster, 1951). A mirror image implies the distribution of transition probabilities (ie. the distribution of transition moments between vibronic states) is similar for  $S_0 0 \rightarrow S_1 b$  and  $S_1 0 \rightarrow S_0 a$  transitions.

✓ The fluorescence quantum yield  $\phi_f$  is the efficiency of  $S_1$  emission relative to the efficiency of all possible fates of  $S_1$ . Therefore in terms of rates,

$$\phi_f = \frac{k_f}{k_f + k_{ic} + k_{isc} + \sum k_D^{S_1}} \quad (L.13)$$

where  $\sum k_D^{S_1}$  refers to all other  $S_1$  deactivation processes, including photochemical reaction and energy transfer. Since  $k_f$  and  $A_{mo \rightarrow la}$  are formally identical,

$$\tau_0 = \frac{1}{k_f} ,$$

and since the actual singlet lifetime can be defined as,

$$\tau_s = \frac{1}{k_f + k_{ic} + k_{isc} + \sum k_D^{S_1}} ,$$

$$\phi_f = \tau_s / \tau_0 \quad (L.14)$$

In addition to absorption and internal conversions, the  $S_1$  state can be populated by intersystem crossing from  $T_1$  (if of course a suitable  $T_1$  vibronic level is available and populated). The singlet lifetime will then equal  $\sim$  the triplet lifetime, but the fluorescence

spectrum will remain unchanged, the process is called delayed fluorescence.

✓ Phosphorescence, defined as radiative emission between states of unlike multiplicities (normally  $T_1 \rightarrow S_0$ ), is usually not observed in room temperature solutions. Since the process is spin forbidden,  $\tau_T$  is relative long ( $\sim 10^{-2}$  sec) and in room temperature fluid solutions radiationless processes and triplet quenching by oxygen and other impurities will dominate depopulation of the  $T_1$  state (Tsai and Robinson, 1968). In rigid matrices (usually at low temperature), however, radiationless processes are less efficient and phosphorescence can often be observed. As with fluorescence, phosphorescence may exhibit a mirror image symmetry with  $S_0 \rightarrow T_1$  absorption (the normal mode of  $T_1$  population however is via  $S_1 \rightarrow T_1$  intersystem crossing). In terms of rates, the phosphorescence quantum yield  $\phi_p$  is usually written

$$\phi_p = \left( \frac{k_{isc(S_1 \rightarrow T_1)}}{k_f + k_{ic(S_1 \rightarrow S_0)} + k_{isc(S_1 \rightarrow T)} + \sum k_D^{S_1}} \right) \left( \frac{k_p}{k_p + k_{ic(T_1 \rightarrow S_0)} + \sum k_D^{T_1}} \right) \quad (I.15)$$

or

$$\phi_p = \phi_{T_1} \delta_p$$

eg.  $\phi_p$  is the product of the efficiency with which the  $T_1$  state is populated  $\phi_{T_1}$  and the efficiency of  $T_1 \rightarrow S_0$  emission  $\delta_p$ .

### Properties of Excited States

Dipole Moment and Spectral Shape. The absorption process will normally reorient one or more electrons without significantly altering the nuclear configuration of most organic molecules. The electric dipole moment, determined by the geometry and charge of the nuclei and surrounding electrons, will therefore be altered in the excited state relative to the ground state and can play an important role in determining spectral properties. Several spectral methods have been developed for measuring excited state dipole moments, they include shifts in absorption and fluorescence spectra in solution compared to gas phase (Bayliss and McRae, 1954), absorption shifts as a function of dielectric constant (Ledger and Suppan, 1967), and the effect of an electric field on the extinction coefficient (Labhart, 1967). The first two methods are of possible use in the present study.

✓ A brief consideration of solvent-solute processes taking place during absorption and emission acts should give an idea of the time scales involved, the origin of solvent effects on dipole moments and the reason for the differing response of absorption and fluorescence properties to a given solvent (assuming  $\tau_S$  for fluorescence is  $\sim 10^{-9}$  sec.). Starting with a ground state molecule surrounded by an

equilibrium solvent geometry, absorption produces a vibronic excitation (Figure I.2). Since major translational reorientation of the solvent cage is not possible during this time interval ( $\sim 10^{-15}$  sec.) the excited molecule temporarily retains its ground state solvent geometry and this configuration is frequently called a "Franck-Condon" excited state (McRae, 1957), and is labelled in Figure I.2 as Franck-Condon State A. Vibrational relaxation ( $\sim 10^{-12}$  sec, three orders of magnitude faster than fluorescence) will leave the molecule in a new state, Franck-Condon State B. The solvent cage then assumes a new geometry of minimum energy consistent with the new electronic configuration ( $\sim 10^{-11}$  sec.), leaving the molecule in a totally relaxed emitting state. Emission then leaves the molecule in the ground electronic manifold, but usually vibrationally excited and with the equilibrium excited state solvent cage. Solvent and vibrational relaxation then return the solvent-solute to the unperturbed ground state configuration. If  $\tau_S$  is less than  $10^{-9}$  sec. or solvent reorientation is slow fluorescence may not occur from a totally relaxed state (See Section II).

The different solvent cage-vibrational states involved in absorption compared to fluorescence leave no reason to expect exactly parallel trends in the solvent effects on these two processes. In view of the possibly large solvent relaxation energies encountered, eg. 5.5 Kcal mole<sup>-1</sup> ( $0.3 \mu\text{m}^{-1}$ ) for highly polar solvents (Hercules and Rogers, 1960), properties inferred only from absorption or fluorescence

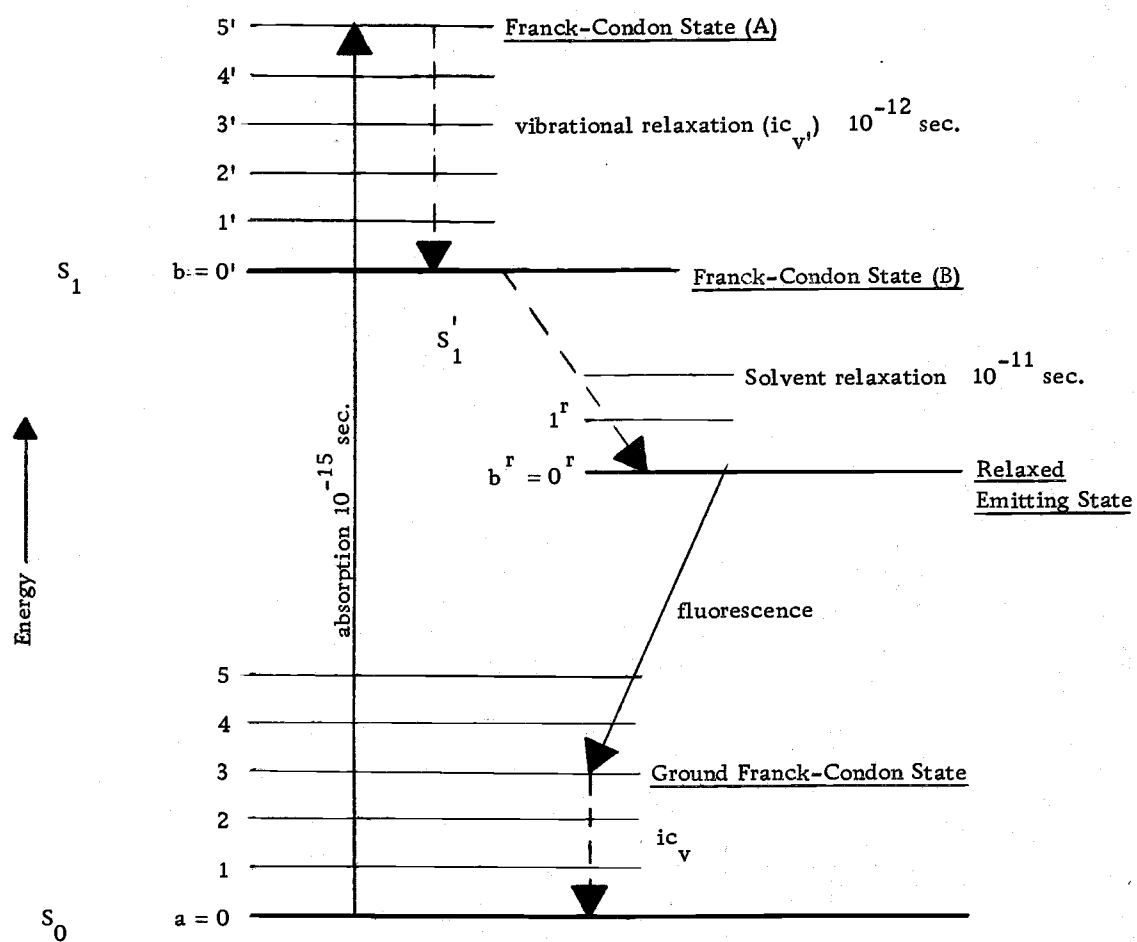


Figure I. 2. Schematic representation of possible Franck-Condon excited and ground states. Ground vibrational states are labelled  $a=0, 1, \dots$ , and excited vibrational states  $b=0', 1', \dots$  or  $b^r=0^r, 1^r, \dots$ .

data should be viewed with caution (Bayliss and McRae, 1954; Wehry, 1967).

There are a number of mechanisms by which a solvent may alter the ground and excited state properties of a given solute and they may be grouped under the general headings of electrostatic dipole effects, dispersive interaction, hydrogen-bonding, viscosity, heavy atom, chemical reaction, and short range effects (as energy or charge transfer). For the specific case of fluorescence from the free nucleic acid bases, heavy atom effects, reaction with the solute, and major short range effects are either avoided or appear to be negligible, and therefore their mechanism of action will not be considered here.

✓ When the solute has a permanent dipole (as the nucleic acid bases), solute-solvent electrostatic effects usually predominate, and the magnitude of the ground and excited dipole moment and the solvent dipole moment will control the size and direction of spectral shifts. Even in the absence of permanent dipoles in both the solute and solvent, if absorption or emission occurs, the necessary transition moment implies a finite transition dipole and temporary dipole-induced dipole effects are possible. There are several able reviews on the subject (Bayliss and McRae, 1954; Basu, 1965; Wehry, 1968). Discussion of specific effects pertinent to the purine and pyrimidine bases is delayed to Section II.

The hydrogen-bonding ability of organic molecules, particularly heterocycles, in protic solvents can be significantly changed by photo-excitation. Therefore protic solvents may effect fluorescence much differently than absorption. Specifically for nitrogen heterocycles, fluorescence from  $n-\pi^*$  transitions are often unaffected by the hydrogen-donating power of the solvent (if the  $\text{>N} \cdots \text{HO-}$  hydrogen-bond is broken in the excited state, emission occurs from the free N-heterocycle to a Franck-Condon ground state in which reformation of the hydrogen bond is unlikely due to the excited state solvent cage). Absorption from the H-bonded ground state will of course be very sensitive to the protic nature of the solvent. Measurements of pyrimidine  $n-\pi^*$  transitions confirm this general conclusion (Baba et al., 1966). The absorption spectrum will blue shift with increasing solvent hydrogen-bonding power due to a larger stabilization of the ground state relative to the excited state. The opposite effect is expected for  $\pi-\pi^*$  transitions owing to the increased basicity of a  $\pi-\pi^*$  excited state on a heterocyclic nitrogen (Weller, 1961; Wehry and Rogers, 1966) and the formation of stronger hydrogen-bonds in the excited state.

The effects of viscosity  $\eta$  and temperature on fluorescence are often inversely parallel (i. e. increasing temperature and decreasing viscosity will give similar results) and are partially related to their effects on diffusion controlled processes in the excited state. A

general equation<sup>1</sup> for the second order rate of a diffusion controlled reaction is

$$k_d = \frac{8RT}{2000\eta} (\text{M}^{-1} \text{sec}^{-1}) \quad (\text{I. 16})$$

and has been shown to give good agreement with experiment (Osborne and Porter, 1965). An increase in both  $\phi_f$  and the energies of fluorescence is usually observed in low temperature glasses and in high viscosity solutions compared to room temperature fluid solutions. Larger  $\phi_f$ 's are due to i) less efficient loss of excitation energy via solvent collision due to the rigid or viscous media usually present (i. e. a smaller  $k_{ic}$  implies a larger  $\phi_f$  (Equation (I.13)), and ii) internal radiationless processes  $k_{ic}$  and  $k_{ics}$  often show a similar decrease with temperature.

The increase in fluorescence energies of low temperature or viscous solutions results from the slower solvent reorientation in the

---

<sup>1</sup> This equation is a generalization from the Smoluchowski equation,

$$k_d = 4\pi\sigma_{AB}(D_A + D_B) \times 10^3$$

where  $\sigma_{AB}$  is the collision radius and  $D_A$  and  $D_B$  are the diffusion coefficients for molecules A and B undergoing a bimolecular collision, using the Stokes-Einstein equation,

$$D_A = \frac{kT}{6\pi r_A \eta}$$

excited state and therefore emission from the higher energy Franck-Condon excited states may occur (Lippert, et al, 1959). That this is primarily a viscosity effect is seen from the similar fluorescence blue-shift observed for aromatic molecules in rigid plastics at room temperature (Bhaumik and Hardwick, 1963).

The primary value of luminescence studies from low temperature, rigid media has been the detection of phosphorescence, rarely observed in fluid solution. For compounds with a low  $\phi_f$  (such as nucleic acid constituents), low temperature fluorescence measurements have also been useful, but several uncertainties arise in extrapolating this data to room temperature which will be discussed later (Section I).

Polarized Emissions. In the previous discussion of absorption probabilities it was implicitly assumed that an isotropic sample was exposed to unpolarized light (i. e. light of randomly oriented electric vectors). However, for a single molecule exposed to polarized light, an additional factor in the overall absorption probability is the overlap of the transition moment and the electric vector. If the angle  $\gamma$  between them is  $90^\circ$  the overlap integral vanishes and therefore the absorption probability is zero. At any other  $\gamma \neq 90^\circ$  the absorption probability is finite and is a maximum at  $\gamma = 0^\circ$ . The probability of absorption is then proportional to  $\cos^2 \gamma$ .

Emission from a geometrically fixed molecule will, in a manner analogous to absorption, also show a directional anisotropy. The

direction of emission polarization will be in the plane of the transition axis, and therefore emission polarization will be a maximum perpendicular to this axis and zero parallel to it (the electric vector is perpendicular to the direction of light propagation). A measurement of fluorescence intensities parallel  $I_{||}$  and perpendicular  $I_{\perp}$  to the axis of the polarized exciting light will give the degree of polarization  $P$ .

$$P = \frac{I_{||} - I_{\perp}}{I_{||} + I_{\perp}} \quad (\text{I. 17})$$

In room temperature solutions of randomly oriented molecules with angle  $\beta$  between absorption and emission transition moments, polarized exciting light will selectively excite those molecules aligned with the polarization axis and emit polarized fluorescence, with the degree of polarization given by (Perrin, 1926; Jablonski, 1935)

$$P = \frac{3 \cos^2 \beta - 1}{\cos^2 \beta + 3} \quad (\text{I. 18})$$

Polarization spectra are plots of Equation (I. 17) vs. absorption energy or emission energy. Since different electronic transitions do not have identically aligned transition moments, a sharp change in  $P$  across an absorption band implies more than one fluorescent electronic state absorbs in the band. A change in  $P$  across an absorption or emission band implies that more than one electronic transition

occurs at a fixed excitation energy. A constant  $P$  usually means that any structure in that band is vibrational in origin and these criteria have been commonly used to distinguish between vibrational and electronic bands in structured spectra (e. g. Feofilov, 1961).

From Equation (I.18) the maximum possible polarization value is  $P = 0.5$ ; however, the highest observed values are  $\sim 0.47$ , and at room temperature no polarization is generally observed. At least a partial explanation is that fluorescence can be depolarized by several mechanisms. Molecular rotations in the excited state will tend to directionally randomize polarized fluorescence, thus reducing  $P$ . In the presence of polarized exciting light, polarization is a function of temperature, the viscosity of the solution  $\eta$ , the singlet lifetime  $\tau_S$ , and the molar volume  $V$ , and is related to them by (Perrin, 1926)

$$\left( \frac{1}{P} - \frac{1}{3} \right) = \left( \frac{1}{P_0} - \frac{1}{3} \right) \left( 1 + \tau_S \frac{RT}{V\eta} \right) \quad (\text{I.19})$$

Depolarization can also occur by energy transfer (although most efficient when transition moments are parallel, dipole-dipole interaction between a donor and acceptor, Equation (I.22), will occur over a range of orientations thus randomizing fluorescence polarizations). The resulting concentration dependence of  $P$  has a form similar to Equation (I.19) (G. Weber, 1954).

## Excited State Acid-Base Equilibria

As early as 1931 a pH effect was noted on fluorescence in solution (K. Weber, 1931) which differed markedly from absorption effects. It was concluded that for systems showing this effect a new acid-base equilibrium is established during the lifetime of the  $S_1$  state having a much different pK from the ground state (Förster, 1950). Several methods have been subsequently developed for determining this excited singlet pK ( $pK^*$ ).<sup>2</sup>

The first method involves measurement of the fluorescence spectra as a function of pH (Weller, 1961). The pH at half fluorescence intensity (for either or both of the acid-base pair, depending on whether they are either or both fluorescent) is then the  $pK^*$ . This technique has the serious disadvantages that at least one of the acid-base pairs must fluoresce and complete equilibrium must be reached in the excited state.

An alternate method, depending on the Förster cycle (Figure I.3) (Förster, 1950; Weller, 1952) avoids the above limitations in some instances and can be used on either absorption or fluorescence spectra. From Figure I.3 it is apparent that

$$\Delta E_1 - \Delta E_2 = \Delta H - \Delta H^*$$

---

<sup>2</sup> It should be noted that triplet excited state pK's have also been determined using T→T absorption and phosphorescence spectra (Jackson and Porter, 1961).

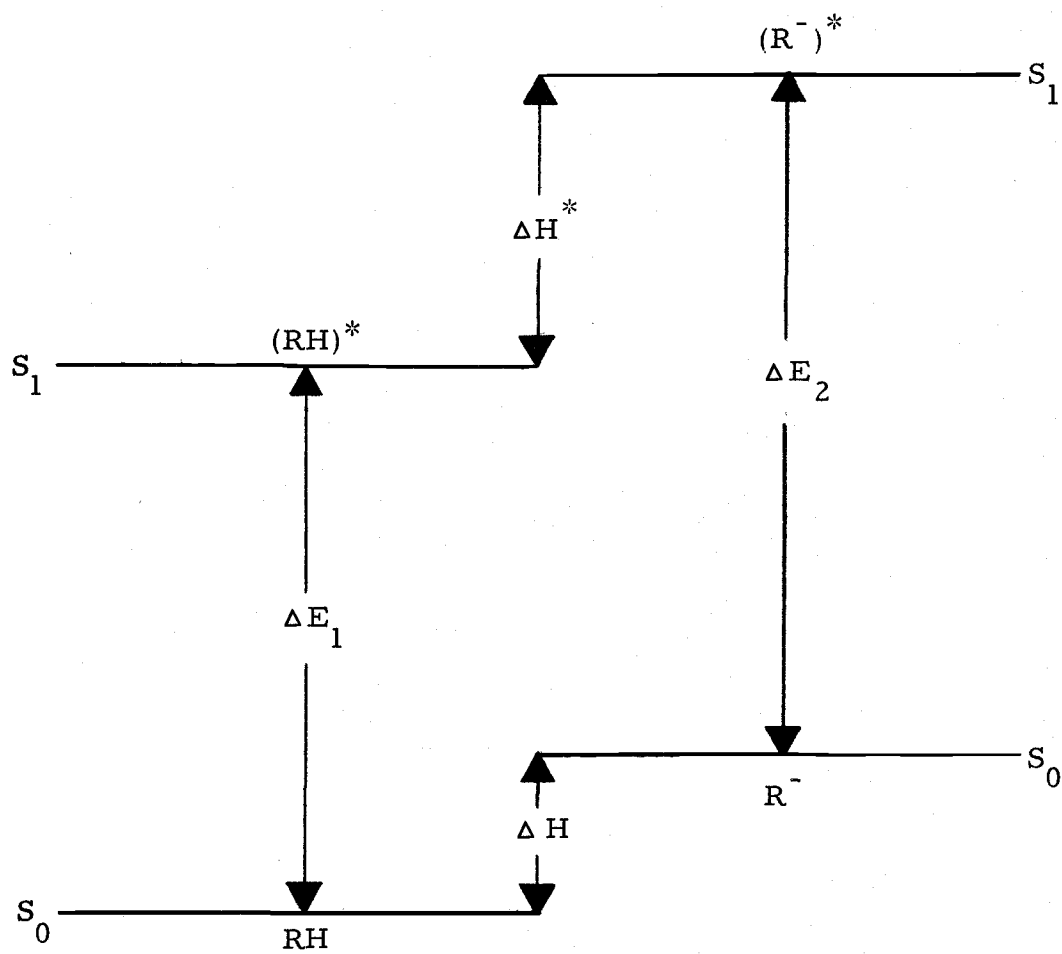


Figure I. 3. Energy levels of acidic and basic forms of an organic molecule.

Defining  $\Delta pK = pK - pK^* = \log(K^*/K)$ , since  $\Delta G = \Delta H - T\Delta S = -RT \ln K$ ,

$$\log(K^*/K) = \frac{\Delta E_1 - \Delta E_2}{2.3RT} + \frac{\Delta S_1 - \Delta S_2}{2.3R} \quad (I. 20)$$

It is assumed that  $\Delta S$  is unchanged upon excitation, then

$$\Delta pK = \frac{6.25 \times 10^3}{T} (\Delta \bar{\nu}_{00'}) \quad (I. 21)$$

where  $\Delta \bar{\nu}_{00'}$  is the difference between 0-0' energies for the acidic and basic forms. The exact position of the 0-0' energy is usually unknown, however, and must be approximated. If the average of the absorption and fluorescence is used, it is assumed that the  $S_0$  and  $S_1$  vibronic spacings are similar and the distribution of transition probabilities are equal for absorption and fluorescence, which is not necessarily valid. If, however,  $\Delta \bar{\nu}$  for the acidic and basic absorption maxima are used (Jaffé and Jones, 1964) it is assumed that these maxima are equal energies above the 0-0' transition and this method suffers from the possibly large differences in Franck-Condon solvent cage effects (Wehry and Rogers, 1965). Calculations of  $pK^*$ 's may aid in defining the exact nature of a fluorescent species when examining the pH effects on fluorescence (Section III).

### Excited State Interactions

An excited state may interact with the surrounding environment to undergo photochemical reaction, energy transfer, or excimer and

exiplex formation. Chemical reaction is obviously undesirable when ascertaining excited state properties and is commonly avoided by using low intensity exciting light for short exposure time.

Electronic energy transfer may occur by a radiative process where a donor molecule emits and a acceptor molecule absorbs ("trivial" transfer), collisional transfer where the dominant exchange interaction is determined by a diffusion controlled rate, Equation (I,16) and Förster transfer which may occur over distances many times normal collisional radii (up to  $\sim 100 \text{ \AA}$ ). Assuming only dipole-dipole interactions Forster (1959) developed a theoretical expression for the rate constant of this long range energy transfer,

$$k_{D \rightarrow A} = (\text{constant}) \frac{\phi_f^D}{n^4 \tau_S^D R^6} \int_0^\infty F^D(\bar{\nu}) \epsilon^A(\bar{\nu}) \frac{d\bar{\nu}}{\bar{\nu}^4}$$

where superscripts D and A refer to the donor and acceptor molecules respectively, R is the distance between A-D pairs,  $F(\bar{\nu})$  is the donor emission spectrum normalized to unity and  $\epsilon(\bar{\nu})$  is the acceptor absorption spectrum. Two fundamental predictions of this expression, the dependence of the transition rate on the inverse sixth power of the distance and on the size of the overlap integral have been experimentally verified for singlet-singlet transfer (Haugland and Stryer, 1967; Haugland et. al., 1969). It is apparent that  $\tau_S$  and the overlap integral are important factors in  $k_{D \rightarrow A}$  and will be discussed in relation

to the possibility of energy transfer in macromolecules (Section I).

Eximer formation (e. g. formation of a dimer-like association between an excited singlet and a ground state molecule) may result in dissociation without emission, fluorescence (at lower energies than the excited monmer) or photochemical reaction, all of which will reduce  $\phi_f$  as a function of concentration. Exiplex formation occurs when energy absorbed in one molecule of a complex is shared by the complex creating a new lower energy "exiplex". The interest in these two processes for this work is that the occurrence of either one will inhibit the efficiency of energy transfer and fluorescence, particularly in macromolecules where pairs of molecules may be closely held together.

## PART B

### Aspects of DNA Excited States and its Constituents

There are, in a general sense, three primary processes involved in the inactivation of a biologically important molecule by exposure to ultraviolet radiation. In order of occurrence they are: i) the initial physical interaction between the molecules and the impinging radiation. This includes absorption of energy to an excited state and all of the other excited electronic and vibrational fates the molecules may undergo while still retaining its initial structure. ii) The chemical process of bond breaking and/or forming, resulting in a new

molecular (or ionic) species. iii) The destruction or alteration of biological function resulting from i) and ii).

Although the primary aim of this work is to investigate certain aspects of the excited states of the purine and pyrimidine bases, the ultimate reason for such a study, must come from what is known chemically and biologically about the action of ultraviolet radiation on DNA itself. The first reason for interest in the free bases arises from the photochemical fact that absorption of UV radiation by DNA occurs in the base constituents. The second arises from the direct implication of their photoproducts as the biological lesions in irradiated DNA and RNA or at least as the sites of initial damage.

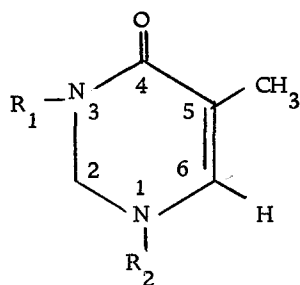
The initial observation linking photodamage to DNA photochemistry was made by Gates in 1928. He noted the similarity between the lethal affect of UV light on bacteria. Sinsheimer and Hastings (1949) reported acid or heat reversible photoproducts from the UV photolysis of uracil and uridine in aqueous solutions. Subsequent investigations (Moore and Thomson, 1958; Wang et al., 1956; Wang, 1958) showed that this reversible product probably resulted from the addition of water across the 5, 6 double bond of the uracil ring. However the relationship of these findings to DNA photodeactivation was not then apparent.

Reasoning that pyrimidine bases in an ice matrix might more closely resemble their arrangement in DNA Beukers et al. (1960),

Rorsh et al. (1960), Beukers and Berends (1960) and Wang (1959, 1960, 1961) were able to isolate an irreversible photoproduct from the UV irradiation of frozen solutions of thymine and suggested that the new product was a cyclobutane type dimer structure (Figure 1.4). Later work confirmed their structure as the cis-head to head dimer (Balckburn and Davies, 1965). More importantly, Beukers et al. (1960) were able to isolate this same dimer product from UV irradiated DNA in vitro, and Wacker et al. (1960) from irradiated DNA in bacteria.

A great deal of subsequent work has been done in isolating and identifying photoproducts from the free bases, their nucleotides, dinucleotides and polynucleotides, and from the natural nucleic acids (reviewed in: Burr, 1969; Fahr, 1969; Johns, 1969; R. G. Setlow, 1966; Smith, 1964; Wacker, 1963). In summary it appears that thymine-thymine dimers and cytosine-thymine dimers are the primary photoproducts isolated from irradiated DNA. Production of these dimers from the free bases requires a fixed geometry such as an ice-pyrimidine crystallite matrix or a dinucleotide sugar-phosphate backbone. It is sufficient here to conclude that the pivotal role of the bases in DNA photochemistry is well established.

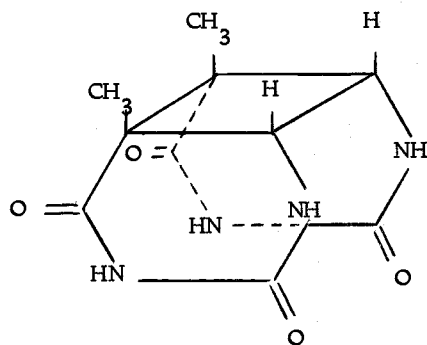
The biological and photochemical observations implicating the bases, particularly the pyrimidines, as primary sites of UV damage are briefly summarized below (see reviews above). i) The mean lethal doses (37% survival) to bacteria, viruses, and transforming DNA



Thymine:  $R_1 = R_2 = H$

Thymidine:  $R_1 = H, R_2 = \text{ribose}$

TMP:  $R_1 = H, R_2 = \text{ribose - phosphate}$



cis - head to head thymine dimer

Figure I. 4. Structure and number system of thymine, its nucleoside, nucleotide, and the major thymine dimer isolated from irradiated DNA.

produce one or more pyrimidine dimers per molecule and make a negligible number of chain breaks (ie. breaks in the sugar-phosphate bonds) or crosslinks. ii) The effects of ultraviolet radiation to inactivate transforming DNA and to destroy the primer ability of the calf thymus DNA - polymerase system yield nucleotide sequences which are resistant to enzymatic hydrolysis and exhibit physical and chemical properties unique to pyrimidine dimers (wavelength dependence of photoreversibility and  $R_f$  values). These properties do not result from photohydration or chain breaking. iii) Many biological systems exhibit the property of photo-reactivation, that is after photochemical damage, reactivation is possibly by reirradiation at a wavelength of 350-420 nm. In vivo and in vitro experiments with purified photoreactivating enzyme system show that the only effect is to destroy dimers, with reactivation occurring to the same extent that dimers are destroyed. iv) Monomerization was the net result of all types of pyrimidine dimer loss. In vivo photoreactivation of bacteria, viruses, and vertebrate cells also exhibit enzymatic photoreactivation where 50 to 90% of the lethal or mutational effects are reversed by monomerization of pyrimidine dimers. v) A similar argument can be made for UV inactivated systems in the absence of enzymes. Since pyrimidine dimers undergo photomonomerization at suitably short wavelengths, it has been shown that light of about 230 nm will reactivate the inhibition of DNA replication. Such photoreactivation in bacterial cells

proceeds to the same extent as monomerization. vi) There is a class of bacteria which are apparently quite resistant to UV radiation. Significant inactivation occurs only after doses which would normally produce over 500 dimers per DNA molecule. These cells contain a unique enzymatic mechanism commonly termed "dark reactivation" which excises dimers from DNA.

Because the lethal and mutagenic effects of UV light are shown to reside in DNA, knowledge of its excited states is important in understanding the route of excitation energy between absorption and photoproduct formation. The complicated secondary structure of native DNA involving stacking interaction, hydrogen bonding, and solvent stabilization makes straight forward interpretations about DNA excited states from simple experiments difficult and often impossible without large risks of error. Nevertheless results from energy transfer studies with polynucleotides (at  $77^{\circ}$  K) (Gueron, 1967), phosphorescence quenching of DNA by paramagnetic ions (at  $77^{\circ}$  K) (Bersohn and Isenberg, 1963; Eisenger and Shulman, 1966) and emission from dyes bound to DNA at  $77^{\circ}$  K (Isenberg, 1964; Galley, 1968) have yielded important interpretations in terms of excited states and energy transfer (both singlet and triplet) in DNA which have been extrapolated to room temperature (reviewed by Eisinger et al., 1970). Comments on some of these interpretations are reserved to Section I.

Although photochemical mechanisms in DNA may well be affected by its secondary structure, many important insights have been gained from nucleotide and free base photochemistry, particularly since the structure and properties of nucleotides or bases in solution can often be more accurately defined than for DNA polynucleotides. The isolated constituents of DNA therefore also seem a logical starting point to study DNA excited states, and from such a premise at least a start has made at understanding energy processes in DNA.

Due to the lack of detectable luminescence, excited state studies of the nucleotides and bases in room temperature aqueous solution have been primarily confined to quenching experiments, photochemical analysis, and flash photolysis (for triplet state parameters). As can be seen from Table I.1 our present knowledge of excited state properties at room temperature is quite incomplete. The majority of previous work on neutral solutions has been carried out in low temperature environments where quantum yields are more easily measurable ( $\phi_f \sim 10^{-1}$ ). Data has been accumulated, principally at 77° K in rigid ethylene glycol/water solutions, on the fluorescence, phosphorescence and e. s. r. properties of the purine and pyrimidine bases and the corresponding nucleotides. This work has been ably reviewed recently (Eisinger, 1968).

One of the most important questions to be answered and the one receiving probably the largest attention is the excited state origin of

Table I.1. Survey of previous measured and estimated excited state properties of nucleic and constituents in a room temperature aqueous environment.

Constituent	$\phi_f$	$\tau_{S_1}$	$\phi_{isc}$
thymine	$\leq 5 \times 10^{-4}$ <sup>(a)</sup>	$< 10^{-11}$	$\geq 4.7 \times 10^{-4}$ <sup>(d)</sup>
TMP	--	$\sim 10^{-12}$ <sup>(c)</sup>	$8 \times 10^{-3}$ <sup>(c)</sup>
uracil	$\leq 5 \times 10^{-4}$ <sup>(a)</sup>	--	$5 \times 10^{-3}$ <sup>(e)</sup>
UMP	--	--	--
cytosine	$\leq 5 \times 10^{-4}$ <sup>(a)</sup>	--	--
CMP	--	$\sim 10^{-12}$ <sup>(c)</sup>	--
adenine	$\sim 6 \times 10^{-4}$ <sup>(b)</sup>	--	--
AMP	--	$\sim 10^{-12}$ <sup>(c)</sup>	$\sim 10^{-4}$ <sup>(c)</sup>
guanine	$\sim 5.5 \times 10^{-4}$ <sup>(b)</sup>	--	--
GMP	--	$\sim 10^{-12}$ <sup>(c)</sup>	$\sim 10^{-4}$ <sup>(c)</sup>

(a) Gill (1970), estimate

(b) Borreson (1965), estimated from graphical data presented therein

(c) Lamola and Eisinger (1969), by europium quenching studies

(d) Fisher and Johns (1970), by photochemical studies, reported value is a lower limit

(e) Brown and Johns (1968), by flash photolysis

the thymine dimer in DNA. Systems of thymine will dimerize from either a singlet or triplet state depending on physical conditions. For example in dilute solution triplet sensitization induces dimerization (Morrison et al., 1968) and triplet quenching reduces dimerization (Greenstock et al., 1967) while dimerization from aggregates in concentrated solution shows temperature and energy dependences indicating a singlet precursor (Fisher and Johns, 1970). Thymine dimer formation in DNA itself can also arise from either a singlet or a triplet precursor, and evidence for both mechanisms is available from energy transfer and triplet sensitization studies (reviewed by Eisinger, 1970). At the present time it seems probable that both dimer mechanisms are functioning in DNA photodeactivation; in fact it has been suggested from acetophenone triplet sensitization of DNA that thymine-thymine dimers arise from a triplet while cytosine-thymine dimers arise from a singlet excimer (Lamola, 1968).

## PART C

### Thesis Aim and Organization

#### Need for Room Temperature Data

From the preceding comments, there appears to be two general systems employed for obtaining experimental information about DNA excited states. For understanding the effects of secondary structure on photochemistry and energy processes, native DNA or synthetic

polynucleotides in a room temperature, neutral aqueous solution are required. For understanding the intrinsic excited state properties of DNA, free bases and their nucleotides have been studied at 77° K. The necessary extrapolation from one system to the other, however, is difficult. Photochemistry of the free bases, even under artificial conditions which may allow an orientation of bases similar to that in a polynucleotide, will not necessarily be analogous to DNA photochemistry. For example irradiation of thymine dinucleotide (TpT) yields four isomeric dimers (Johns et al., 1964) while only one major isomer can be isolated from irradiated DNA. Stacking interaction, the large number of bases in a close fixed geometry, and hydrogen bonding between bases pairs have a very imprecisely-known effect on energy processes in DNA and they undoubtedly play a large role in observed photochemical differences. Further careful work on DNA and model systems should begin to reconcile this problem.

A more fundamental problem is the uncertainties existing in the direct extrapolation of excited state properties determined at 77° K in ethylene glycol:water glasses to the biologically-significant conditions of room temperature aqueous solution. There appear to be several, rather distinct reasons for the uncertainty. i) A generally observed red-shift in the fluorescence emission maximum has been reported for several purines (Borreson, 1965, 1967; Drobnik et al. (1967) upon warming 77° K glasses and a similar effect is

expected for the pyrimidines. A viscosity-dependent mechanism as suggested by Hercules and Rogers (1960) has been used to explain this effect (Eisinger, 1968). Solvent and vibrational relaxation from the Frank-Condon excited state are best considered as two separate relaxation processes. The rate of vibrational deactivation may be relatively independent of solvent viscosity, but solvent cage reorientation will be quite sensitive to changes in viscosity and temperature. In rigid matrices at  $77^{\circ}$  K, although emission is probably from the vibrationally relaxed molecule (vibrational state  $b = 0$ ), few solvent molecules will have relaxed from their ground state configuration and the emission will be of generally higher energy than at room temperature where quick solvent reorientation takes place. (It is noted that a factor opposing this red shift is the shorter singlet lifetime  $\tau_S$  at room temperature; if sufficiently short it may compete with solvent reorientation even at room temperature resulting in emission from a state similar in energy to that at  $77^{\circ}$  K.) To ascertain the exact effect of temperature requires, of course, measurement of heretofore undetectable fluorescence at room temperature. ii) Radiationless electronic deactivation processes may also be temperature dependent, but in a manner specific for the solute. For example, low temperature  $\phi_{isc}$  for GMP is 0.15 (Gueron, 1967) and  $\sim 0$  for TMP but at room temperature the order is reversed (Table 1), TMP being orders of magnitude higher than GMP. Clearly excited states of DNA cannot

be easily deduced from low temperature data on the nucleotides or bases. The need and importance of excited state data in a room temperature neutral, aqueous environment is therefore apparent.

### Thesis Organization

It is the purpose of this work to develop a method of detecting the weak fluorescence of the purine and pyrimidine bases and to evaluate the resulting excited singlet parameters in light of present theories on energy absorption, localization and photochemistry in UV irradiated DNA. In view of the dominant role of thymine in the photochemistry and photobiology of DNA, more complete studies are carried out on the effects of pH and solvent on thymine fluorescence. Accordingly the thesis has been divided into three parts: Section I deals with the detection and evaluation of the fluorescence from adenine, guanine, thymine, cytosine, and uracil; Section II evaluates some solvent effects on thymine emission; and Section III is concerned with the pH effects on thymine fluorescence. Each section contains a brief specific introduction and a statement of new materials and methods not previously described.

I. FLUORESCENCE OF THE PURINE AND  
PYRIMIDINE BASES OF THE NUCLEIC  
ACIDS IN NEUTRAL AQUEOUS  
SOLUTION AT 300° K

Introduction

Luminescence studies of DNA constituents at room temperature have proceeded slowly and new knowledge of excited state properties under these conditions is marked by either increased detection sensitivity or by the indirect measurements of energy transfer or photochemical studies. The earliest attempts at direct detection (Shore and Pardee, 1956; Weber, 1957) reported no room temperature luminescence from any bases of DNA. Then fluorescence was detected from adenine in acid solution, from guanine in acid and alkaline solution, and from thymine in alkaline solution (Udenfreind and Zaltzman, 1962). These fluorescences have now been quite extensively characterized (Börreson, 1967, 1965, 1963; Gill, 1968; Berens and Wierzchowski, 1969), with quantum yields in the range  $1.6 \times 10^{-3}$  (alkaline thymine) to  $1.7 \times 10^{-2}$  (alkaline guanine). Except for the minor base 5-methyl cytosine (Gill, 1970) there remained no observed emission from neutral aqueous solutions of the bases. An upper limit on the quantum yield of purine and pyrimidine fluorescence at 300° K was placed at  $10^{-3}$  (Eisinger and Shulman, 1968). More recently this limit has been lowered to  $\sim 5 \times 10^{-4}$  (Gill, 1970) and it is apparent that increased

instrumental sensitivity is required to detect base fluorescences.

The importance the fluorescence of the DNA constituents at room temperature was emphasized in the Introduction. In addition, recent studies on polyribonucleotides containing purine base analogues (Ward et al., 1969) have shown that energy transfer and excimer formation do not occur at room temperature (possibly consistent with the expected short lifetimes) as opposed to polynucleotides at liquid nitrogen temperature (Eisinger, 1968). The value of excited singlet data on the bases therefore assumes even more significance. This section is aimed at detecting and evaluating the fluorescence from the purine and pyrimidine bases of DNA and RNA.

#### Materials and Methods

All purine and pyrimidine bases were purchased from Calbiochem; adenine, cytosine, and uracil were A grade (chromatographically homogeneous) and guanine CfP grade (chromatographically pure). Thymine used for fluorescence studies was obtained from three sources 1) Calbiochem (A grade), 2) Sigma Chemical Company ( $\Sigma$  grade) and 3) Mann Research Company (M. A. grade). A fourth brand of thymine, used only for comparisons of absorption spectra, was from Schwartz Bioresearch Company (C. H. grade). 2,4-Diethoxythymine was supplied by Cyclo Chemical Corp. (Grade I) and 2,5-diphenyloxazole (PPO) was Packard Scintillation grade. All water

used was triply distilled and cyclohexane was Matheson, Coleman and Bell Spectroquality. Other solvents and reagents were: ethylene glycol, Fisher certified reagent; sodium dihydrogen phosphate, B & A reagent; glucose, B & A reagent; and sulfuric acid, B & A reagent.

All the bases were used without further purification. Buffers were avoided (except where indicated) in order to minimize interference from their scattering and possible photochemical reaction, and the pH of each solution was determined immediately before and after fluorescence measurements. The relative insolubility of guanine required dissolution first in 0.05M sulfuric acid and then neutralization with sodium hydroxide (fluorometric grade, Harleco Co.). A fluorescence blank for guanine was made similarly, all other blanks contained only triply-distilled water.

A Turner Model 210 "Spectro" was used for fluorescence and absorption measurements with fixed bandwidths of  $250 \text{ \AA}$  for the emission monochromator and  $150 \text{ \AA}$  for excitation except where otherwise noted. The wavelength accuracy of the monochromators was checked by replacing the source Zenon lamp with a 50 w Hg lamp and reflection of this light into the emission monochromator with a polished aluminum foil. Excitation and emission monochromators were either corrected to or were within  $\pm 5 \text{ \AA}$  of the nominal reading. All fluorescence data was scanned at  $3 \text{ \AA/sec}$ .

The weakness of the fluorescences required signal enhancement procedures in which the data was transferred via a Nuclear Data

82-0059 voltage-frequency converter to the memory of a Nuclear Data Model 2200 Multi-channel Analyzer. Operating the analyzer in a multi-scaling mode, it was possible to digitize the fluorescent signal and store it in 1024 successive channels during a scan. A number of repetitive scans were then added to the memory until an adequate total spectrum was obtained. Background scatter from the exciting light was recorded for an identical number of scans and subtracted in the memory before print-out on a Hewlett-Packard 7595 (S)X-Y recorder. Generally 2 to 4 scans were required for each spectra. In a typical run the fluorescence signal of the Turner was sampled and stored every 0.4 seconds (signal sensitivity was one part in 1024 full scale) during a scan of about 410 seconds covering a 2000 Å range. In order to make the voltage and impedance requirements for the two instruments compatible an eleven to one (220 K to 22 K) voltage divider was inserted between the output of the Turner and the multichannel analyzer.

Due to the uniqueness of the procedure for detecting fluorescence from the purine and pyrimidine bases, the length of the presentation, and the need for experimental verification of certain aspects of the method, it is presented as an independent unit in Appendix I. A sample of fluorescence data manipulation from initial Turner 210 output to final spectrum plotting is given in Appendix II. It is sufficient here to state that the method involves right angle detection of fluorescence from finite absorbing solutions. ✓ Additional corrections to the

fluorescence data involve i) a wavelength dependent factor accounting for the variable response of the instrument as a function of absorbance (for excitation only), and ii) standard transformations to quantal excitance and to constant wavenumber resolution.

Quantum yields were calculated according to the ratio method (Turner, 1964) relative to PPO in nitrogen flushed cyclohexane which has a quantum yield of 1.00 (Berlman, 1965, p. 147). Corrections were made to account for the finite absorbance (Equation A.1.18) and for the different refractive indices (Equation A.1.19). In order to avoid using different emission bandwidths in calculating the relative quantum yields of the bases, the yield of guanine at pH 10.9 (no added buffer, pH measured immediately before and after fluorescence measurements) was determined relative to PPO at a 25 Å emission bandwidth as  $1.65 \times 10^{-2}$  which agrees with a reported value of  $1.7 \times 10^{-2}$  (Börreson, 1965). All other quantum yields were then calculated relative to pH 10.9 guanine at a 250 Å emission bandwidth.

## Results

Emission spectra (Figures 1.1-1.5) are compared to reported data at low temperature. The relatively minor changes observed for neutral nucleotide absorption spectra while going from room to liquid nitrogen temperatures (Shinsheimer and Hastings, 1949; Gueron, 1967), also presumably holding true for the bases, might lead one to

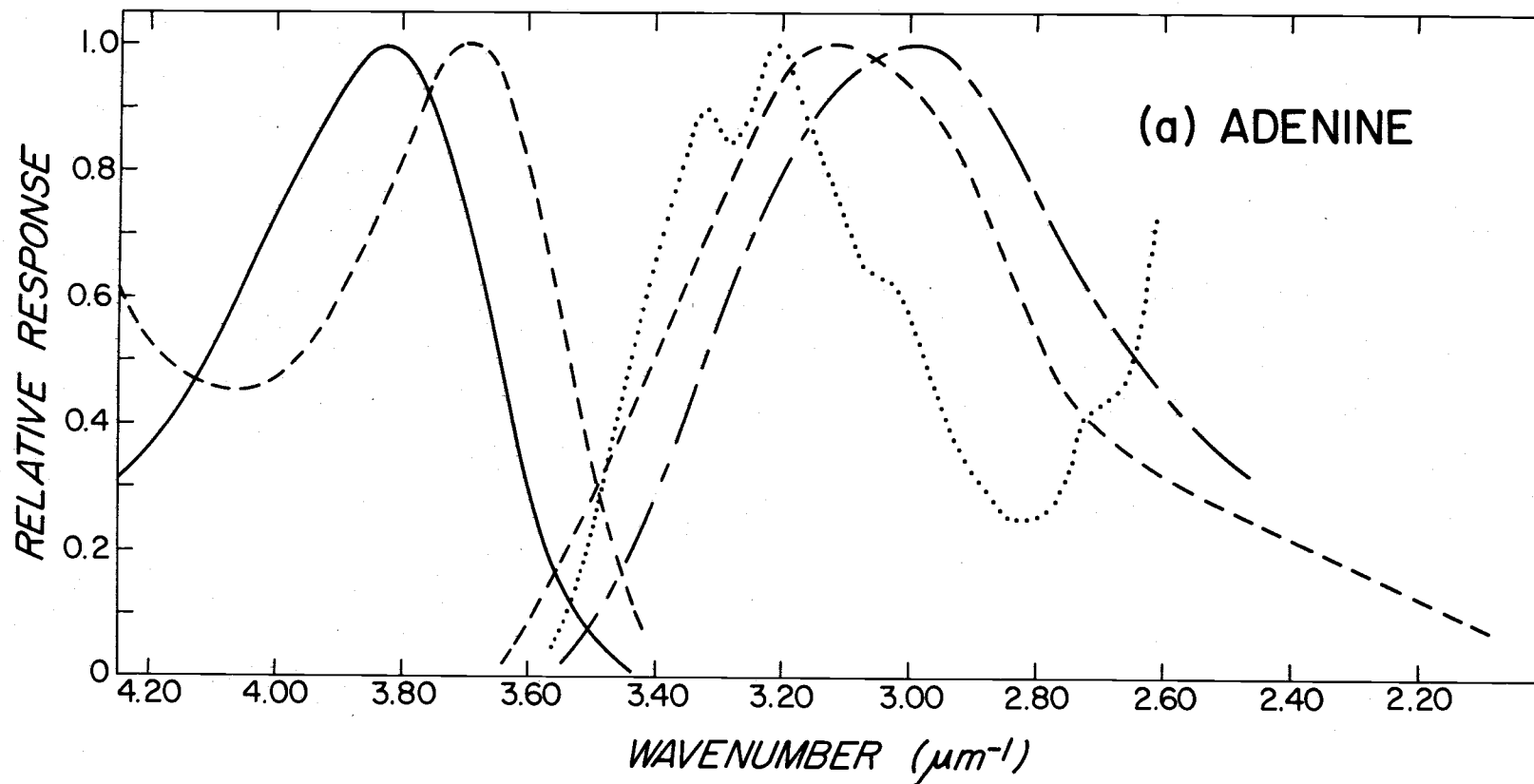


Figure 1.1. Corrected fluorescence excitation (dashed line, left) and emission spectra (dashed line, right) and absorption spectrum (solid line) for adenine, 2 scans (signal to noise  $> 25$ ), emission compared to that at  $77^{\circ}$  K in ethylene glycol:  $H_2O$  (1:1) (Honnäs and Steen, 1970) (dotted line), fluorescence excited at  $3.82\mu m^{-1}$  and emission monitored at  $3.13\mu m^{-1}$ . Solid-dash-solid curve is the emission curve when excited at  $4.17\mu m^{-1}$ .

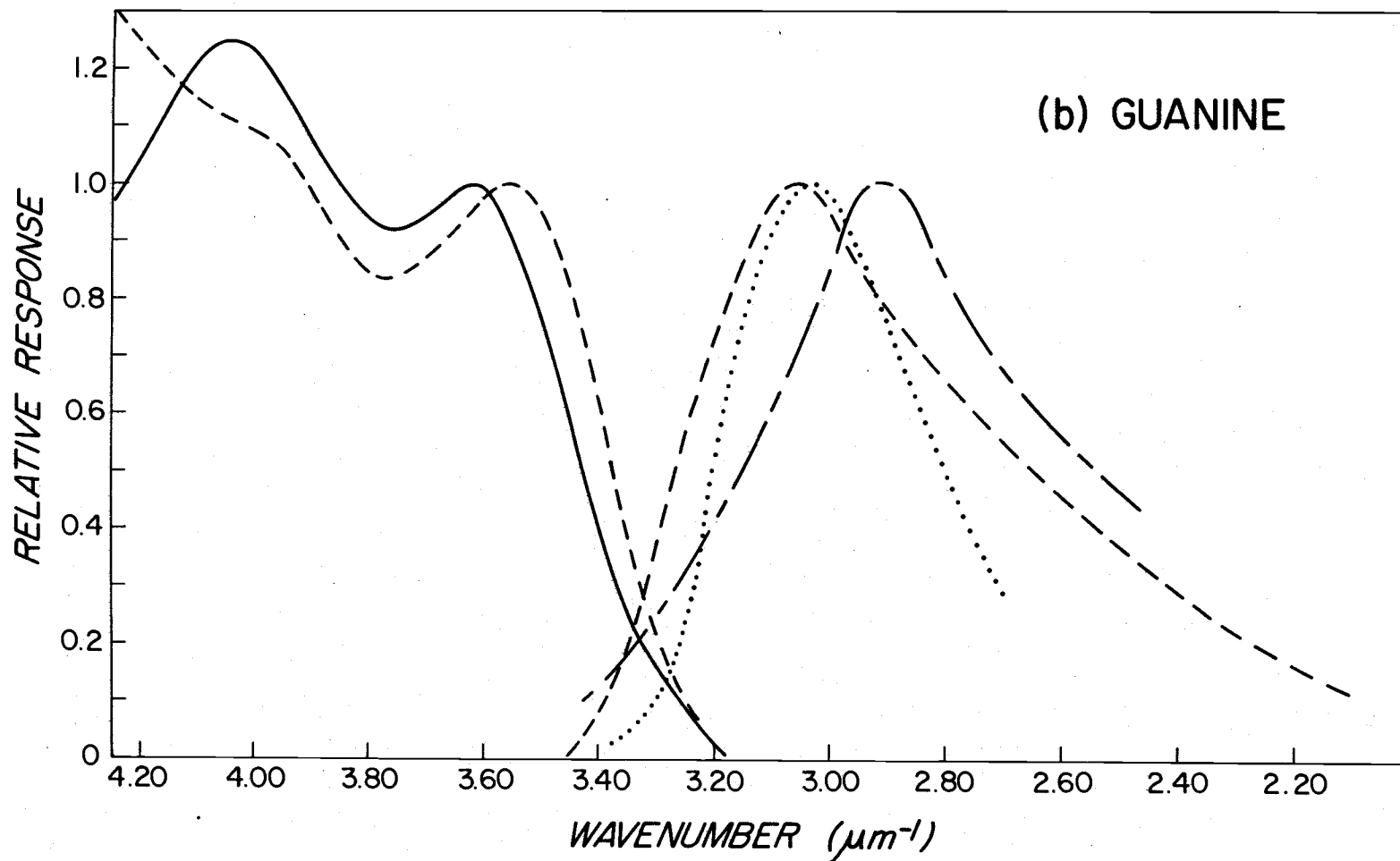


Figure 1. 2. Corrected fluorescence excitation (dashed line, left) and emission spectra (dashed line, right) and absorption spectrum (solid line) for guanine, 2 scans (S/N > 25), emission compared to that at 195<sup>o</sup> K (Callis et al., 1964), excited at 3.63  $\mu\text{m}^{-1}$  and monitored at 3.30  $\mu\text{m}^{-1}$ . Solid-dash-solid curve is the emission spectrum when excited at 4.17  $\mu\text{m}^{-1}$ .

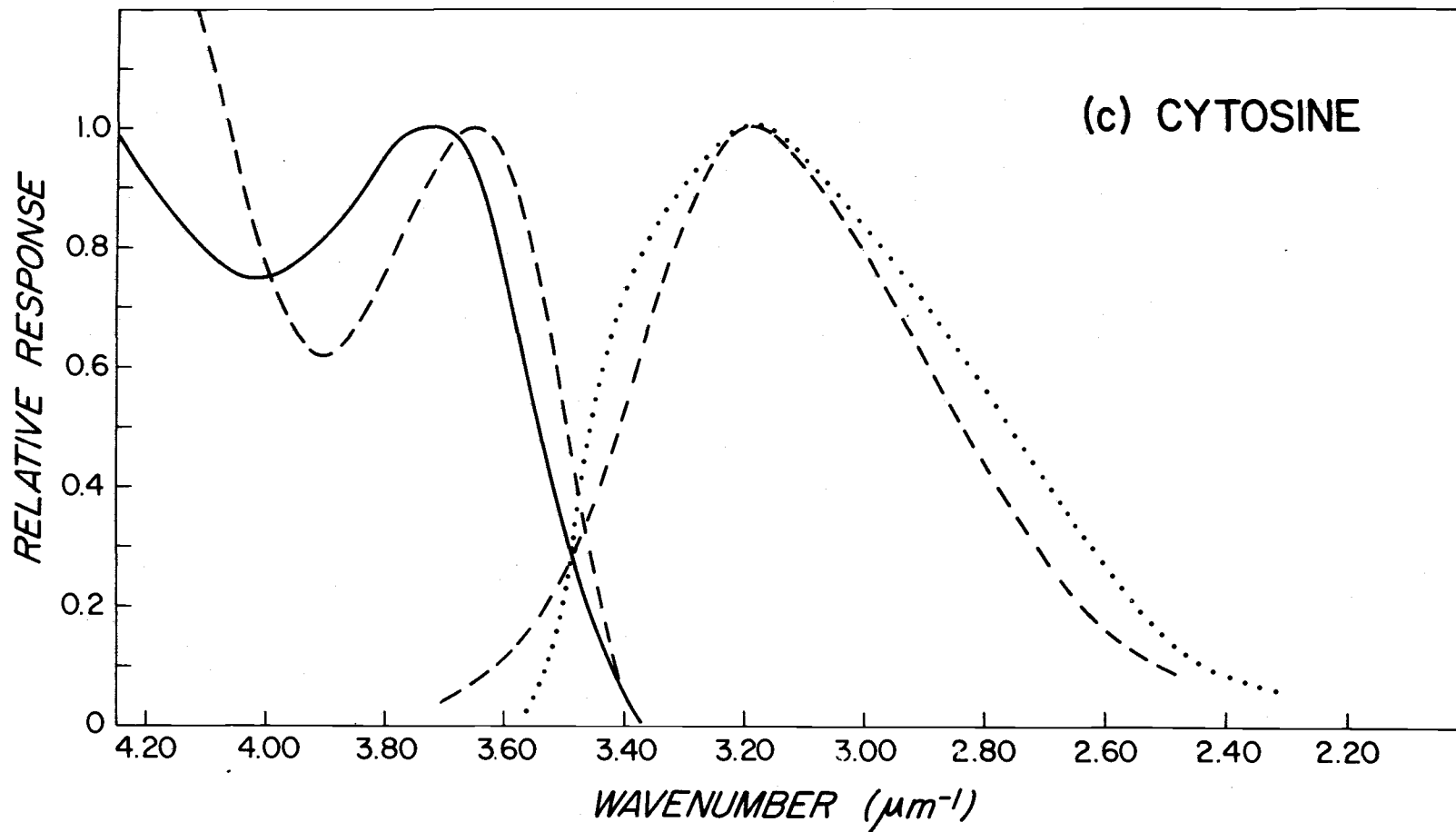


Figure 1. 3. Corrected fluorescence excitation (dashed line, left) and emission spectra (dashed line, right) and absorption spectrum (solid line) for cytosine, 4 scans ( $S/N > 15$ ), emission compared to that at  $77^{\circ}$  K (Longworth *et al.*, 1966), (dotted line), excited at  $3.75 \mu\text{m}^{-1}$  and monitored at  $3.13 \mu\text{m}^{-1}$ .

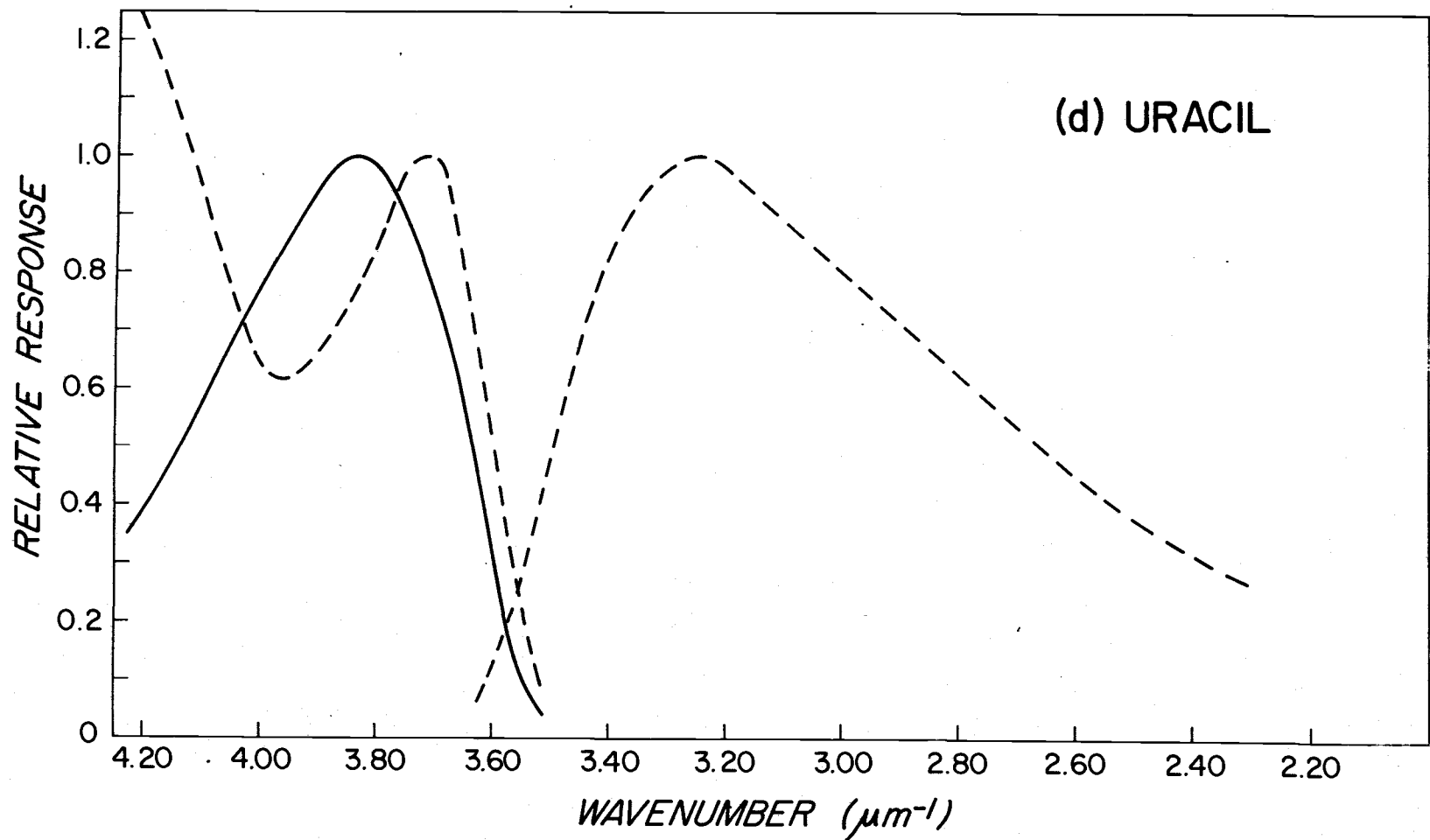


Figure 1.4. Corrected fluorescence excitation (dashed line, left) and emission spectra (dashed line, right) and absorption spectrum (solid line) for uracil, 4 scans ( $S/N > 15$ ), excited at  $3.87 \mu\text{m}^{-1}$  and monitored at  $3.23 \mu\text{m}^{-1}$ .

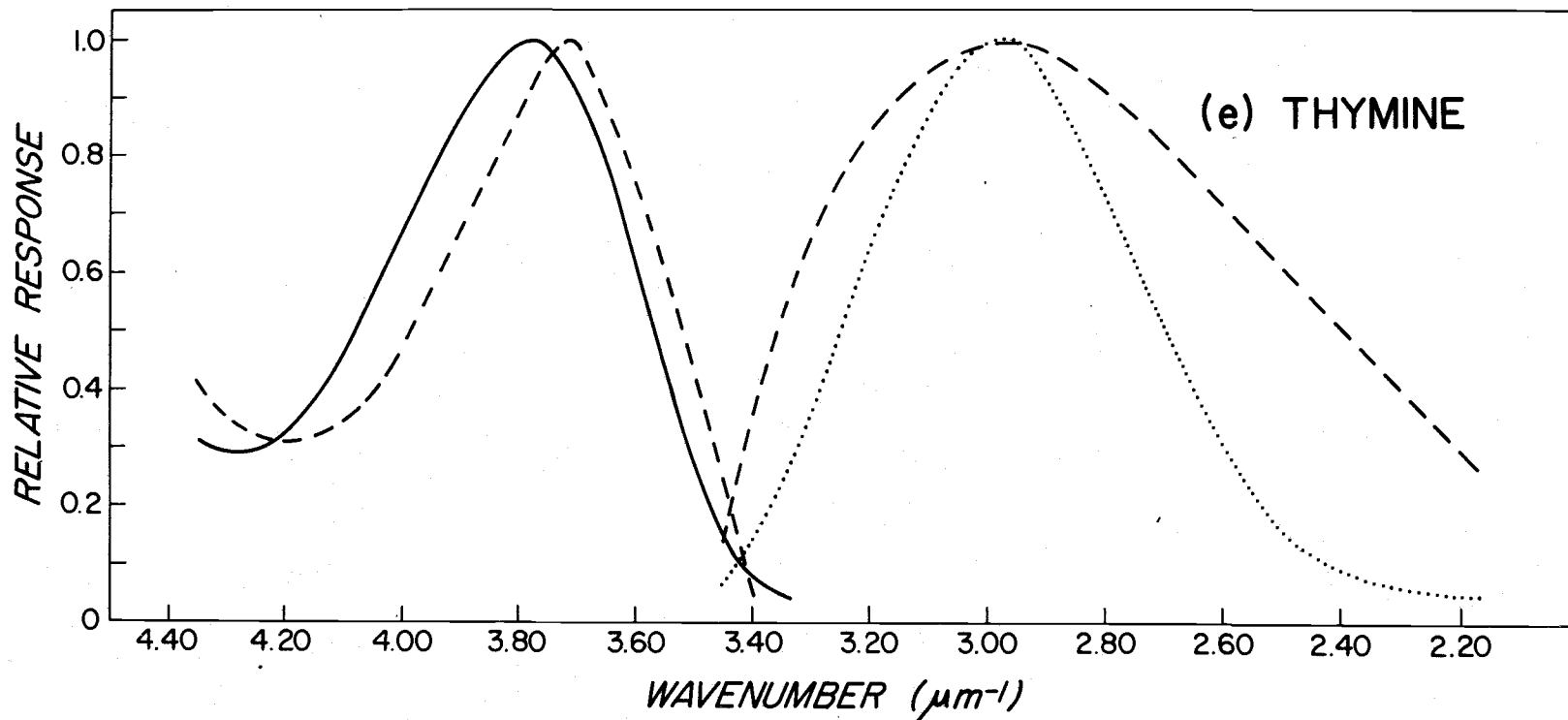


Figure 1.5. Corrected fluorescence excitation (dashed line, left) and emission spectra (dashed line, right) and absorption spectrum (solid line) for thymine, 6 scans ( $S/N > 25$ ), emission compared to that at  $77^{\circ}\text{K}$  (Honnas and Steen, 1970) (dotted line), excited at  $3.77\ \mu\text{m}^{-1}$  and monitored at  $3.00\ \mu\text{m}^{-1}$ .

expect correspondingly small changes in emission spectra. It has been noted however that there is no fundamental reason to expect spectral agreement; in fact the large environmental changes accompanying the change of solvent and a temperature reduction to 77° K and the attendant uncertainty in the state of the solute (ie. whether still isolated molecules or crystallite aggregates) argues for differences. The comparison is included primarily to show the general reasonableness of the observed emissions. Since corrected 77° K data is only available for thymine and adenine, no significance can be attributed to minor disagreements with 300° K data for the other bases.

In view of the weakness of the emission it is important to establish whether impurities are present which may give rise to the signal. All four commercial sources of thymine were claimed to be chromatographically homogeneous in either one or two solvent system; these claims have been substituted by chromatography in n-butanol: water: acetic acid (80 : 30 : 13). Absorption ratios of these samples have been determined on the Cary Model 15 and are compared with the standard literature reference (Shuger and Fox, 1952) in Table 1.1. The samples are virtually indistinguishable among themselves; the small differences between the present data and that of Shugar and Fox

Table 1.1. Comparison of absorption spectra ratios for several brands of thymine taken on a Turner Model 210 and a Cary Model 15. The sources of thymine were CB = Calbiochem Co., M = Mann Research Co.,  $\Sigma$  = Sigma Chemical Co., and S = Schwartz BioResearch Co.

Absorbance Ratios (nm/nm)	Turner 210		Cary 15				Beckman DU
	CB <sup>a</sup>	CB <sup>b</sup>	CB	M	$\Sigma$	S	S
250/260	.67	.70	.70	.69	.70	.70	.67
280/260	.52	.53	.52	.51	.52	.52	.56
290/260	.10	.16	.10	.10	.10	.10	.12

a) 25 Å bandwidth

b) 150 Å bandwidth

(1952) may be instrumental in origin<sup>3</sup>. Included in Table 1.1 are some ratios determined on the Turner Model 210 at fixed bandwidths of 150 Å (which was also used for the determination of excitation spectra) and 25 Å.

On the basis of 1) the similarity between the low temperature and room temperature emission spectra, 2) the independence of the source of thymine and 3) our inability to detect fluorescing impurities, it is concluded that the emission is a genuine fluorescence of thymine. Absorption spectra from the other bases (all from a single commercial source) were also in agreement with standard values. Because of this, their similarity with low temperature emission data, and the reasonableness of their calculated quantum yields (Table 1.2) (the purine  $\phi_f$ 's larger than thymine and lower  $\phi_f$ 's for cytosine and uracil), all observed fluorescence signals appear to be genuine.

Fluorescence excitation spectra are reported in all cases and are compared with absorption spectra taken on the same instrument with identical bandwidths (a valid comparison is only possible in this manner (Fletcher, 1969)).

---

<sup>3</sup> A discrepancy exists between the absorption ratio values given in "Specifications and Criteria for Biochemical Compounds", Publication 719, NAS/NRC, Washington, D. C. 1960 and the original data from which these specifications and criteria are derived. Shugar and Fox (1952) seem to be the only data source for thymine and we have compared our results with it.

Table 1. 2. Fluorescent properties of the bases at room temperature.

Compound	Concentration (M x 10 <sup>5</sup> )	pH	Excitation energy ( $\mu\text{m}^{-1}$ )	Fluorescence Quantum Yield (x 10 <sup>4</sup> )	0-0' Energy* ( $\mu\text{m}^{-1}$ )	Singlet Lifetimes <sup>+</sup> (x 10 <sup>12</sup> sec.)	
						(a)	(b)
Adenine	5	7.3	3.83	2.6	3.56	1.0	8.9
Guanine	8	6.3	3.63	3.0	3.34	1.4	3.0
Thymine	5	6.7	3.77	1.02	3.45	0.9	1.5
Cytosine	10	6.5	3.75	0.82	3.49	0.2	0.9
Uracil	8	6.8	3.87	0.45	3.57	0.7	1.4

\* determined by the absorption-emission intersection

+ method of calculation explained in the text

Adenine emission is unstructured, contrary to corrected low temperature data (Honnäs and Steen, 1970) (Figure 1.1). There appear to be two possible explanations for such unresolved peaks. i) The emission bandwidth of 250 Å is too wide to resolve the bands of about 100 Å separation occurring at 77° K (Although several scans with 100 Å bandwidths also failed to reveal structure). ii) At room temperature there is a higher density of rotational and vibrational states within a vibronic level which allows some energy overlap of vibrational states normally resolved at 77° K. Thus, assuming the bands in adenine emission are vibrational in origin (at 170° K constant polarization is observed over the emission band from 3.33 to 2.85 μm<sup>-1</sup> (Eastman, 1969)), a resolution loss with increasing temperature may occur. It seems most likely that this latter effect of temperature is the dominant cause for the smooth emission of adenine at 300° K. The spectrum is roughly an envelope enclosing the vibrational bands, but is slightly red-shifted relative to corrected 77° K data. Such a shift at higher temperatures is expected (Lippert *et al.*, 1959).

At a pH of 7.3 adenine is definitely in its neutral form, more than two pH units from either ground state pK's of 4.15 and 9.8 or the fluorescence pK of 4.2 (Borreson, 1963). The observed emission is therefore a genuine property of neutral adenine at room temperature.

From the work of Weber and Teal (1958) who reported the quantum yields for a number of compounds to be invariant with excitation energy which implies coincidence of normalized absorption and excitation, agreement between absorption and emission is expected. For adenine, however, such agreement is not evident (Figure 1. 2). This observation is not an instrumental artifact because the wavelength reliability of the Turner 210 has been established (see Methods, this section), and the quantum yield determined with excitation at  $4.17 \mu\text{m}^{-1}$  is 2.76 times that with  $3.83 \mu\text{m}^{-1}$  excitation which agrees with the factor of 2.73 determined from the excitation and absorption spectra. In addition a wavenumber dependence on the excitation spectrum at  $170^\circ \text{K}$  (in ethylene glycol:water, 70:30) was observed by Eastman (1969) and the resulting effect on the quantum yield as a function of excitation energy is similar to our data (Figure 1. 6). The shift in excitation relative to absorption seems therefore real and since it appears to be a general effect for all the bases, the possible mechanisms will be discussed together in a later section.

Guanine gives the most intense fluorescence (Table 1. 2) and an unstructured emission spectrum (maximum at  $3.05 \mu\text{m}^{-1}$ , Figure 1. 2) close to the uncorrected low temperature emission (Callis *et al.*, 1964). The structured phosphorescence bands  $> 2.80 \mu\text{m}^{-1}$  at  $77^\circ \text{K}$  are not present at room temperature because of the very low  $\phi_p$ . As with adenine, guanine excitation is not coincident with absorption.

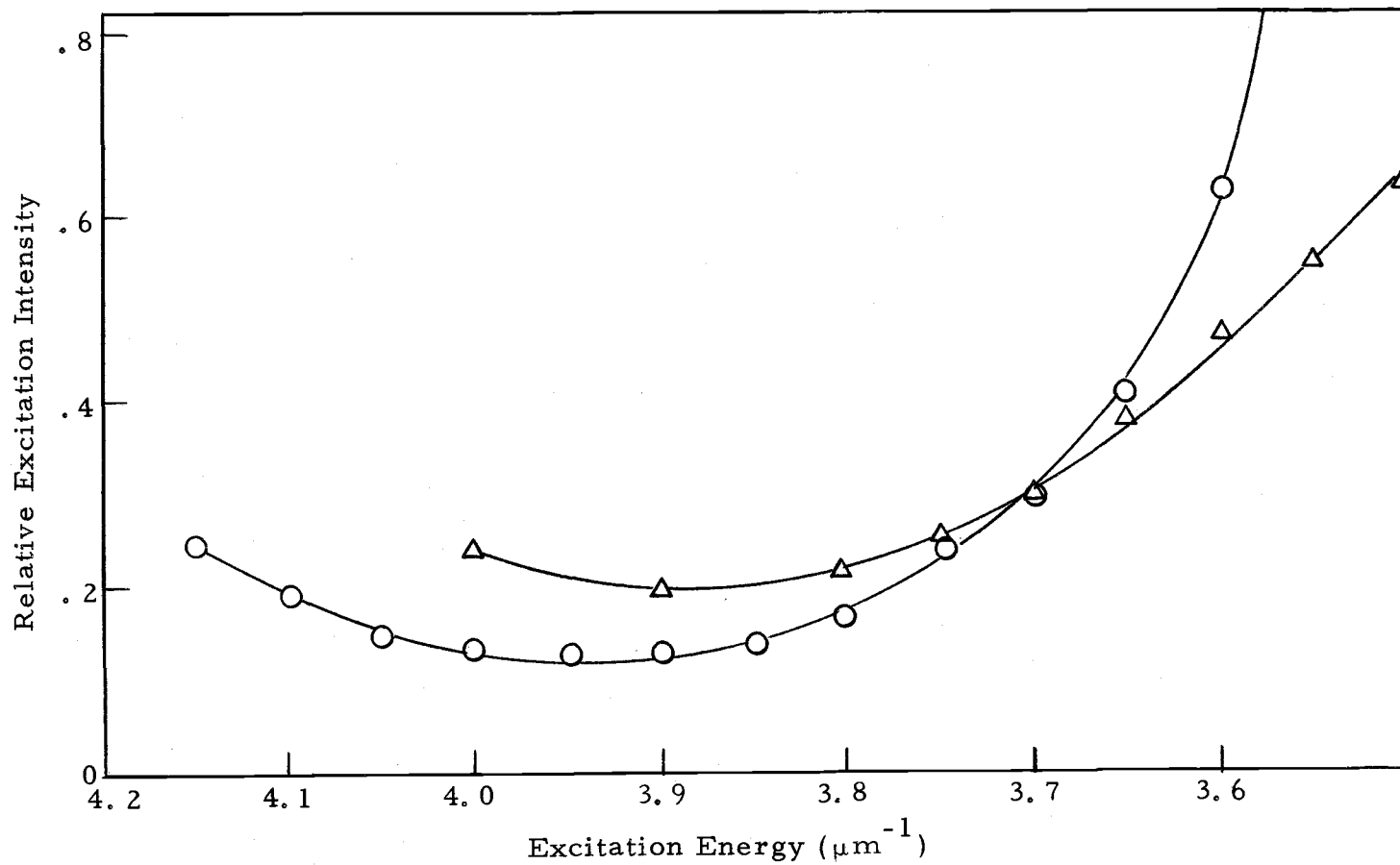


Figure 1.6. Relative fluorescence excitation intensity vs. energy. Adenine in aqueous solution at 300° K (O — O), adenine in 70/30 ethylene glycol at 170° K ( $\Delta$  —  $\Delta$ ) (Eastman, 1969).

At pH 6.5 guanine is between its ground state  $pK$ 's of 3.3 and 9.2, and the observed emission therefore originates in the neutral molecule.

Cytosine (Figure 1.3) and uracil emission spectra (Figure 1.4) are in reasonable agreement with uncorrected  $77^{\circ}$  K data (Longworth et al., 1966) (Only an emission maximum at  $3.18 \mu\text{m}^{-1}$  is reported for uracil). Similar to the purines, all pyrimidine fluorescence excitation spectra are shifted to lower energies than their absorption.

Thymine emission (Figure 1.5) is independent of its commercial source and has  $\bar{\nu}_{\text{max}}$  at  $2.96 \mu\text{m}^{-1}$ . It is essentially unaltered in 0.5 M  $\text{H}_2\text{SO}_4$ , 0.1 M phosphate (pH 6.70), and 0.1 M phosphate + 0.25% glucose. In ethylene glycol:water (1:1) the emission maximum is shifted to  $3.07 \mu\text{m}^{-1}$  (see Section II, Figure 2.1). The emission spectrum in ethylene glycol:water (1:1) (Honnäs and Steen, 1970) is compared to ours in water (Figure 1.5). Although the room temperature emission is broader there is general agreement, particularly at the maxima which are essentially coincidental at  $2.96 \mu\text{m}^{-1}$ . Other reports for  $77^{\circ}$  K list the emission maximum as  $3.05 \mu\text{m}^{-1}$  (corrected, Kleinwachter et al., 1966) in 0.1 M phosphate + 0.25% glucose, and  $3.16_5 \mu\text{m}^{-1}$  (uncorrected, Longworth et al., 1966) in ethylene glycol:water (1:1).

## Discussion

✓ The most striking aspect of the fluorescent data is the disagreement of all the bases between their absorption and fluorescence excitation spectra. Processes which may explain this type of shift include the existence of two tautomeric structures in the first absorption band, only one of which is fluorescent (Hauswirth and Daniels, 1970a; Eastman, 1969; Borreson, 1967), the changing efficiency of radiationless deactivation processes as a function of excitation energy (Hauswirth and Daniels, 1970a), emission from an  $n-\pi^*$  or  $\pi-\pi^*$  state hidden in the red edge of the absorption band (Hauswirth and Daniels, 1970a; Witten and Lee, 1970; Miles et al., 1969). The relevance of these processes in terms of each individual base is presented along with a more detailed account in the case of thymine.

Pyrimidines

Excitation Spectra. Circular dichroism data for the pyrimidines has resolved the low energy absorption of their nucleosides into two electronic transitions for thymidine and uridine, and a single transition for cytidine (Miles et al., 1967), all of a  $\pi-\pi^*$  nature. The shift between absorption maxima and the lowest energy CD maxima is compared to the shift between absorption and excitation spectra of the pyrimidine bases observed in this work in Table 1.3. Although

Table 1. 3. Comparison of the shift in low energy maxima from circular dichroism (CD) spectra of the pyrimidine nucleosides and fluorescence excitation spectra of the corresponding free bases with the low energy absorption maxima of each nucleoside or base.

	Nucleoside Abs. Max. ( $\mu\text{m}^{-1}$ )	CD Max. <sup>(a)</sup> ( $\mu\text{m}^{-1}$ )	$\Delta\mu\text{m}^{-1}$ Abs. - CD	$\Delta\mu\text{m}^{-1}$ (free bases) Abs. - Fl. Excitation
Cytidine	3.70	3.70	0	+0.06
Uridine	3.82	3.75	+0.07	+0.12
Thymine	3.75	3.61	+0.14	+0.08

(a) Data taken from Miles et al., (1967).

there is not good agreement between the magnitudes, the direction of CD shifts are the same as observed fluorescence excitation shifts. This at least makes it possible that a  $\pi-\pi^*$  transition exists in the red edge of the pyrimidine absorption spectrum (except for cytosine) which may account for a majority of fluorescence.

There has been no evidence of stable tautomers of the neutral pyrimidine bases; this however does not eliminate their existence. For example, it is possible that a ground state tautomer of thymine, existing in a small percentage, may be fluorescent. 2,4-Diethoxythymine is equivalent in structure to the 2,4-dienol or lactim structure of neutral thymine. However the 2,4-diketo or lactam tautomer is commonly considered to predominate in neutral aqueous solution. We find this model compound has an emission with  $\bar{\nu}_{\max}$  at  $3.22 \mu\text{m}^{-1}$  and  $\phi_f = 1.6 \times 10^{-3}$  (Figure 1.7). If the tautomer model is valid, only ~7% of the thymine would have to exist in the lactim form to give a net quantum yield of  $1.04 \times 10^{-4}$ , assuming the intrinsic fluorescence yield of the tautomer to be similar to its model. Such a small proportion would be difficult to detect in aqueous solution by other spectroscopic techniques.

Excited State Processes. Consideration of a simple Grotrian diagram (Figure 1.8) shows how the fluorescent quantum yield may be related to excitation into higher vibronic levels. The independence of the fluorescence emission spectrum on exciting wavelength is usually

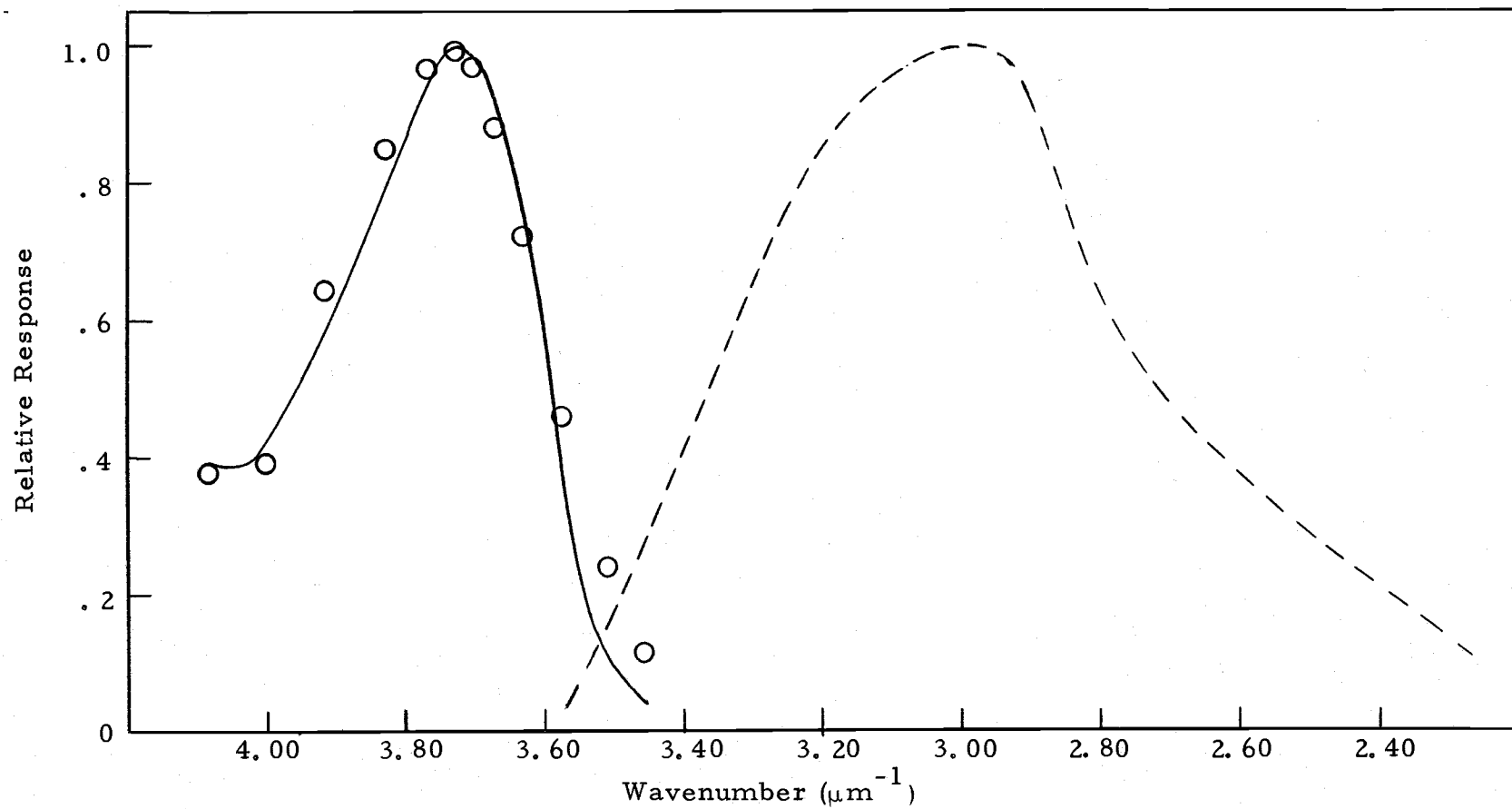


Figure 1. 7. Relative absorption spectrum (—), relative corrected fluorescence excitation intensities (O), and relative emission spectrum (---) for  $5 \times 10^{-5}$  M 2,4-diethoxy thymine, pH 6.8, emission excited at  $3.73 \mu\text{m}^{-1}$ , and excitation monitored at  $3.00 \mu\text{m}^{-1}$ .

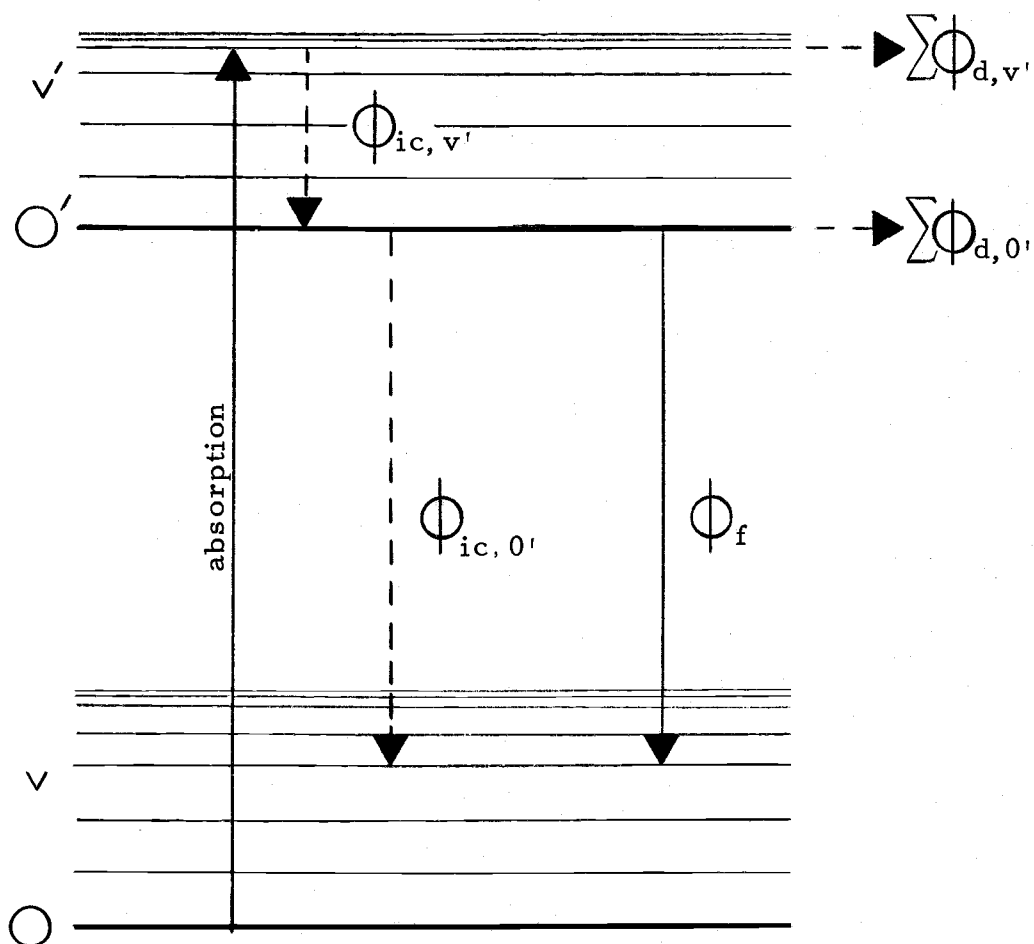


Figure 1.8. Grotrian diagram of possible deactivation pathways following excitation into the first vibronic manifold (symbols defined in text).

considered to be evidence that emission occurs from the lowest vibronic level of the first excited state and this is observed for thymine for excitation between  $3.45$  and  $4.00 \mu\text{m}^{-1}$ . If excitation occurs in the  $0'$  level, then the fluorescence quantum yield,  $\phi_{f,0'}$ , is the fraction of molecules in this state which fluoresce. Processes not leading to fluorescence may be internal conversion to ground state,  $\phi_{ic,0'}$ , and other deactivation processes such as photochemical product formation and intersystem crossing to the triplet manifold,  $\Sigma\phi_{d,0'}$ . If excitation takes place to higher vibronic levels  $v'$  of the first excited state, then the total fluorescence quantum yield will be given by the fluorescence yield from the  $0'$  level multiplied by the fraction of molecules reaching that level by internal conversion from  $v'(\phi_{ic,v'})$ ,

$$\phi_{f,v'} = \phi_{ic,v'}\phi_{f,0'} \quad (1.1)$$

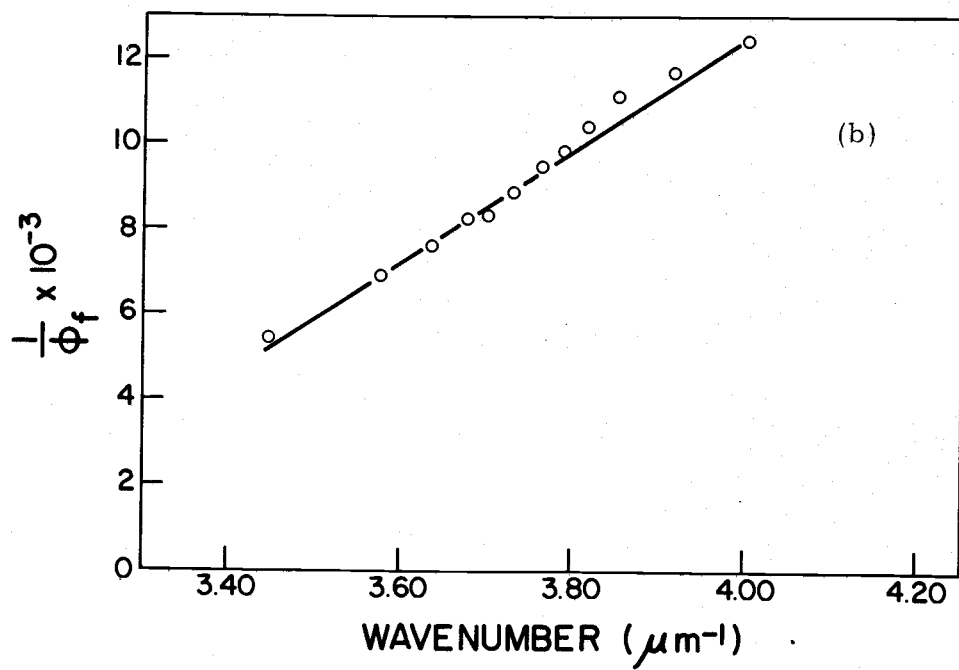
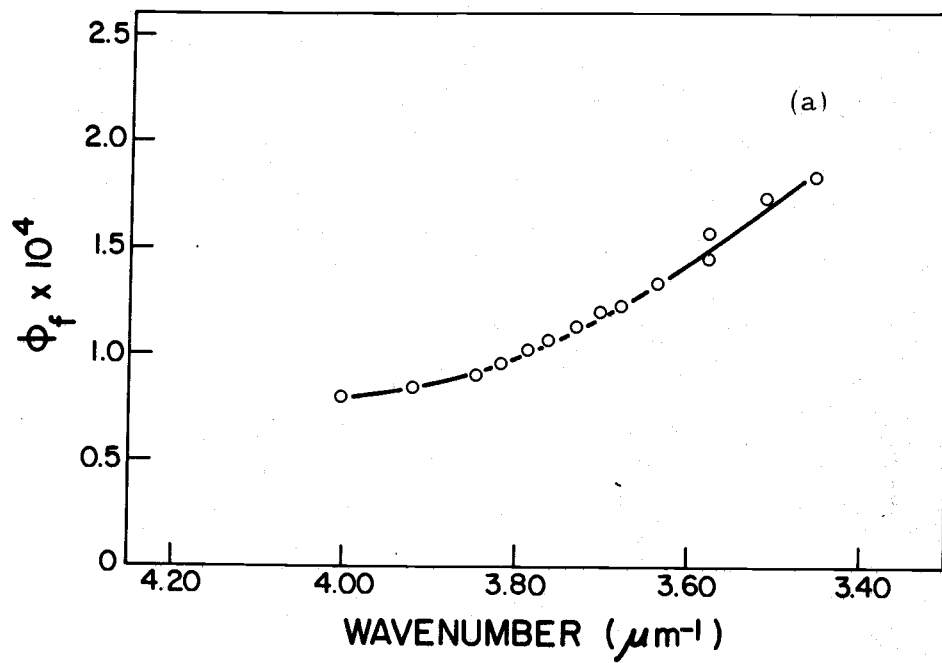
Clearly, since  $\phi_{ic,v'} \leq 1$ ,  $\phi_{f,v'}$  can be at most equal  $\phi_{f,0'}$  and will probably be less; the latter case is in agreement with our findings (Figure 1.9a). Writing  $\phi_{ic,v'}$  in terms of rate constants for processes occurring from level  $v'$ , then  $\phi_{ic,v'} = \left(\frac{k_{ic}}{k_{ic} + \Sigma k_d}\right)^{v'}$  where  $\Sigma k_d$  is for all deactivation processes not leading to the fluorescent  $0'$  level, including photochemical reaction, direct internal conversion to the ground or some other non-fluorescing state and intersystem crossing to the triplet state. Then

Figure 1.9. Variation in fluorescence quantum yield with excitation energy.

a.  $\phi_{fl}$  vs. excitation energy

Quantum yield calculated by dividing the excitation spectrum by the absorption spectrum (Figure 1.5) and adjusting the quantum yield to that determined for excitation at  $3.77 \mu\text{m}^{-1}$ .

b.  $1/\phi_{fl}$  vs. excitation energy



$$\frac{1}{\phi_{f, v'}} = \frac{1}{\phi_{f, 0'}} \left[ 1 + \left( \frac{\sum k_d}{k_{ic}} \right) \right]^{v'} \quad (1.2)$$

and this suggested the empirical relation between  $\frac{1}{\phi_{f, v'}}$  and excitation energy shown in Figure 1.9b, from which  $\frac{\sum k_d}{k_{ic}}$  appears to be approximately a linear function of the energy of excitation above  $0'$ .

Cytosine and uracil also show a linear increase in  $1/\phi_f$  with excitation energy (Figure 1.10). However at  $3.90 \mu\text{m}^{-1}$  for uracil and  $3.85 \mu\text{m}^{-1}$  for cytosine the plots abruptly change to linear segments with negative slopes. It is difficult to accommodate such a change in  $1/\phi_f$  at higher energies within a simple vibronic manifold. If a different electronic state were populated at these energies a different slope of  $1/\phi_f$  vs. energy might be expected, particularly if the new state had different emission characteristics. Further work on the emission of the pyrimidines at various excitation energies is necessary before any definite conclusions can be made.

It is interesting to note that the photochemical corollary to this fluorescence behavior has been reported. As excitation occurs into higher vibronic levels  $v'$ ,  $\phi_{ic, v'}$  decreases and  $\sum \phi_{d, v'}$  increases; these deactivation processes include intersystem crossing, and it has recently been shown for aqueous solutions of thymine (Fisher and Johns, 1970) orotic acid (Whillans and Johns, 1969) and uracil (Brown and Johns, 1968) that chemical effects attribute to intersystem crossing occur with increasing efficiency as the excitation energy is increased above the  $0-0'$

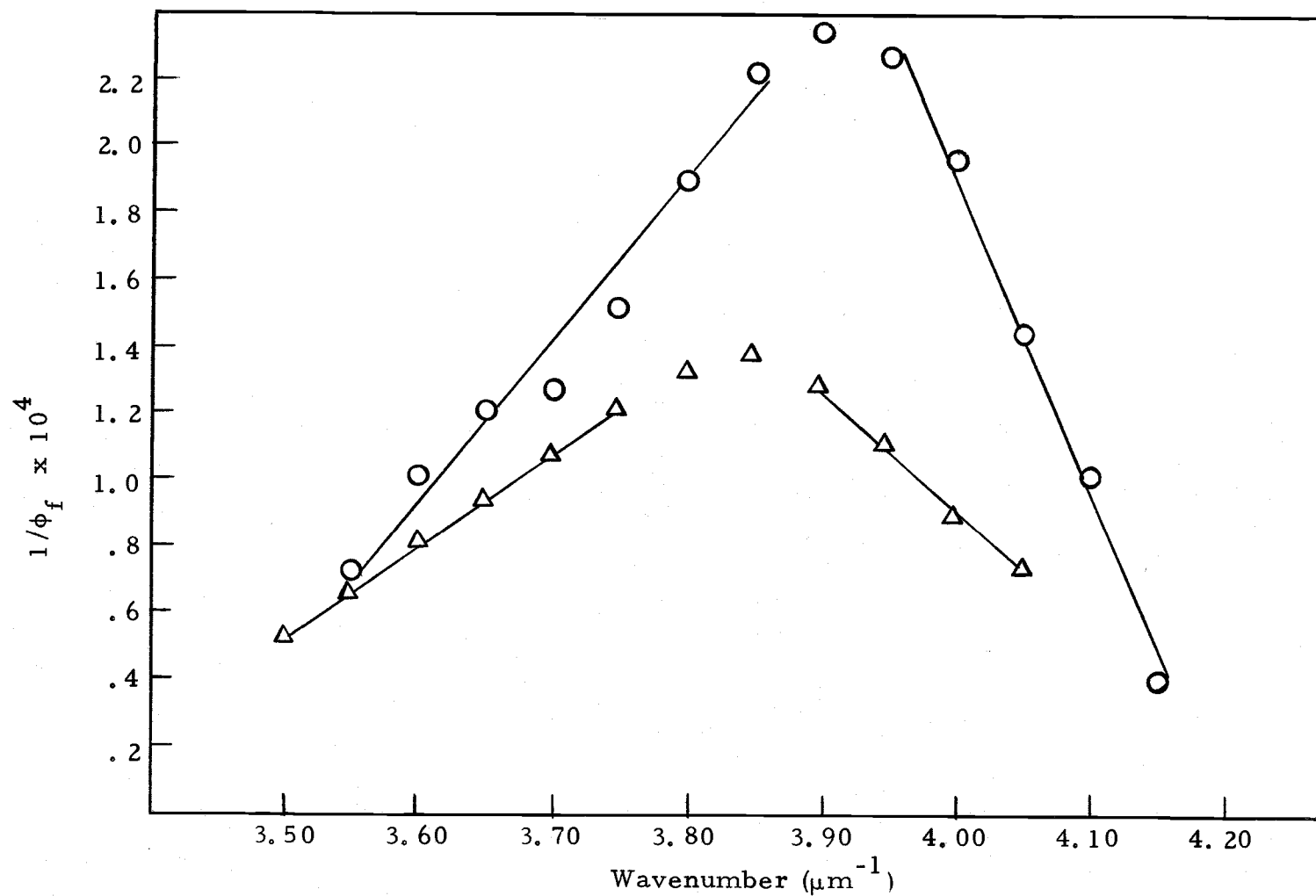


Figure 1.10.  $1/\phi_f$  vs. excitation energy; O—O uracil,  $\Delta$ — $\Delta$  cytosine.

level. Specifically for thymine the intersystem crossing yield has been found to increase about five-fold across the first absorption band.

Although it has not been possible as yet to evaluate the empirical relationship in Figure 1.9b in terms of the rate constants implicit in Equation (1.2), it is possible to analyze the rates for processes occurring from the lowest vibrational level of the first excited state (level 0'). The quantum yield for intersystem crossing from the 0' level can be expressed in terms of rate constants,

$$\phi_{isc, 0'} = \frac{k_{isc, 0'}}{k_f + k_{ic, 0'} + k_{isc, 0'} + \Sigma k_{d, 0'}} \quad (1.3)$$

where  $k_{isc}$  was formerly included in  $\Sigma k_{d, v'}$ . Then from the definition of  $\phi_{f, 0'}$  (Equation 1.13),

$$\frac{\phi_{isc, 0'}}{\phi_{f, 0'}} = \frac{k_{isc, 0'}}{k_f} \quad (1.4)$$

Since

$$k_f = 1/\tau_0, \quad (1.5)$$

$$k_{isc, 0'} = \frac{\phi_{isc, 0'}}{\tau_0 \phi_{f, 0'}} \quad (1.5)$$

From assignment of the 0-0' energies (Table 1.2), it is possible to determine  $\phi_{isc, 0'}$  (Fisher and Johns, 1970; Lamola and Eisinger, 1969; Brown and Johns, 1968) and  $\phi_{f, 0'}$  for thymine and uracil.  $\tau_0$ 's were evaluated (Table 1.2) according to Equation (1.11).

For emission spectra not showing a mirror image relationship with absorption, radiative lifetimes calculated as in Table 1.2 have been shown to be generally low (Strickler and Berg, 1962; Ware and Baldwin, 1963) and therefore  $k_{isc, 0'}$ 's calculated from this  $\tau_0$  are probably an upper limit.

Further development is possible using measured photochemical yields. If the major term in  $\Sigma k_{d, 0'}$  is photochemical reaction  $k_c$  then

$$\phi_{c, 0'} = \frac{k_{c, 0'}}{k_f + k_{ic, 0'} + k_{isc, 0'} + k_{c, 0'}} \quad (1.6)$$

and in a manner analogous to Equation (1.5) it can be shown,

$$k_{c, 0'} = \frac{\phi_{c, 0'}}{\tau_0 \phi_{f, 0'}} \quad (1.7)$$

Since the value of  $\phi_c = 2 \times 10^{-3}$  for uracil does not vary with excitation energy (Brown and Johns, 1968), it may be assumed that  $\phi_c$  for thymine is also constant and the value of  $\phi_c = 4.3 \times 10^{-4}$  (Daniels and Grimison, 1963) excited at  $3.94 \mu\text{m}^{-1}$  can be used for  $\phi_{c, 0'}$ . Substituting calculated values of  $k_{isc, 0'}$  and  $k_{c, 0'}$  into Equation (1.6),  $k_{ic, 0'}$  can be evaluated, and these rate constants for thymine and uracil are shown in Table 1.4.

Although these values cannot be used to interpret excited state processes occurring above the  $0'$  level, in the specific case of low

Table 1.4. Calculated rate constants for some excited state processes.

	Rate ( $\text{sec}^{-1} \times 10^{-9}$ )		
	$k_{c, o'}$	$k_{isc, o'}$	$k_{ic, o'}$
Thymine	0.20	2.0	460
Uracil	0.34	1.5	728

energy excitation ( $3.45 - 3.60 \mu\text{m}^{-1}$ ) they should be of use in predicting and accounting for excited state processes. The roughly equal  $k_{isc, 0'}$ 's for thymine and uracil imply about equal efficiencies in populating the triplet state from the  $0'$  level. Fisher and Johns (1970), however, quote preliminary triplet-triplet absorption data which implies uracil populates its triplet  $\sim 20$  times more efficiently than thymine. Intersystem crossing from  $v'$  levels must be much more facile in uracil compared to thymine to account for this observation.

### Purines

Polarized fluorescence excitation and absorption studies on neutral adenine at low temperature have detected two  $\pi-\pi^*$  transitions within the low energy absorption envelope (Callis et al., 1964; Stewart and Davidson, 1963), but the lowest energy band appears to be coincident with the absorption maximum ( $3.83 \mu\text{m}^{-1}$ ). CD measurements and solvent shifts have detected a weak  $n-\pi^*$  band at  $\sim 3.45 \mu\text{m}^{-1}$  (Miles et al., 1969), but this is at markedly lower energy than our excitation maxima ( $3.70 \mu\text{m}^{-1}$ ).

The nature of the absorption shoulder at  $\sim 3.74 \mu\text{m}^{-1}$  (poorly resolved by the Turner 210 in Figure 1.3) is still questionable. It has been assigned to both a  $n-\pi^*$  transition (Hoffman and Ladik, 1964) and also to vibrational structure in the main band (Kleinwachter et al.,

1966; Miles et al., 1969), and polarization studies confirm the latter assignment (Callis et al., 1964). If one concurs with these most recent conclusions, there appears to be no electronic mechanism in adenine to account for the shift in fluorescence excitation.

Eastman (1969) estimates a fluorescence excitation spectrum for adenine at low temperature (assuming a mirror image relationship for emission and absorption as in Equation (I.12)). The red edge of this calculated excitation spectrum is shifted  $\sim 1.0 \mu\text{m}^{-1}$  to lower energies than the absorption spectrum. The fluorescence species ( $\sim 6\%$  of total adenine) is assigned a minor tautomeric structure. Our excitation spectrum agrees in its shift relative to absorption with Eastman's calculated spectrum and fluorescence may therefore arise from this tautomer. Eastman's estimate of the tautomeric concentration is not a reliable guide for aqueous systems since it was determined in isobutanol at  $170^\circ \text{K}$ .

A plot of  $1/\phi_f$  vs. excitation energy for adenine (Figure 1.11) shows two linear segments with different slopes. At low energies  $1/\phi_f$  increases, as with thymine (Figure 1.9b), but at  $\bar{\nu} > 3.95 \mu\text{m}^{-1}$   $1/\phi_f$  is linear with a negative slope. This behavior may imply the presence of two different emitting species. To confirm this, the fluorescence emission spectrum was recorded with excitation at  $4.17 \mu\text{m}^{-1}$  (Figure 1.1). A new emission maximum is observed, red-shifted  $1.4 \mu\text{m}^{-1}$  to  $2.99 \mu\text{m}^{-1}$  which substantiates this preliminary

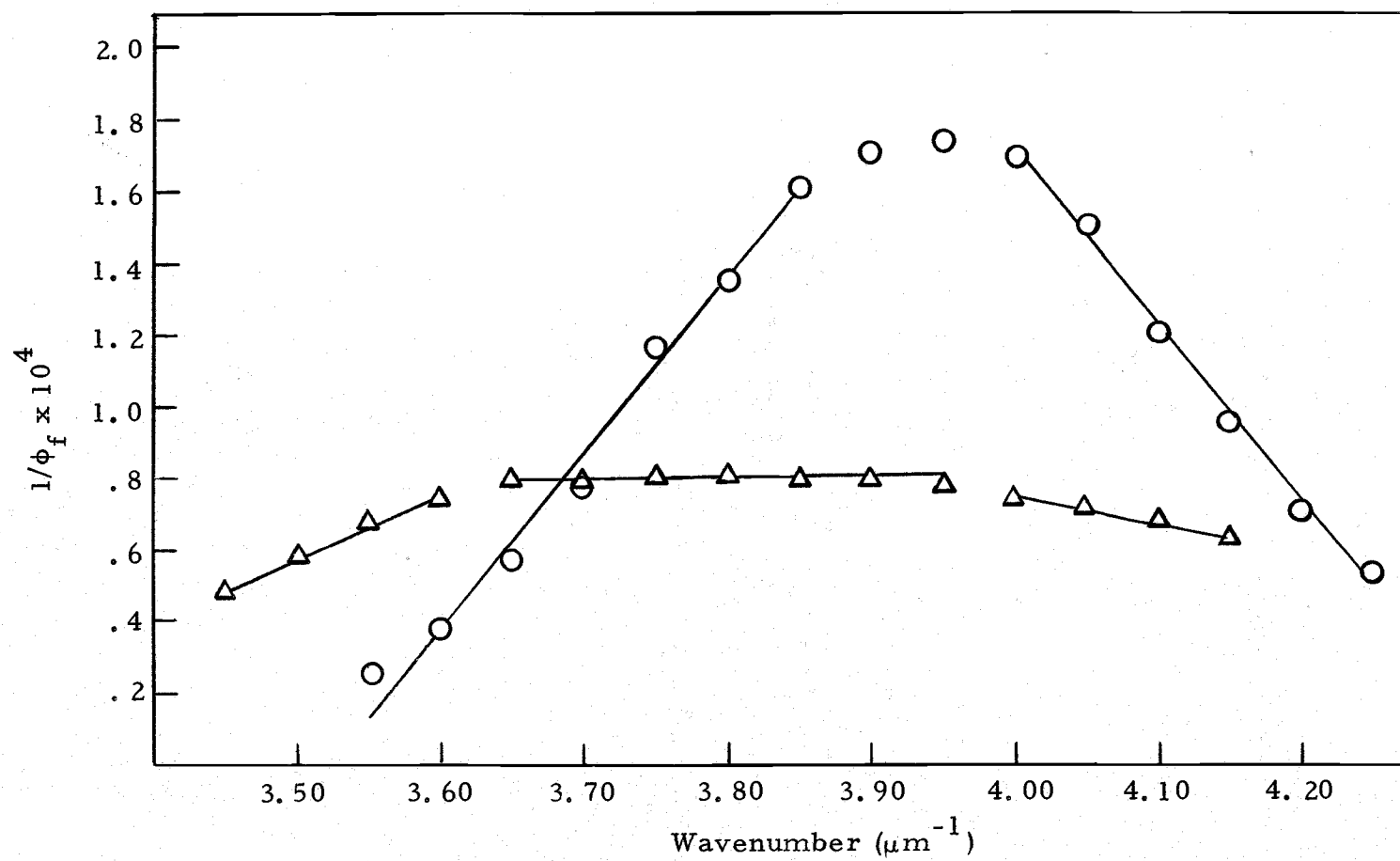


Figure 1.11.  $1/\phi_f$  vs. excitation energy; O—O adenine,  $\Delta$ — $\Delta$  guanine.

observation. Additional data is necessary before any firm conclusion can be made concerning a second emitting species.

Callis et al. (1964) noted a rather broad overlap of  $\pi-\pi^*$  states in neutral guanine at low temperature by polarization studies across the first absorption band. There does not appear to be sufficient overlap however to red-shift the low energy component the necessary  $0.08 \mu\text{m}^{-1}$  (see Figure 1.2) but the shift is in the proper direction. There are no previous comments on possible tautomers of neutral guanine, but guanine at pH 11 (Börreson, 1965) shows about a  $-0.10 \mu\text{m}^{-1}$  shift in excitation maximum compared to absorption.

In Figure 1.11 an inverse quantum yield vs. excitation energy plot for guanine shows three linear segments with much less difference in slopes than for the two linear portions of the adenine plot. Excitation at  $4.17 \mu\text{m}^{-1}$  also gives a new emission maximum red-shifted  $1.4 \mu\text{m}^{-1}$  to  $2.92 \mu\text{m}^{-1}$ .

Since all the bases exhibit similar linear segments with opposite slopes (except thymine which may require additional measurements at higher energies) a general property of the free bases may be that higher energy excitation within the first absorption envelope does not populate a higher vibronic state of the same transition, but populates a new electronic transition having different emission properties. CD measurements detect a  $\pi-\pi^*$  transition different from the lowest energy transition at  $\sim 4.17 \mu\text{m}^{-1}$  for uridine (Miles et al., 1967) and

for some adenine nucleoside derivatives (Miles et al., 1969) and confirm the existence of another transition at this energy.

### Quantum Yields and Lifetimes

The emission quantum yields (Table 1. 2) are sufficiently low to escape previous detection. At room temperature the purines fluoresce at least three times more intensely than pyrimidines, whereas at 77°K cytosine is reported (Longworth et al., 1966) as efficient as the purines, and thymine (Honnäs and Steen, 1970) has more than twice their yield. These changes in the relative order of emission yields as a function of temperature (e. g. from 77 to 300°K the guanine yield is reduced 200-fold, but the thymine yield is reduced over 2000-fold) emphasize the uncertainties in direct application of low temperature results to room temperature.

The low observed quantum yields imply correspondingly short singlet lifetimes,  $\sim 10^{-12}$  sec. This has been interpreted as making singlet energy transfer in DNA improbable (Eisinger et al., 1970). (The estimated transfer rate is  $10^{12}$  sec<sup>-1</sup> under the most favorable conditions (Gueron et al., 1967)). The possibility, however, of emission arising from a tautomer or excited state hidden in the first absorption band makes the true quantum yields and the oscillator strengths of the fluorescing species somewhat uncertain. Calculated singlet lifetimes are all  $\sim 10^{-12}$  or less (Table 1. 2, column (a)) if it

is assumed the entire low energy absorption band for each base is responsible for emission. If, however, the fluorescent oscillator is assumed to be the fluorescence excitation fitted to the low energy absorption band (which may give an estimate of that portion of the total absorption actually responsible for fluorescence (Eastman, 1969) all lifetimes are significantly increased (Table 1. 2, column (b)). Room temperature singlet lifetimes calculated directly from the quantum yield and absorption spectrum must therefore be considered a lower limit. In addition, the slightly broader emission spectra reported for all the bases at 300° K relative to 77° K may mean a different overlap integral for singlet transfer. The role of singlet energy transfer in DNA at room temperature must remain an open question.

The presence of oxygen in solution will often reduce the observed quantum yield (for example see Berlman, 1965, p. 35-37). The quantum yield in the absence of oxygen  $\phi_0$  can be related to the quantum yield in an air equilibrated system and the singlet lifetime by a Stern-Volmer type quenching formula (Berlman and Walter, 1962),

$$\frac{\phi_0}{\phi} = 1 + \tau_S k_q [O_2] \quad (1.8)$$

where  $k_q$  is the second order quenching rate. For known values of  $\frac{\phi}{\phi_0}$ ,  $\tau_S$ , and  $[O_2]$  in various solvents,  $k_q$  can be evaluated and is found to be a diffusion controlled process,  $\sim 10^{10} \text{ m}^{-1} \text{ sec}^{-1}$ . The

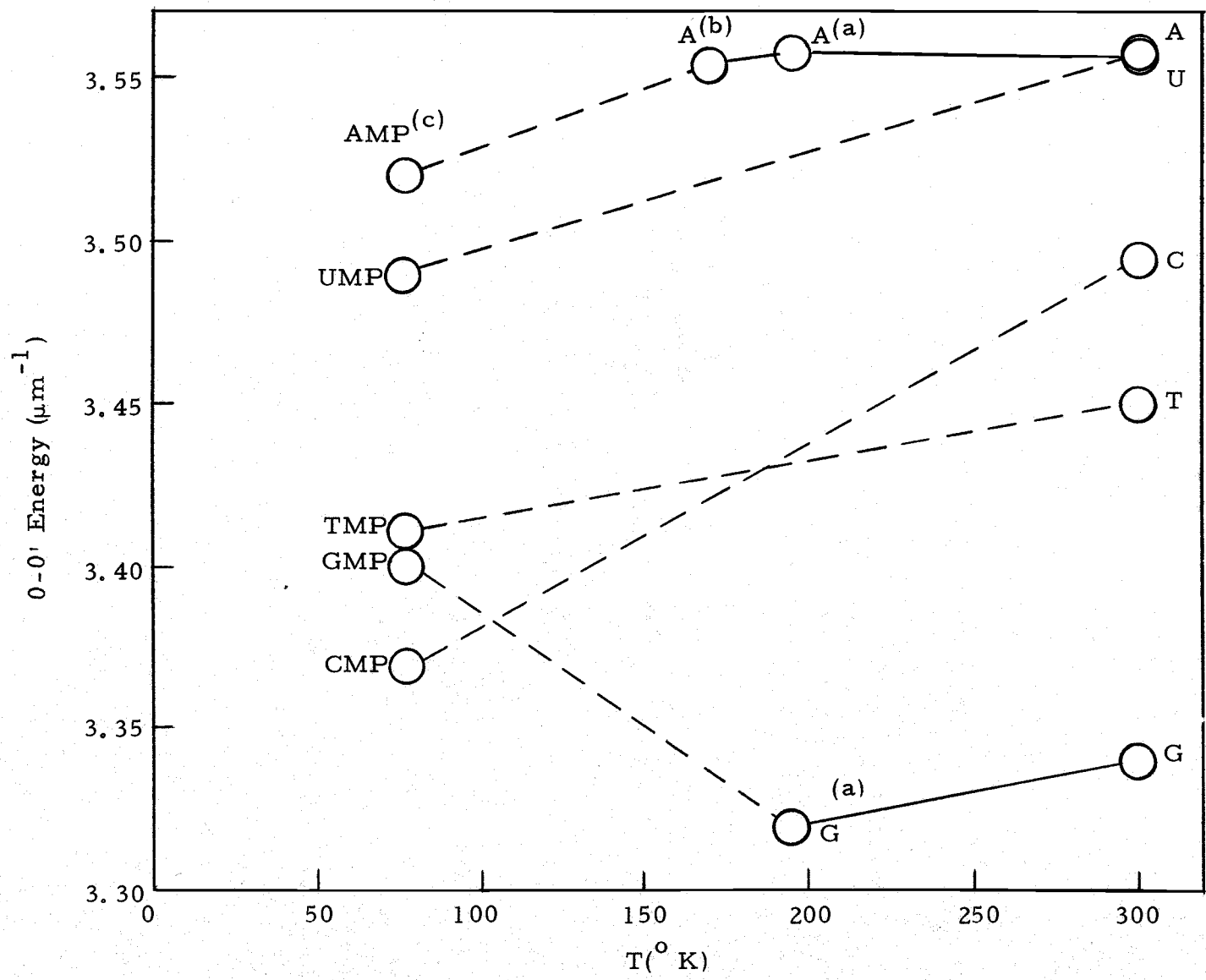
removal of  $O_2$  from thymine in aqueous solution does not, however, alter its quantum yield (within  $\pm 5\%$ ). This implies that either  $O_2$  does not quench the thymine singlet by collisions or that  $\tau_S < 10^{-8} \text{ sec}^{-1}$ . The calculated thymine  $\tau_S$  confirms the second implication but does not rule out the first.

### 0-0' Energies

The 0-0' energies (Table 1.3) are in the order adenine > uracil > cytosine > thymine > guanine. In Figure 1.12 these energies are compared with low temperature 0-0' energies for the nucleotides (Gueron et al., 1967) and for adenine and guanine (Callis et al., 1964; Eastman, 1969). Although different from the order for the nucleotides at  $77^\circ \text{K}$  (Gueron et al., 1967), particularly in the position of guanine, our values are very similar to those determined at intermediate temperatures of  $195^\circ \text{K}$  for adenine ( $3.56 \mu\text{m}^{-1}$ ) and guanine ( $3.32 \mu\text{m}^{-1}$ ). Although room temperature data on the nucleotides would be preferred for comparison, present results may mean that the relative excited state energies of the bases are sufficiently altered by temperature to affect the possibility of energy transfer.

In view of the significant differences in excited singlet properties between  $77^\circ \text{K}$  and  $300^\circ \text{K}$ , extrapolation from low temperature work to processes occurring in DNA under biological conditions may require careful re-evaluation. Extension of the present technique to

Figure 1.12. Comparison of the 0-0' energies for the purines and pyrimidines and their nucleotides as a function of temperature (solvent differences are ignored). (a) from the overlap of absorption and fluorescence emission spectra of Callis et al, (1964). (b) from the overlap of absorption and fluorescence emission spectra of Eastman (1969). (c) Tabulated data of Gueron et al, (1967).



investigate the fluorescent properties of the nucleotides, eximer formation in the dinucleotides, and the fluorescence behavior of DNA itself is now feasible and will no doubt be rewarding.

## II. SOLVENT EFFECTS ON THYMINE FLUORESCENCE

### Introduction

There have been very few attempts to experimentally determine the excited state electronic structure of the base components of DNA and RNA, primarily because the most directly useful property, that of fluorescence, has been heretofore undetected. Some information has been reported on the direction of the transition moments for 1-methylthymine and 9-methyladenine (Stewart and Davidson, 1963; Stewart and Jensen, 1964) and on the ground state dipole moments of adenine and 1,3-dimethyluracil (de Voe and Tinoco, 1962). The possibility of obtaining excited state dipole moments from studies of an electric field on the absorption spectrum has been shown (Labhart, 1967) and is currently in progress (Siebold and Labhart, 1970). The preponderance of information on the electronic structures of the constituents of DNA and RNA, particularly in the excited state, has resulted from theoretical calculations based on quantum mechanics (reviewed by Pullman, 1970), but application of this data to a biological situation should await experimental verification.

Because of the accessibility of room temperature fluorescence data for thymine in a neutral aqueous solution (see Section I), its apparent role as major center for energy localization in DNA, and the lack of previous data, it is desirable to ascertain additional excited

state properties of thymine from fluorescence data. The purpose of this section is therefore to determine the effect of various solvents on the fluorescence of thymine and to deduce information, where possible, on the structure and properties of the excited molecule from these effects.

### Materials and Methods

Thymine (Calbiochem, A grade) was dissolved in dimethylsulfoxide, p-dioxane, acetonitrile, methyl formate (all Matheson, Coleman, and Bell, spectroquality), D<sub>2</sub>O (E. Mark Co., spectroscopic grade, 99.75%), methanol (Baker and Adams, reagent grade), ethylene glycol (Fischer, reagent), and triply distilled water.

Emission spectra were determined on a Turner Model 210 with signal accumulation and corrections as described in Section I and Appendix I. Absorption spectra were taken on a Cary 15. Emission quantum yields were calculated relative to guanine at pH 10.9 (Section I) and are corrected for variations in solvent refractive index relative to water according to Equation (A.1.19).

### Results and Discussion

Different solvents can alter fluorescence data in two fundamental ways. They can change the shape and maxima of the emission (and absorption) spectra and/or they can alter the magnitude of the

fluorescence quantum yield. Although these effects may not always be treated independently, for convenience they will be treated separately here.

### Spectral Shifts and Shape

Theory. The effect of solvent environment on absorption and emission spectra, if treated rigorously, is a prohibitively complex problem for which a complete analysis is as yet unavailable. However the spectral shifts accompanying a change in solvent for a given solute offer a direct experimental approach to the study of molecular excited states and therefore several somewhat different approaches have been taken toward constructing a simplified theory of solvent effects (e. g. McRae 1957; Lippert, 1957). Critical reviews of these theories have appeared recently (Basu, 1964; Suppan, 1968) and only the main features and assumptions of the development are presented here.

The frequency shift in the absorption  $\Delta\bar{\nu}_a$  and emission  $\Delta\bar{\nu}_f$  spectra for a molecule in solution relative to the gas can be related to the classical Onsager (1936) reaction field by perturbation theory. This tie to classical theory is necessary to correlate macroscopic solvent properties to the quantum mechanical result for one solute molecule and a surrounding set of solvent molecules.

Assuming only dipole-dipole interaction and no specific interaction such as hydrogen bonding an expression for the solvent shift can be derived. Such a result is clearly deficient since it assumes no change in the reaction field upon excitation (i. e. the solvent does not have time to reorient during the excitation process, but the new excited state solute dipole will induce a different dipole in the solvent, and this dipole-induced dipole interaction will be a function of the solvent polarizability). Accordingly, Lippert (1957) assumes a two term expression for the absorption solvent shift, the first involving only the polarizability as manifested in the solvent index of refraction, and the second involving presumably only the dipole interaction,

$$\Delta \bar{\nu}_a = \frac{1}{hc} \frac{\mu_g^2 - \mu_e^2}{a^3} \left( \frac{n^2 - 1}{2n^2 + 1} \right) + \frac{2}{hc} \frac{\mu_g (\mu_g - \mu_e)}{a^3} (\Delta f) \quad (2.1)$$

and similarly for the fluorescence shift,

$$\Delta \bar{\nu}_f = \frac{1}{hc} \frac{\mu_g^2 - \mu_e^2}{a^3} \left( \frac{n^2 - 1}{2n^2 + 1} \right) + \frac{2}{hc} \frac{\mu_e (\mu_g - \mu_e)}{a^3} (\Delta f) \quad (2.2)$$

where

$$\Delta_f = \frac{\epsilon - 1}{2\epsilon + 1} - \frac{n^2 - 1}{2n^2 + 1}$$

$\mu_g$  and  $\mu_e$  = the ground and excited dipole moments

$a$  = solute cavity radius ~ molecular radius .

These expressions have been shown (Suppan, 1968) to give good agreement with the more rigorous inclusion of the polarizability (McRae, 1957) for solvents with  $n^2 = 2 \pm 0.2$ . In general, this theory appears usable only when there is a large range of dielectric constants (i. e.  $\Delta\epsilon > 20$ ) since there is little correlation within groups of solvents of similar polar properties (cf. Lippert, 1957).

By including the solvent polarizability in the Onsager reaction field, McRae (1957) more rigorously accounted for solute dipole-induced solvent dipole interactions in the excited state. Included in this development is a term for dispersive interactions (i. e. non-polar interactions) which has questionable reliability (Suppan, 1968) and is only a minor contribution to spectral shifts when the solvent possesses a permanent dipole. McRae's total equations are cumbersome and generally useful only for a series of solvents of nearly identical refractive indices (Baba et al., 1966).

In the present study, the selection of solvents was severely limited by the need for significant solvent light transmission at  $\sim 3.80 \mu\text{m}^{-1}$  ( $> 50\%$  T), the relative insolubility of thymine in many solvents, and the required lack of fluorescent impurities under these very sensitive conditions. It was therefore neither possible to use an extensive series of solvents with similar refractive indices nor to apply McRae's theory to observed spectral shifts. For these reasons the theory of Lippert has been employed. Some properties of the

solvents used are listed in Table 2.1.

From Equations (2.1) and (2.2)

$$\Delta\bar{\nu}_a - \Delta\bar{\nu}_f = \frac{2}{hc} \frac{(\mu_e - \mu_g)^2}{a^3} \Delta f \quad (2.3)$$

In practice, the absorption and fluorescence maxima are the only well defined spectral positions and hence  $\Delta\bar{\nu}_a$  and  $\Delta\bar{\nu}_f$  are usually calculated from differences in maxima. The theory was developed, however, for the 0-0' electronic transition and the general usefulness of Equation (2.3) is limited to cases where changes in maxima reflect changes in the 0-0' energy. For large solvent shifts ( $> 0.05 \mu\text{m}^{-1}$ ) the use of spectral maxima is a reasonable assumption (Suppan, 1968).

Since for any solvent  $\Delta\bar{\nu}_a$  and  $\Delta\bar{\nu}_f$  are the wavenumber differences between the respective gas phase maxima,

$$\Delta\bar{\nu}_a - \Delta\bar{\nu}_f = \bar{\nu}_{a, \max} - \bar{\nu}_{f, \max}$$

A plot then of  $(\bar{\nu}_{a, \max} - \bar{\nu}_{f, \max})$  against  $\Delta f$  should be linear with a

slope of  $\frac{2}{hc} \frac{(\mu_e - \mu_g)^2}{a^3}$ .

Excited State Dipole Moment. Fluorescence emission and absorption spectra were determined for thymine at 27° C in several protic solvents (Figure 2.1, spectra in water shown in Figure 1.5) and in several aprotic solvents (Figure 2.2). From these spectra the

Table 2.1. Properties of solvents. (a)

Solvent	Dielectric Constant $\epsilon$			Refractive Index $n$			Viscosity in centipoise (cp) $\eta$
H <sub>2</sub> O	77.6	(27)	b	1.332	(25)	c	0.851 (27) c
D <sub>2</sub> O	77.8	(27)	b	1.329	(25)	b	0.969 (30) f
Methanol	32.2	(27)	c	1.326	(25)	c	0.532 (27) c
EG:H <sub>2</sub> O	63.2	(27)	d	1.387	(27)	d	3.47 (27) d
Dimethylsulfoxide	47.8	(20)	e	1.476	(25)	c	1.98 (25) e
Acetonitrile	37.5	(25)	c	1.342	(25)	c	0.345 (25) c
Methyl Formate	8.5	(20)	c	1.358	(25)	c	-----
p-Dioxane	2.2	(25)	c	1.420	(25)	c	1.30 (25) c

(a) Temperature in parentheses

(b) Collie *et al* (1948)

(c) Chemical Rubber Company (1968) p. E-221 - E-222, F-34 - F-42, E-58

(d) Timmermans (1960)

(e) Crown Zellerbach Corporation (1967)

(f) Eisenberg and Kauzman (1969) p. 223

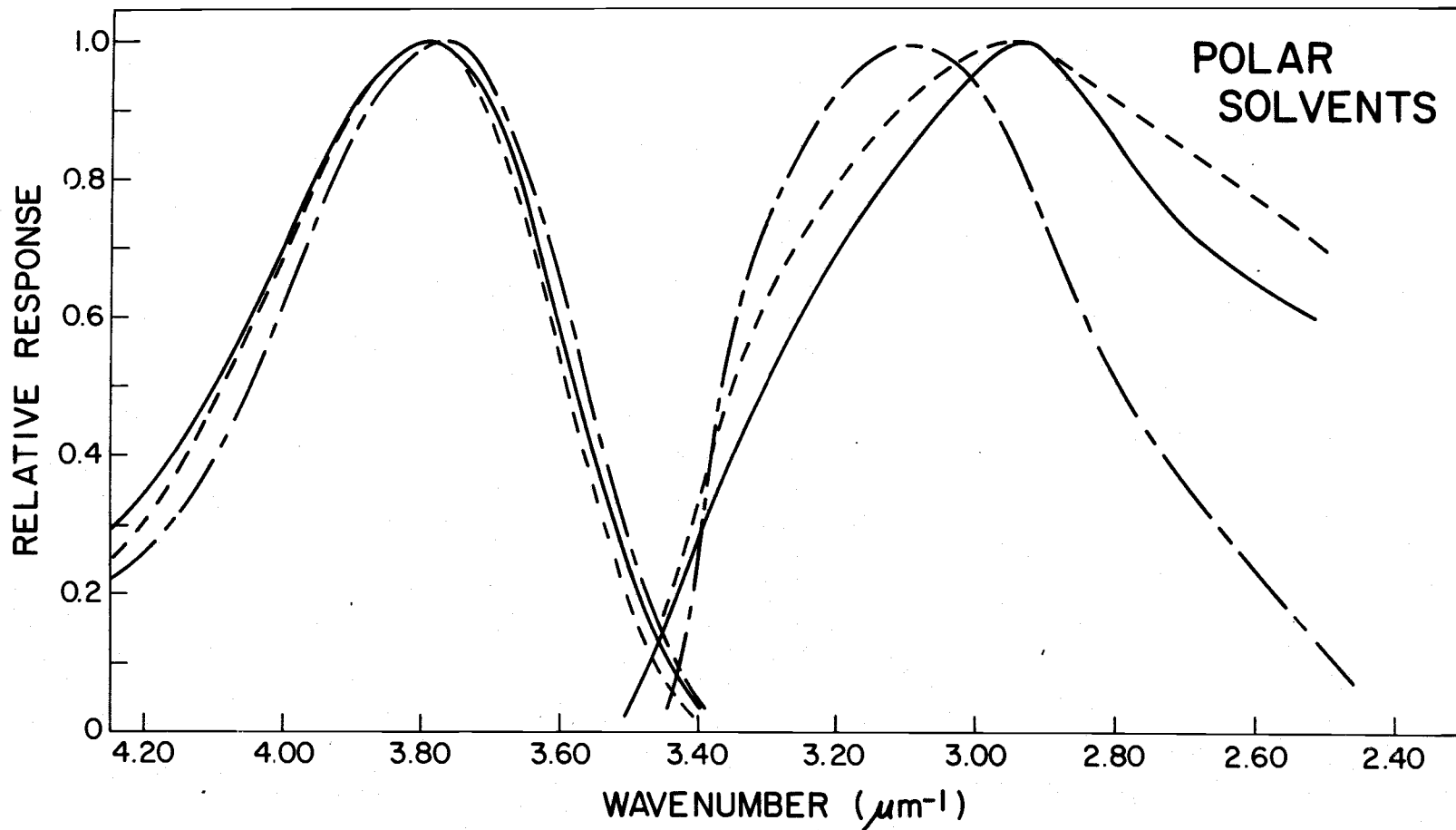


Figure 2.1. Absorption spectra (curves on the left) and fluorescence emission spectra (curves on the right) for thymine in hydrogen bonding solvents:  $\text{D}_2\text{O}$  (—), methanol (-----) and ethylene glycol:water 1:1 (— · — · — ·).<sup>2</sup>

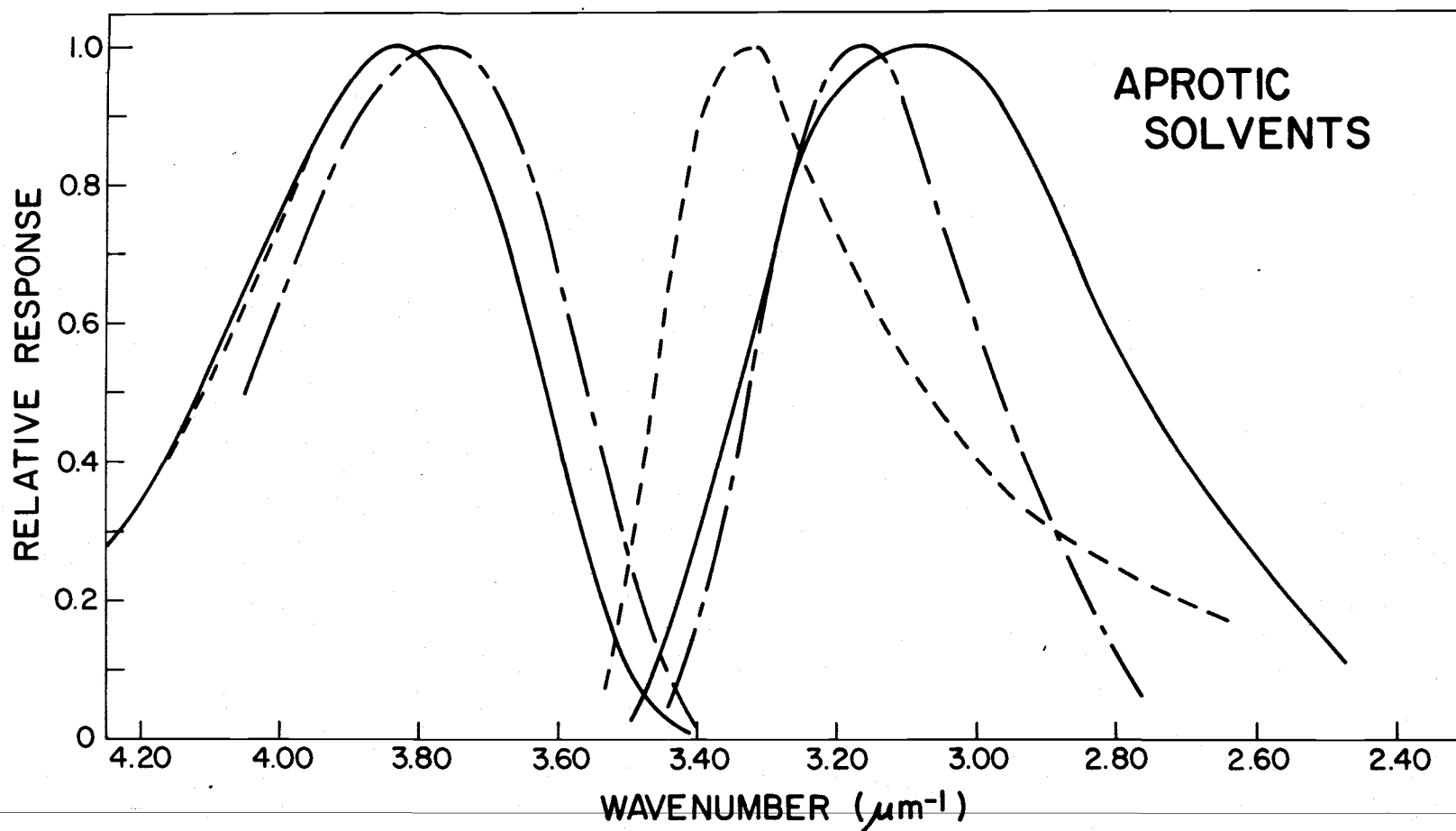


Figure 2. 2. Absorption spectra (curves on the left) and fluorescence emission spectra (curves on the right) for thymine in non-hydrogen-bonding solvents: acetonitrile (————), dimethylsulfoxide (-----) and dioxane (— · — · —).

frequencies of absorption and fluorescence maxima are tabulated in Table 2. 2 (data is also included for thymine in methyl formate for which only maxima were determined). Spectral shifts relative to water and emission quantum yields are also listed. Approximate 0-0' energies calculated from absorption and emission averages (Table 2. 2(b)) demonstrate the general reasonableness of using shifts in maxima for the calculations.

In Figure 2. 3 a plot of Equation (2. 3) is shown for the aprotic solvents. The straight line was fit to the data points by the method of least squares and has a slope of  $0.285 \mu\text{m}^{-1}$  with a 77% correlation. Assuming the cavity radius for thymine is similar to that for pyrimidine =  $3.9 \text{ \AA}$  (Baba et al., 1966)

$$\mu_e = \mu_g \pm 4.1D. \quad (2.4)$$

To decide whether  $\mu_e$  is larger or smaller than  $\mu_g$  requires an examination of the magnitude of the spectral shifts for absorption relative to fluorescence. It has been generally observed that for  $\pi-\pi^*$  transitions involving a polar aromatic molecule,  $\mu_e > \mu_g$  (some evidence for this conclusion is reviewed by Wehry, 1967). Since an increase in solvent polarity will produce relatively greater stabilization in the excited state relative to the ground state, solvents with larger dielectric constants will red-shift the fluorescence spectrum to a greater degree than the absorption. On the other hand, promotion of

Table 2. 2. Absorption and fluorescence properties of  $5 \times 10^{-5}$  M thymine in various solvents.

Solvent	Absorption		Fluorescence		0-0' Energy		$\phi_f$ $\times 10^4$
	$\bar{\nu}_{a, \max}$ ( $\mu\text{m}^{-1}$ )	$\Delta\bar{\nu}_{a, \max}$ ( $\text{cm}^{-1}$ ) <sup>(a)</sup>	$\bar{\nu}_{f, \max}$ ( $\mu\text{m}^{-1}$ )	$\Delta\bar{\nu}_{f, \max}$ ( $\text{cm}^{-1}$ ) <sup>(a)</sup>	(b) ( $\mu\text{m}^{-1}$ )	(c) ( $\mu\text{m}^{-1}$ )	
H <sub>2</sub> O	3.79	----	2.96	----	3.37	3.45	1.04
D <sub>2</sub> O	3.80	+100	2.94	-200	3.37	3.43	1.48
Methanol	3.80	+100	2.96	0	3.37	3.46	1.41
EG:H <sub>2</sub> O	3.78	-100	3.10	+1400	3.44	3.43	2.53
Acetonitrile	3.83	+400	3.09	+1300	3.46	3.48	1.12
Dimethylsulfoxide	3.76	-300	3.16	+2000	3.46	3.43	2.47
Methyl Formate	3.84	+500	3.32	+3600	----	----	----
Dioxane	3.84	+500	3.32	+3600	3.58	3.52	1.57

(a) relative to water

(b) from the average of  $\bar{\nu}_{a, \max}$  and  $\bar{\nu}_{f, \max}$

(c) from the absorption-emission overlap

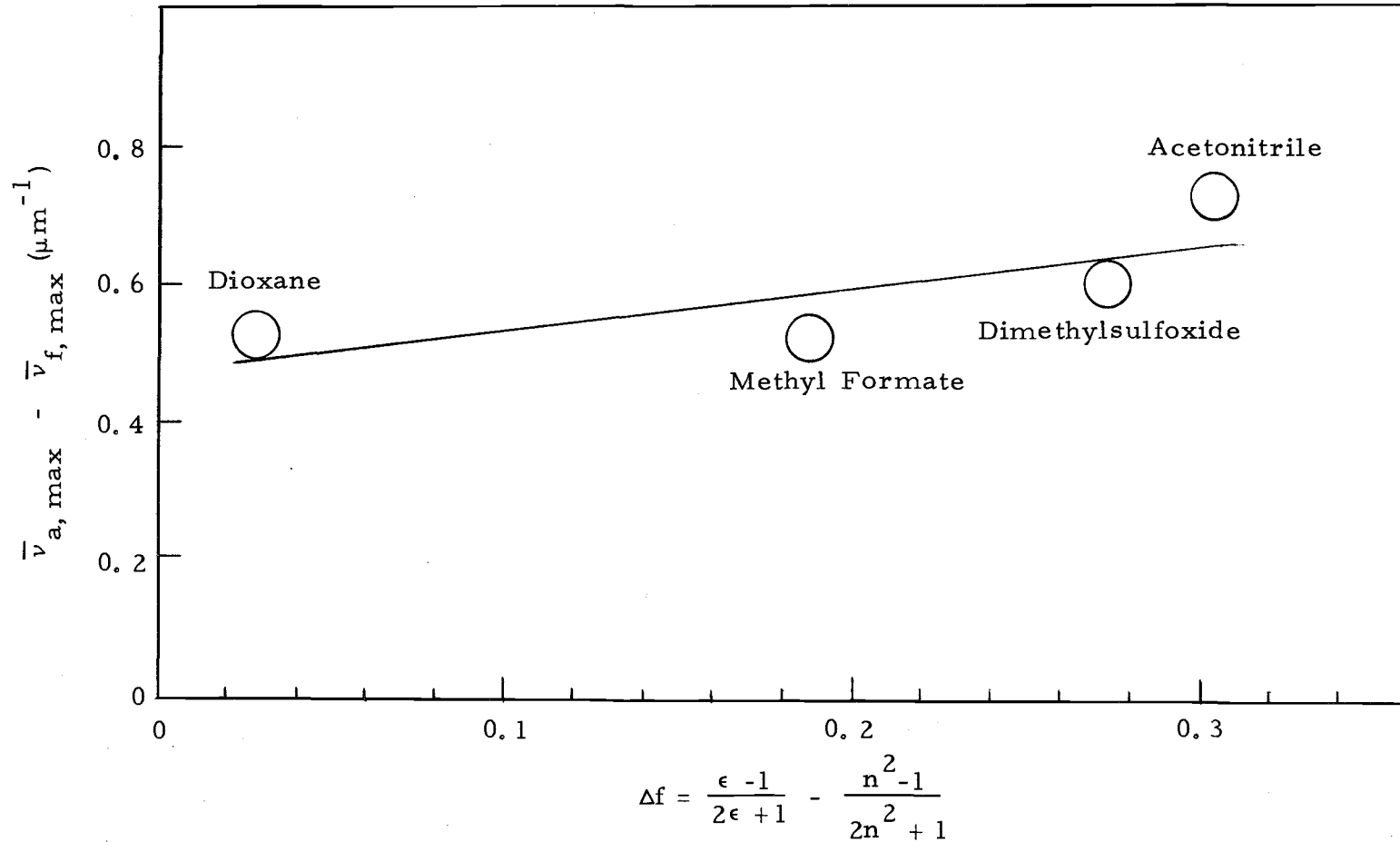


Figure 2.3. Plot of the difference between absorption and fluorescence spectral maxima of thymine vs.  $\Delta f$ .

a non-bonded electron to a  $\pi$ -orbital,  $n-\pi^*$  transitions, generally reduces  $\mu_e$  relative to  $\mu_g$  because n-orbitals are localized on one atom of a molecule while  $\pi$ -orbitals are usually delocalized over a large portion of an aromatic ring. Increasing the solvent dielectric constant will generally blue-shift the absorption with only small effects on the fluorescence spectrum specific for the solute.

From a consideration of Table 2.2 it is apparent that increasing solvent polarity has markedly red-shifted the fluorescence spectra and affected the absorption very little; this implies a  $\pi-\pi^*$  transition with  $\mu_e > \mu_g$  for neutral thymine. The lack of any consistent trend in either  $\bar{\nu}_{a, \max}$  or  $\bar{\nu}_{f, \max}$  implies the transition is not of a  $n-\pi^*$  nature (see Introduction).

Assuming the ground state dipole moment of thymine is equal to that for 1,3-dimethylthymine =  $3.9 \pm 0.4$  D (de Voe and Tinoco, 1962) which is the only data available for a structure similar to thymine, from Equation (2.4)  $\mu_e$  for thymine is calculated as

$$\mu_e = 8.0 \pm 2.2 \text{ D} .$$

This value is not quite in agreement within experimental error with a value for thymine of  $\mu_e = 5.25 \pm 0.4$  D (Seibold and Labhart, 1970). It is significant however that both values are greater than the ground state dipole moment and of roughly the same size considering the large changes ( $> 20$  D) often calculated (e. g. Lippert, 1957).

Other Causes for Spectral Shifts. Most previous studies on spectral shifts as a function of solvent used molecules with large fluorescence quantum yields ( $\sim 0.1$ ) and this normally implied singlet lifetimes  $\sim 10^{-9}$  sec. From a consideration of Figure I. 2, a molecule with a  $\tau_S = 10^{-9}$  sec. will probably emit from a totally relaxed excited state. Thymine, however, has a calculated lifetime  $\sim 10^{-12}$  sec. and it seems most likely that solvent reorientation cannot occur during this time, and therefore probably emits from a Franck-Condon excited state B (Figure I. 2, vibrationally relaxed but having a ground state solvent atmosphere.). In fact  $\tau_S$  is so short that emission may even come from a vibrationally excited Franck-Condon state, but this does not seem likely because the small absorption-emission overlap and the normal Stokes' shift of the emission spectrum to lower energies implies some relaxation has occurred. This conclusion implies vibrational relaxation must be faster than  $\sim 10^{-12}$  sec.

If emission does occur from a vibrationally relaxed excited state before solvent relaxation can occur, it is difficult to see how dipole-dipole effects could cause spectral shifts. Stabilization of an excited state dipole by electrostatic interaction requires a change in solvent orientation relative to its ground state configuration. Water has one of the shortest dielectric relaxation lifetimes ( $\sim 7.7 \times 10^{-12}$  sec., Collie et al., 1948) and even this may not be short enough to compete effectively with a singlet lifetime of  $10^{-12}$  sec. Solute dipole

induced solvent dipole interactions can be very fast ( $\sim 10^{-13}$  -  $10^{-14}$  sec., not much slower than the absorption process) and could account for spectral shifts in aprotic solvents. The theories of Lippert (1957) and McRae (1957) account for both dipole-dipole and dipole-induced dipole effects and they seem to work with moderate success on thymine. Perhaps for molecules possessing very short lifetimes as thymine, better results could be obtained by placing more emphasis on the induced solvent dipole interaction (measured by the solvent polarizability and manifested in the index of refraction terms).

For the protic solvents the specific short range effects of hydrogen bonding generally dominate dipole and induced dipole interactions (Suppan, 1968). It is conceivable that the  $\pi-\pi^*$  transition of thymine could cause relatively stronger hydrogen bonding in the excited state. An excited  $\pi$ -electron system will have more negative charge on the extremities of an aromatic ring and thus for thymine stronger hydrogen bonds are likely between its carbonyl oxygens and the solvent hydrogens. This type of stabilization may account for the general redshift of the fluorescence maxima in protic solvents (the top three solvents in Table 2. 2) compared to the non-hydrogen bonding solvents (the effect of ethylene glycol may be dominated by its relatively high viscosity and is discussed later.). An opposite destabilizing effect has been observed for  $n-\pi^*$  transitions for carbonyl compounds in hydrogen bonding solvents due to a weakening or cleavage of the

hydrogen bond in the excited state.

### Quantum Yields

Isotope Effect. A deuterium isotope solvent effect on  $\phi_f$  has been reported for several molecules containing ionizable protons (Stryer, 1966) and was interpreted on the basis of its effect on excited state proton transfer reactions. In the case of thymine  $\phi_{f, D_2O} / \phi_{f, H_2O} = 1.42$ , but it is not possible for proton reactions to occur in the excited state responsible for fluorescence (see Section III). Another, more general explanation of this effect emphasizes that solute-solvent interactions are at least partially responsible for the rate of internal conversions, the major process competing with fluorescence, and this conclusion therefore classes the deuterium isotope effect as a general solvent effect on the fluorescence quantum yield (Förster and Rokos, 1967). The effect of  $D_2O$  on  $\phi_f$  for thymine might therefore be due to less efficient internal conversion processes in  $D_2O$  while  $k_f$  (a solute property more independent of solvent environment) remains unchanged.

If this latter interpretation is at least qualitatively accurate, the  $D_2O$  effect on  $\phi_f$  should also appear on  $\phi_{isc}$  since the rate constants for both fluorescence and intersystem crossing are of the same order of magnitude for thymine (see Table 1.4) and are several orders of magnitude less than  $k_{ic}$ .

For dilute solutions of uracil it has been shown (Brown and Johns, 1968) from oxygen quenching and kinetic studies that water addition across the 5-6 double bond occurs from the excited singlet state and that dimerization occurs from the triplet. It is reasonable to assume therefore that deuterium isotope effects on the dimer yield will monitor qualitatively the effects on  $k_{isc}$ . Applying the quantum yields for the photolysis of 1-methyluracil (Shugar and Wierzchowski, 1958) to the proportions of UMP<sup>4</sup> hydrate and dimer detected by Nnadi and Wang (1969) in H<sub>2</sub>O and D<sub>2</sub>O, the yields shown in Table 2.3 can be calculated. The decrease in hydrate yield in D<sub>2</sub>O relative to H<sub>2</sub>O is attributed to the slower rate of D-O bond breakage during the water addition process (Shugar and Wierzchowski, 1958). Since dimer formation does not require such solvent bond cleavage, another type of explanation is required to explain the increase in  $\phi_{Dimer}$  for both UMP and thymine in D<sub>2</sub>O. The same proposal that explained the increased  $\phi_f$  in D<sub>2</sub>O can also be used to explain the increased  $\phi_{Dimer}$  since a decreased  $k_{ic}$  in D<sub>2</sub>O also implies a larger  $\phi_{isc}$  and therefore more triplet state from which dimers may form.

In a quantitative sense there is at least approximate agreement; for UMP,  $\phi_{Dimer}$  increases by a factor of 1.3 in D<sub>2</sub>O and for

---

<sup>4</sup> 1-methyluracil is a suitable structural model for UMP and in view of the lack of reported quantum yields in D<sub>2</sub>O it seems reasonable to assume  $\phi$  of 1-methyluracil photolysis in D<sub>2</sub>O equals that for UMP.

Table 2.3. Comparison of the quantum yield for hydrate and dimer formation in  $\text{H}_2\text{O}$  and  $\text{D}_2\text{O}$  for UMP and thymine (see the text for the method of calculation).

Compound	Solvent	$\times 10^3$	
		$\phi$ Hydrate	$\phi$ Dimer
UMP	$\text{H}_2\text{O}$	11.9	0.6
UMP	$\text{D}_2\text{O}$	4.9	0.8
Thymine	$\text{H}_2\text{O}$	----	0.4
Thymine	$\text{D}_2\text{O}$	----	0.9

thymine,  $\phi_{\text{Dimer}}$  increases by a factor of 2.2 while  $\phi_f$  increases by a factor of 1.4 in  $\text{D}_2\text{O}$ . It appears therefore that for at least  $\text{D}_2\text{O}$  the mechanism for the increases in  $\phi_{\text{Dimer}}$  and  $\phi_f$  involves a decrease in  $k_{\text{ic}}$ . An interesting note is that the dielectric relaxation time of  $\text{D}_2\text{O}$  is about 20% slower than water (Collie et al., 1948). This could account for a factor of 1.2-1.3 increase in  $\phi_{\text{Dimer}}$  and  $\phi_f$  if  $k_f$  and  $k_{\text{isc}}$  are unchanged in  $\text{D}_2\text{O}$  and if internal conversions are related to dipole interactions and solvent reorientation in the excited state. It would be interesting to analyze  $\phi_{\text{Dimer}}$  for thymine in other solvents and compare them to the observed change in  $\phi_f$  to see if the proposed mechanism for the effect of  $\text{D}_2\text{O}$  is a general solvent effect on  $k_{\text{ic}}$ .

Hydrogen Bonding. Thymine has a singlet lifetime in  $\text{H}_2\text{O}$ ,  $\text{D}_2\text{O}$  and methanol of  $\sim 10^{-12}$  sec. and it is quite possible that the dielectric relaxation of even water is too slow to effect  $\phi_f$  and hence the analysis of the isotope solvent effect above may not be correct. Since internal conversion processes may often be the major factor causing a variation in  $\phi_f$ , a mechanism is required which will alter internal conversion processes within  $\sim 10^{-12}$  sec. Vibrational energy transfer through a hydrogen bond could occur as fast as the vibrational period ( $\sim 10^{-13}$  sec.). Vibrational energy transfer could occur on about the same time scale as vibrational periods ( $\sim 10^{-13}$  sec.) and this may account for the changes in  $\phi_f$  from  $\text{H}_2\text{O}$  to  $\text{D}_2\text{O}$  and

methanol. Stronger hydrogen bonds would more effectively couple the thymine molecule to the solvent and therefore increase the efficiency of vibrational relaxation. This hypothesis is affirmed by experiment since the strongest bonding solvent,  $H_2O$ , has the lowest  $\phi_f$ , with the weaker bonding solvents,  $D_2O$  and methanol, having higher and roughly equal  $\phi_f$ 's. It is interesting to note that this type of hydrogen bonding interaction may also be present in the adenine-thymine base pairs of DNA and may account for a major proportion of internal conversions in double stranded polynucleotides.

Viscosity. Some aspects of the data in Table 2. 2 can be most easily explained if  $\tau_S$  is  $> 10^{-12}$  sec. An example is the apparent effect of viscosity on the spectral shift in ethylene glycol and on the magnitude of the quantum yields in the aprotic solvents. All the strongly hydrogen bonding, protic solvents ( $H_2O$ ,  $D_2O$ , Methanol and EG: $H_2O$ ) have almost identical absorptions and fluorescence maxima, except for the ethylene glycol mixture whose  $\bar{\nu}_{f,max}$  is blue shifted  $\sim 1400$   $cm^{-1}$ . No trend in dielectric constant is apparent, but while  $H_2O$ ,  $D_2O$  and methanol all have a viscosity less than 1.0 cp.,  $\eta$  for the ethylene glycol mixture is ca. 3.47 cp. In addition,  $\phi_f$  is markedly higher in ethylene glycol than in the other three hydrogen-bonding solvents. An explanation of the fluorescence blue-shift is that an excited thymine molecule in a vibrationally relaxed Franck-Condon excited state B (see Figure I. 2) sees relatively slow solvent relaxation ( if

$\tau_S > 10^{-11}$  sec.) and emits from a higher energy state to states having more closely ground state solvent environments compared to molecules in a less viscous mechanism. Increasing  $\phi_f$  as a function of increasing viscosity has been discussed previously (see Introduction) and may also account for the order of quantum yields dimethylsulf-oxide > dioxane > acetonitrile. It is not possible to judge at this time whether another explanation of these trends if necessary or whether  $\tau_S$  is  $> 10^{-12}$  sec. Care must be taken in interpreting processes occurring on a molecular level in terms of a macroscopic property such as viscosity and therefore the foregoing discussion of possible viscosity effects may not be valid.

Concluding Comments. A good portion of the discussions in this section has been qualitative and possibly even vague. No excuse is needed for this except to point out that studies on excited states with lifetimes as short as that calculated for thymine forces any discussion of the excited state processes into a realm in which there is no experimental evidence.

In summary the relative energy of absorption and fluorescence transitions for thymine in the various solvents can be schematically drawn as in Figure 2.4. Relative to the gas phase transitions, in hydrogen bonding solvents the excited state is more stabilized than the ground state due to stronger hydrogen bonding in the excited state. Absorption is therefore of lower energy than in the gas and of

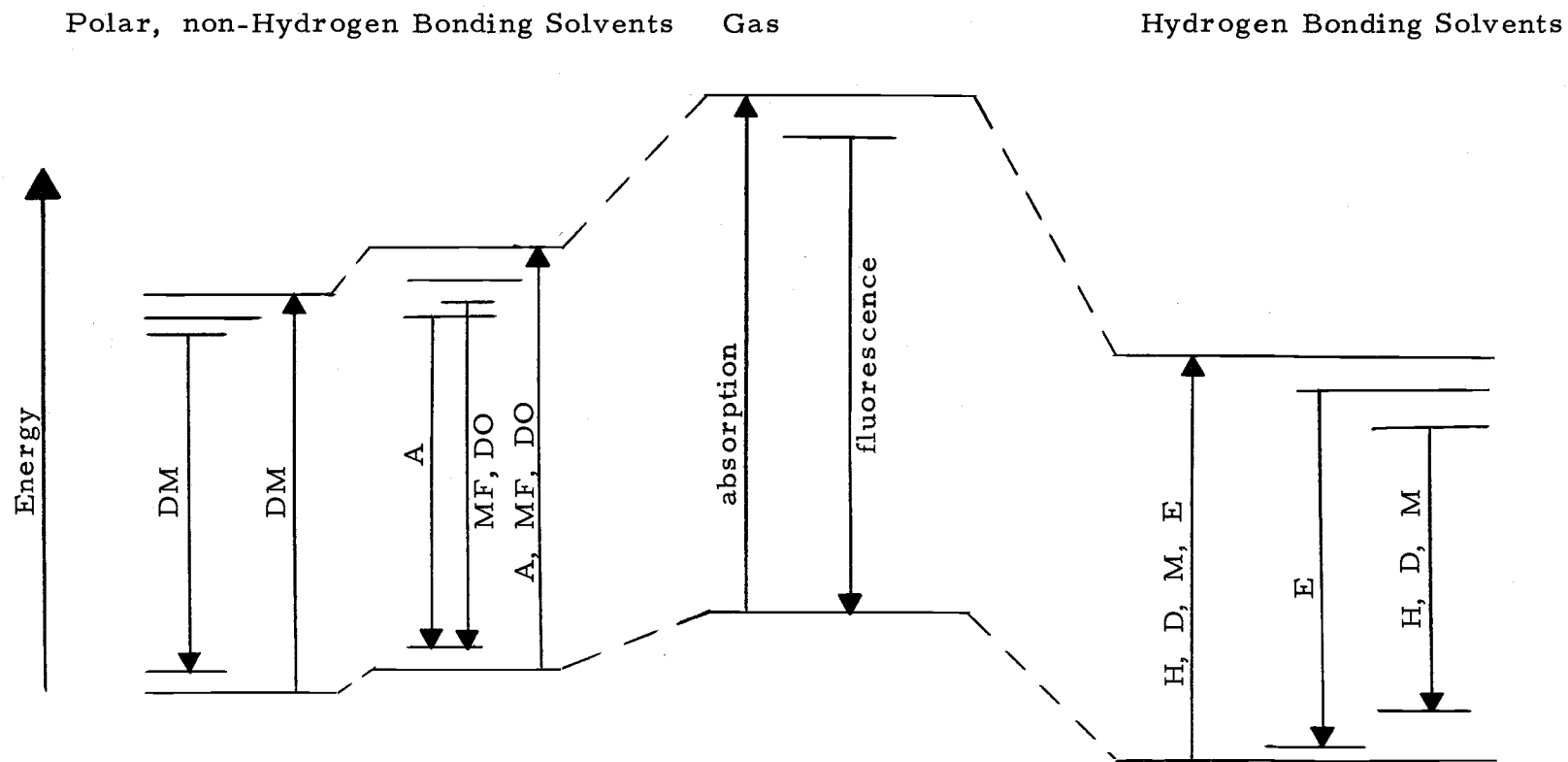


Figure 2.4. Schematic diagram of the effect of various solvents on the absorption and fluorescence energy at thymine. DM = dimethylsulfoxide, A = acetonitrile, DO = p-dioxane, MF = methyl formate, H = water, D = D<sub>2</sub>O, M = methanol, and E = ethyleneglycol:H<sub>2</sub>O 1:1.

approximately equal energies in any hydrogen bonding solvent. In all four solvents vibrational relaxation occurs to Franck-Condon excited state B (FCB) but solvent reorientation for the more viscous ethylene glycol mixture is slow and hence its fluorescence maximum is higher than for  $H_2O$ ,  $D_2O$  and methanol. For the polar, aprotic solvents larger stabilization again occurs in the excited state relative to the ground state because  $\mu_e > \mu_g$ , but it is not as large a stabilization as a specific interaction such as hydrogen bonding. Hence acetonitrile methyl formate and dioxane have roughly equal  $\bar{\nu}_{a, \max}$  all larger than for the protic solvents. Dimethylsulfoxide must have an additional specific interaction with thymine which further stabilizes the ground state and accounts for its low  $\bar{\nu}_{a, \max}$ . For all these solvents relaxation then occurs to the FCB state. Additional stabilization depends on the dipole strength of the solvent and hence  $\bar{\nu}_{f, \max}$  for methyl formate and dioxane are equal and higher than that for acetonitrile. Dipole interactions then place  $\bar{\nu}_{f, \max}$  for dimethylsulfoxide at an intermediate value.

### III. pH EFFECTS ON THYMINE FLUORESCENCE AT 300° K

#### Introduction

In its ground electronic state thymine at pH 12 has been shown (Wierzchowski et al., 1965) to exist in tautomeric equilibrium between two singly ionized structures, 1 HT<sup>-</sup> and 3 HT<sup>-</sup> (See Figure 3.1 for nomenclature and structures).

Since alkaline thymine was the only naturally occurring pyrimidine to fluoresce at room temperature (Udenfriend and Zaltzman, 1962) it has been the subject of several studies (Kleinwachter et al., 1966; Longworth et al., 1966). Fluorescence has been shown to originate only from the 3 HT<sup>-</sup> (Gill, 1968; Wierzchowski and Berens, 1969) at pH 12, where the ground state is monoionic. In all cases, however, data has been reported only at pH 11 or 12 with no attempt to ascertain the effect of changing pH on fluorescence properties.

Interest in alkaline thymine concerning its biological importance has been the subject of some controversy. At 77° K, TMP at pH 12 was shown to populate the triplet level and have e. s. r. properties similar to those in DNA (Shulman and Rahn, 1966). Subsequently, acetone sensitization of the neutral TMP triplet showed its e. s. r. properties to be even more similar to DNA (Lamola et al., 1967) and a thermodynamic argument was presented against proton transfer

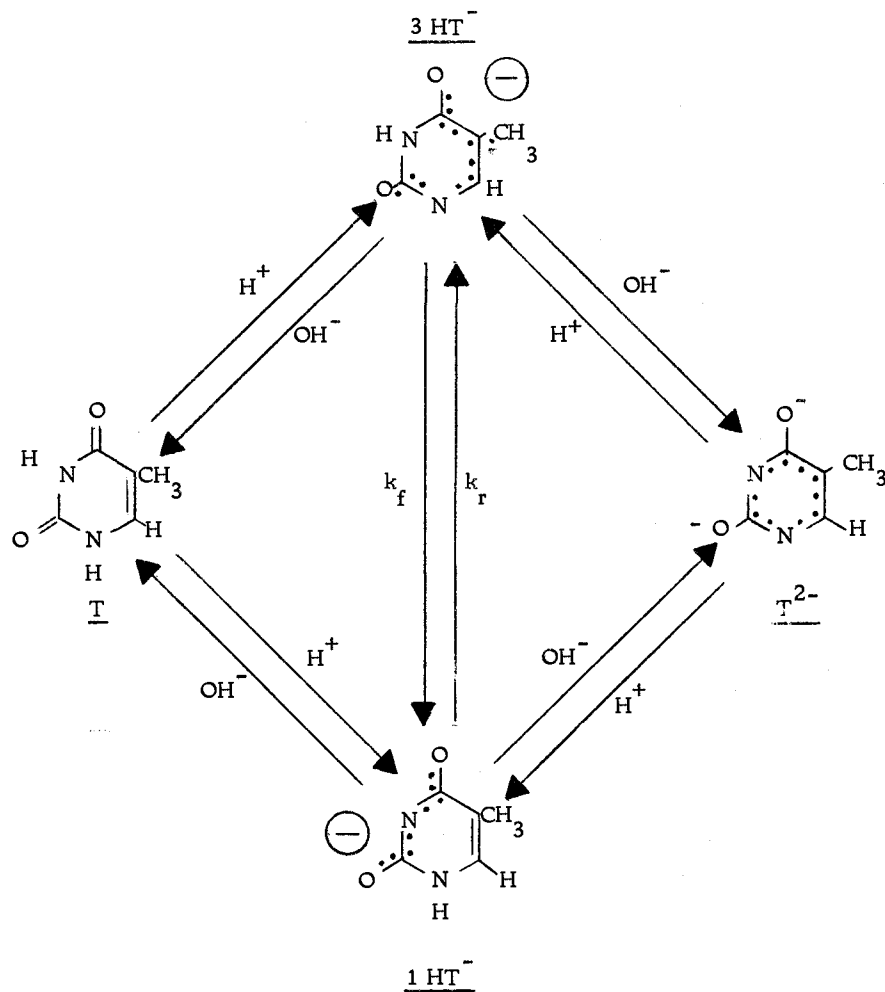


Figure 3.1. Nomenclature of the neutral and ionized forms of thymine from neutral pH to 10 M NaOH.  $k_f/k_r = K$ , the tautomeric equilibrium constant between  $1HT^-$  and  $3HT^-$ .

between adenine and thymine pairs in DNA (which would be necessary to produce an ionized thymine in DNA) because the transfer would require 6.5 Kcal as calculated from ground state and estimated excited state  $pK$ 's of thymine and adenine. Recently Taylor *et al.*, (1969) have shown the occurrence of a photo-induced two proton tautomerization between two hydrogen-bonded 7-azaindole molecules and they suggested that this process may be of importance in DNA since a two proton exchange between adenine-thymine pairs does not have a large thermodynamic barrier. This suggested process has been questioned by Eisinger *et al.*, (1970) but no evidence was given against it. The role of singly ionized thymine in the excited state behavior of DNA is still somewhat uncertain. Alkaline thymine is of additional interest since it photolyzes at room temperature much more rapidly than neutral thymine and appears to form several dimers of as yet uncertain structure (Hauswirth and Daniels, 1970b).

In view of these observations it seems desirable to extend the fluorescence studies on alkaline thymine to lower  $pH$ 's where the first ionization occurs, and to higher  $pH$ 's where  $T^{-2}$  is produced, with the aim of better understanding the emitting states of thymine and detecting possible protic reactions of the excited states.

## Materials and Methods

Thymine was purchased from three sources: California Biochemical Company (A grade), Sigma Chemical Company ( $\Sigma$  grade), and Mann Research Laboratories (M. A. grade). All were found to be chromatographically homogeneous and their absorption spectra agreed with published specifications (see Section I). NaOH was obtained from Harleco Company (fluorometric grade) as a 10 Molar aqueous solution. Its absorption spectrum (10 M, 1 cm path length) had a smooth tail in the  $4.55 - 4.45 \mu\text{m}^{-1}$  region (absorbance  $< 0.1$ ) indicating a minimum of heavy metal impurities. The sodium borate buffer (0.025 M) (Baker and Adamson, reagent grade) was adjusted to the proper pH's with additions of either HCl or NaOH.

Absorption spectra were recorded on a Cary 15 spectrophotometer. Corrected fluorescence emission and excitation spectra were taken on a Turner Model 210 spectrofluorimeter as were absorption spectra used for comparison with fluorescence excitation spectra. The emission polarization was measured on an instrument built by Evett and Isenberg (1968); its construction and operation are described therein.

## Results

The absorption, fluorescence emission and excitation spectra,

and emission polarization for alkaline thymine at 300° K are compared in Figures 3.2 - 3.4 for three representative pH's. In the case of  $10^{-2}$  M NaOH our excitation spectra agree with those of Gill (1968) and Berens and Wierzchowski (1969) also taken at 300° K, (Figure 3.2; also see Appendix I, Table A.1.5). The fluorescence quantum yield (excited at  $3.43 \mu\text{m}^{-1}$ ) for thymine at pH 12 was calculated to be  $1.7 \times 10^{-3}$ . This value compares well with a previous report (Gill, 1968,  $\phi_f = 1.6 \times 10^{-3}$ ).

Curves showing the concentration of absorbing species as a function of pH (Figure 3.5) were calculated from absorption spectra (Figures 3.6 and 3.7) taken at the indicated pH's. To evaluate component concentrations at an intermediate pH knowledge of extinction coefficient curves for each component is required. Extinction coefficients for neutral thymine ( $\epsilon_{\nu}^{(T)}$ ) were calculated directly from a neutral absorption spectrum and for the dianion of thymine ( $\epsilon_{\nu}^{(2)}$ ) from a spectrum in 10 M NaOH, assuming only dianion at this pH (This assumption is consistent with the data in Figure 3.5 and with an earlier estimate of thymine's second pK at >13.5 (Shugar and Fox, 1952)).  $1 \text{ HT}^-$  and  $3 \text{ HT}^-$  extinction coefficients ( $\epsilon_{\nu}^{(1)}$  and  $\epsilon_{\nu}^{(3)}$ ) were calculated assuming:

- a. The relative absorption spectrum of  $3 \text{ HT}^-$  is equivalent to the fluorescence excitation spectrum at pH 12. (Probably reasonable in view of assignment of the  $3 \text{ HT}^-$  tautomer as

Figure 3. 2. Fluorescence excitation and emission spectra and absorption spectrum of  $5 \times 10^{-5}$  M thymine in 0.01 M NaOH.

- Absorption spectrum (taken on a Turner Model 210 with a 150 Å bandwidth).
- - - - - ■ Fluorescence excitation spectrum (emission at  $2.65 \mu\text{m}^{-1}$  with a 250 Å bandwidth and 150 Å excitation bandwidth).
- - - - - ● Fluorescence emission spectra (excitation at  $3.42 \mu\text{m}^{-1}$  with 150 Å bandwidth and 100 Å emission bandwidth).
- Excitation data of Berens and Wierzchowski (1969)
- △ Excitation data of Gill (1968)
- △ - - - - △ Emission spectrum of Gill (1968)
- ▲ ——— ▲ Emission Polarization

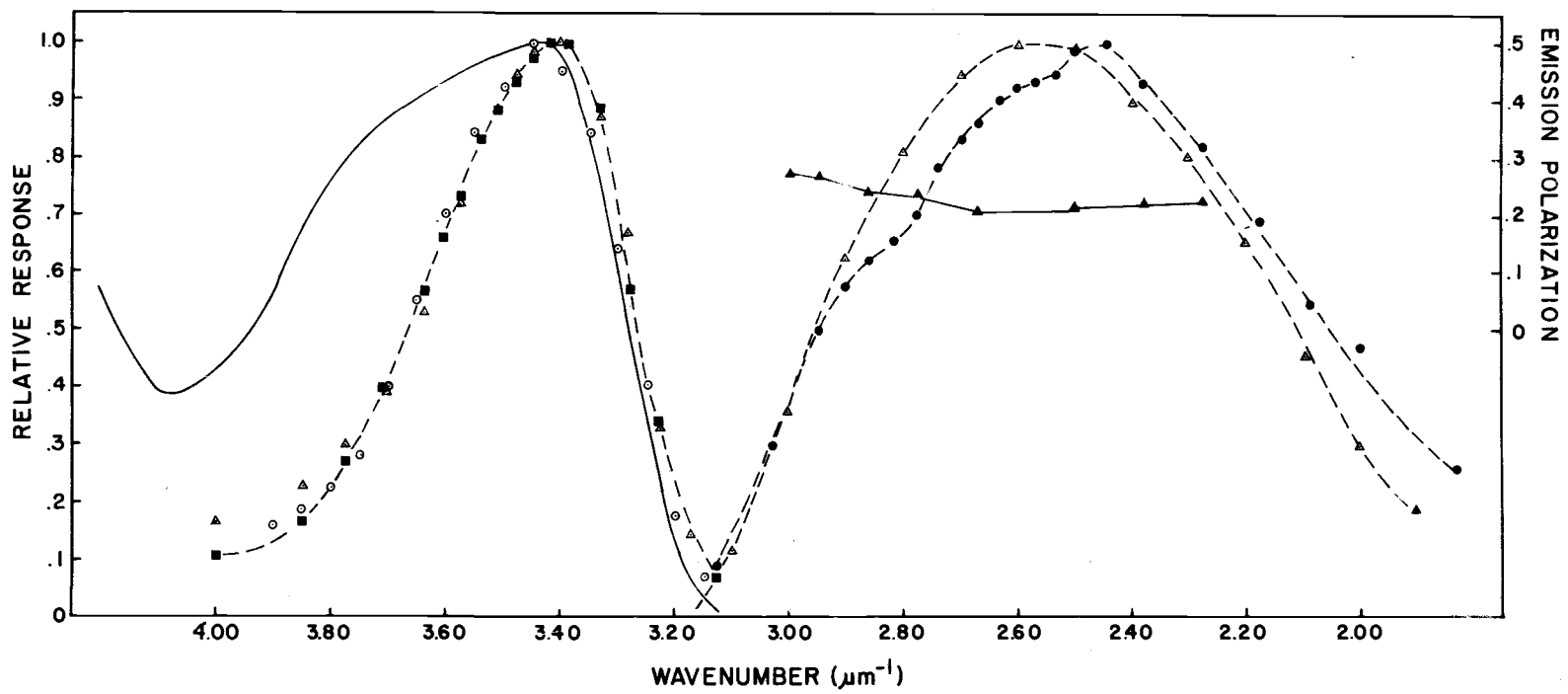
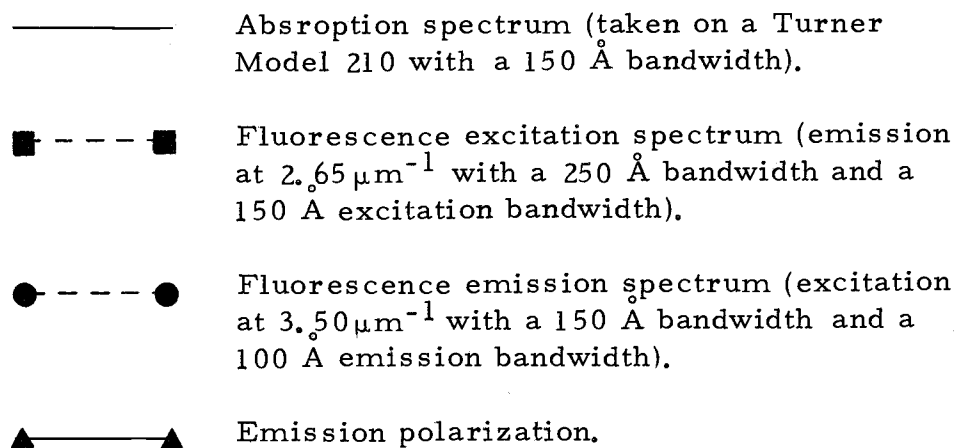


Figure 3.3. Fluorescence excitation and emission spectra and absorption spectrum of  $5 \times 10^{-5}$  M thymine in 1 M NaOH.



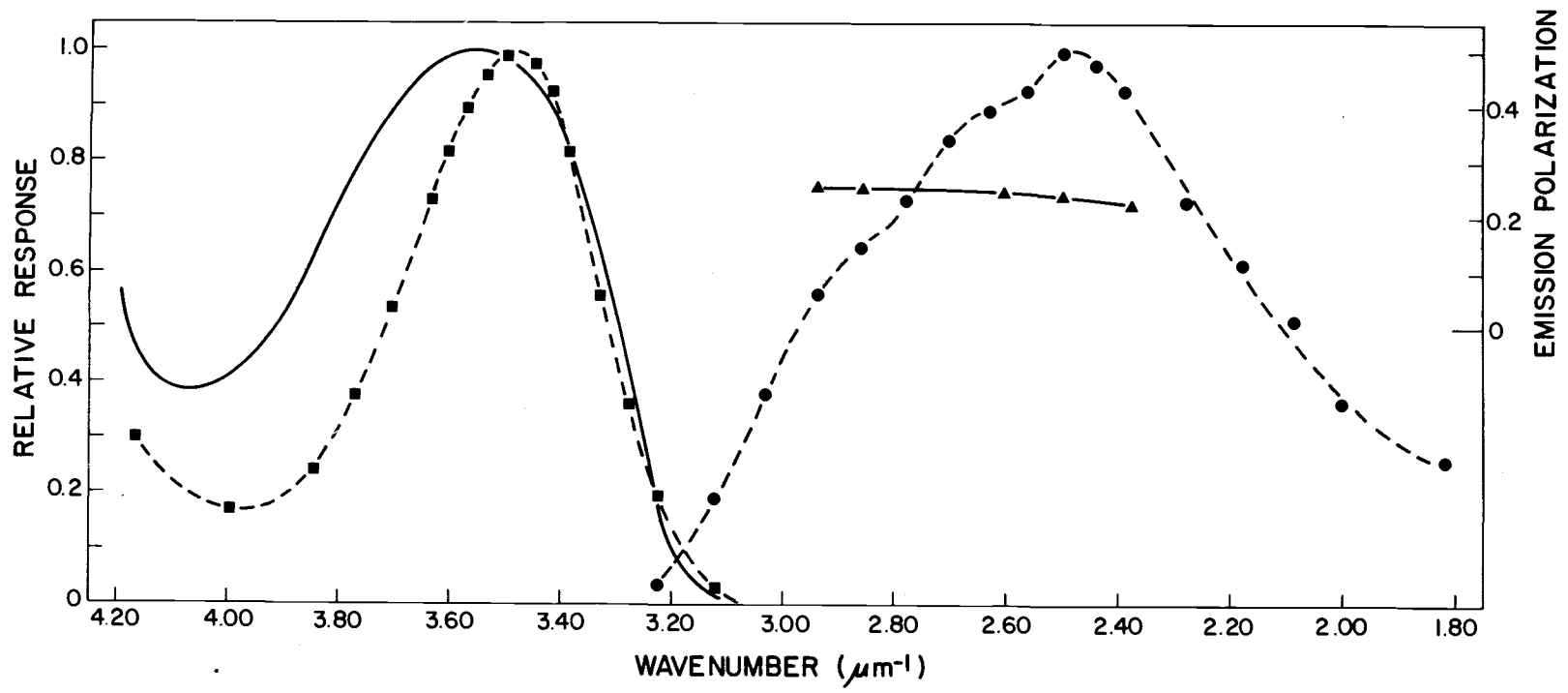
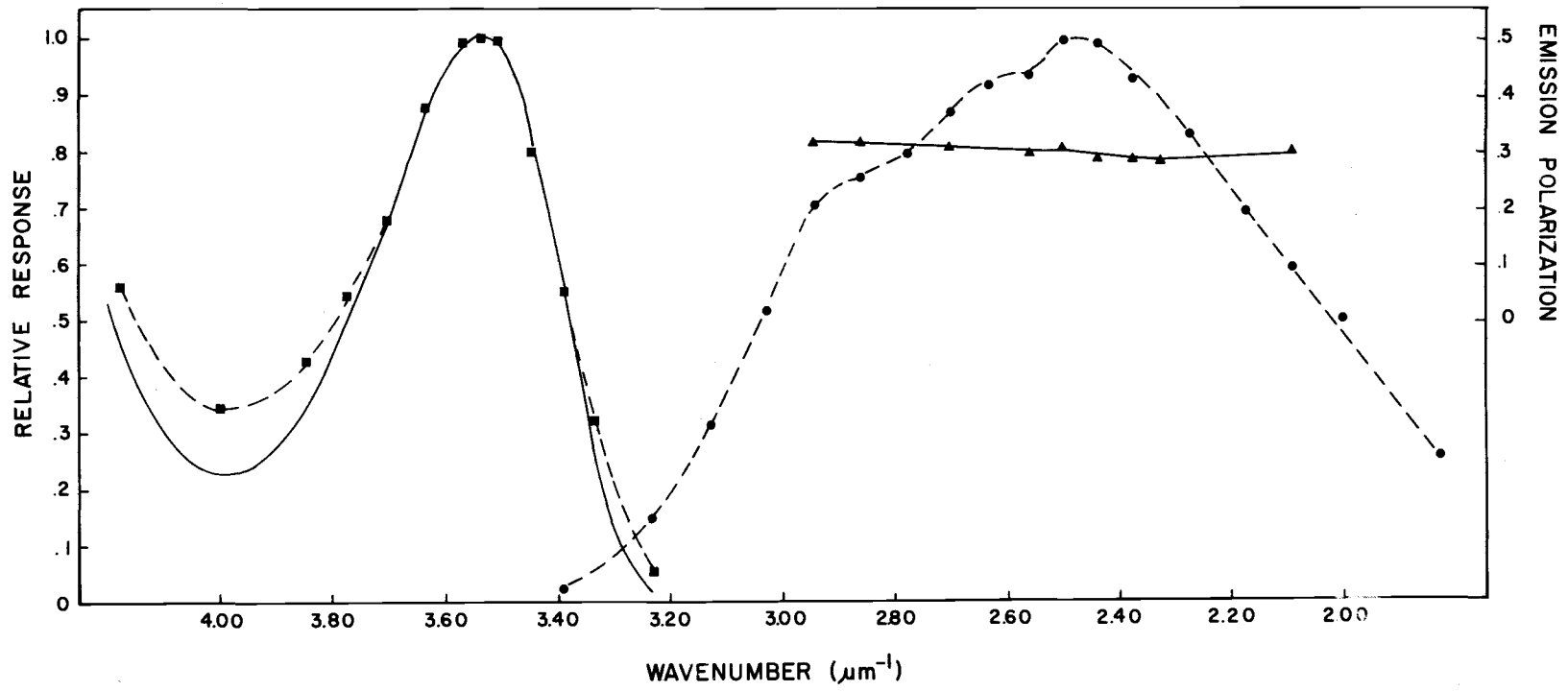


Figure 3.4. Fluorescence excitation and emission spectra and absorption spectrum of  $5 \times 10^{-5}$  M thymine in 10 M NaOH.

- Absorption spectrum (taken on a Turner Model 210 with a 150 Å bandwidth).
- - - - - ■ Fluorescence excitation spectrum (emission  $2.65 \mu\text{m}^{-1}$  with a 250 Å bandwidth and a 150 Å excitation bandwidth).
- - - - - ● Fluorescence emission spectrum (excitation at  $3.53 \mu\text{m}^{-1}$  with a 150 Å bandwidth and a 100 Å emission bandwidth).
- ▲ ——— ▲ Emission polarization.



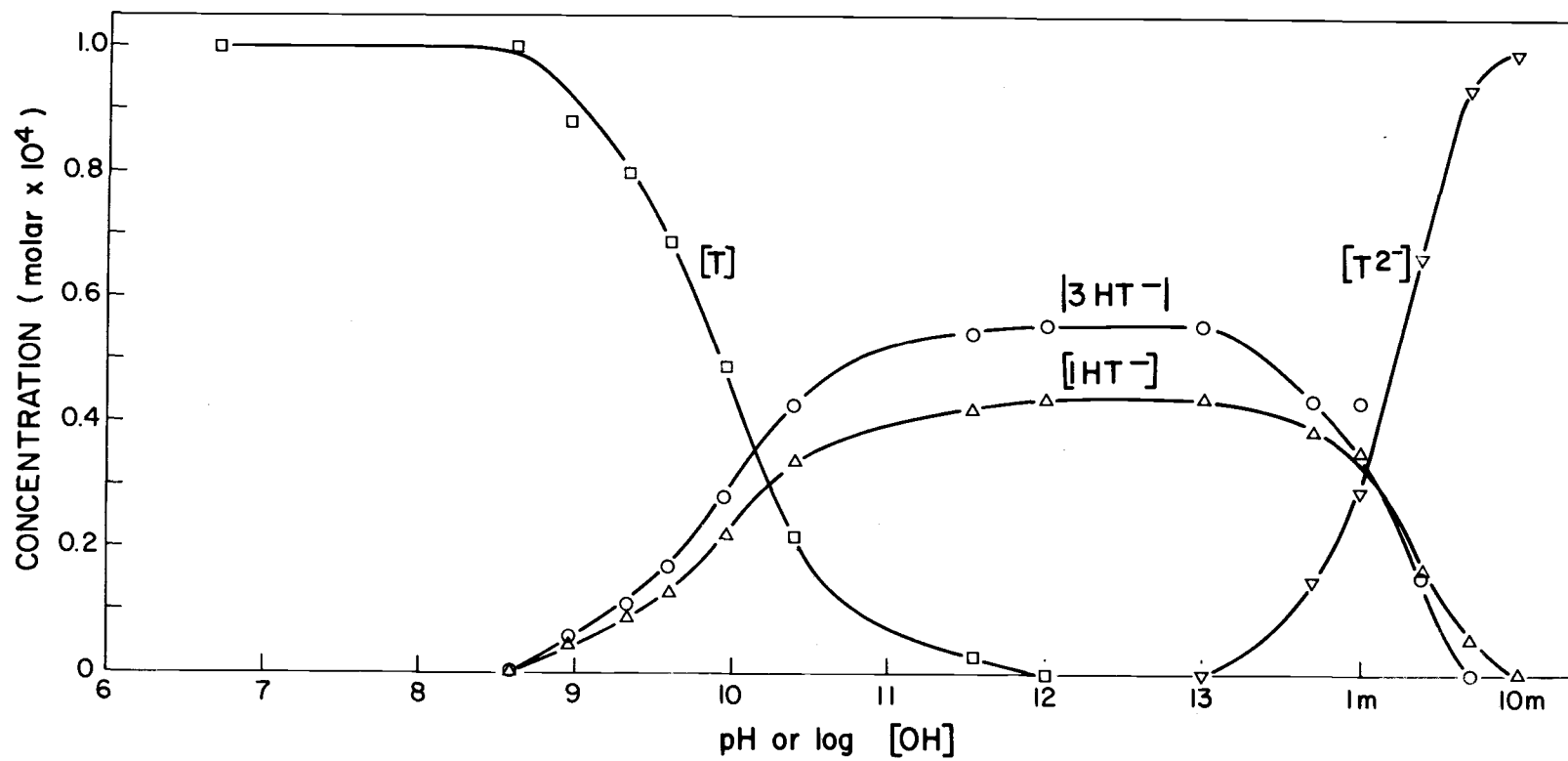


Figure 3.5. Concentration of absorbing species of thymine as a function of pH.

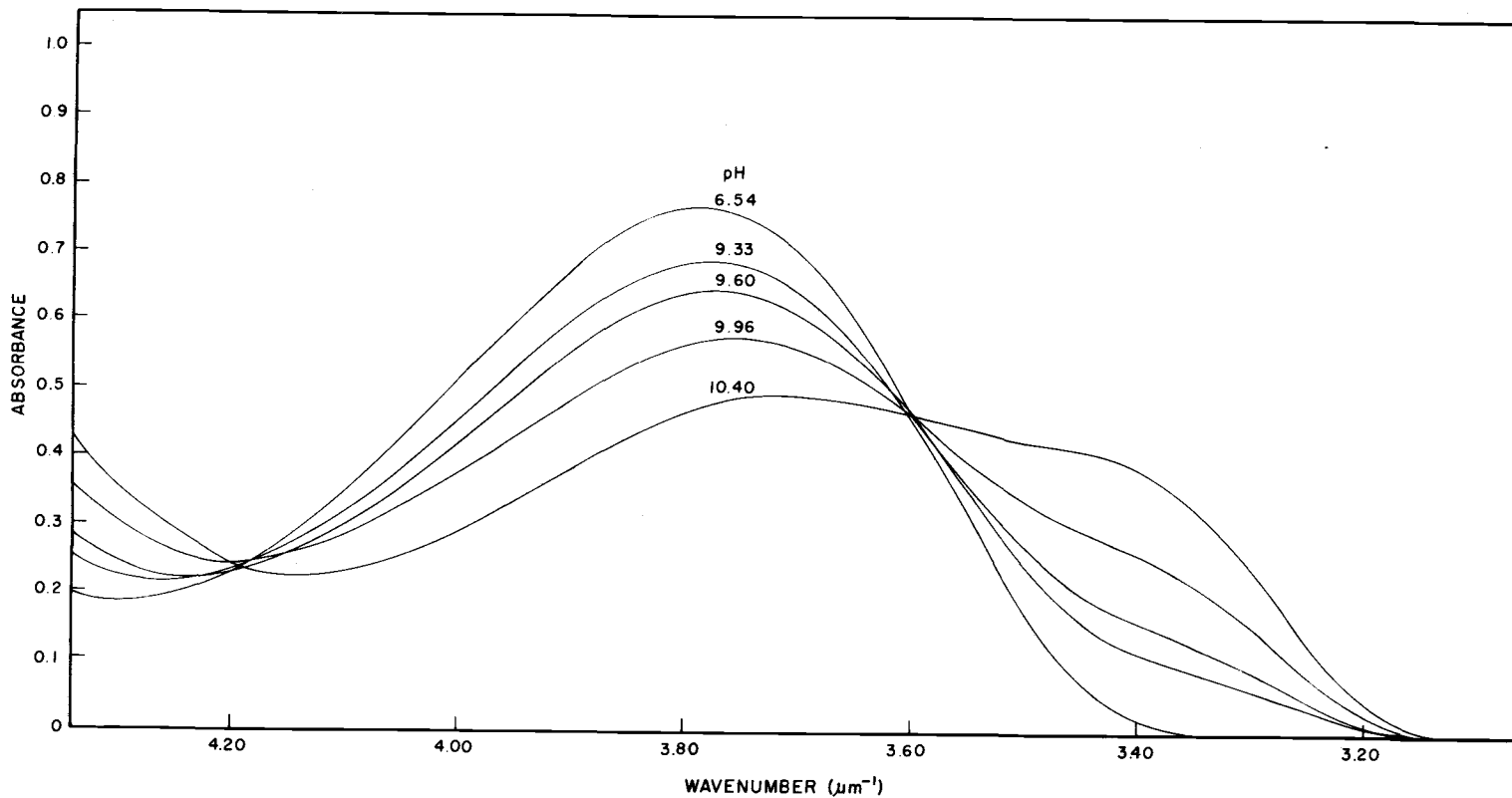


Figure 3.6. Absorption spectra of  $10^{-4}$  M thymine taken on a Cary 15 in 0.025 M borax buffers between pH 6.54 and 10.4 (pathlength 1 cm).

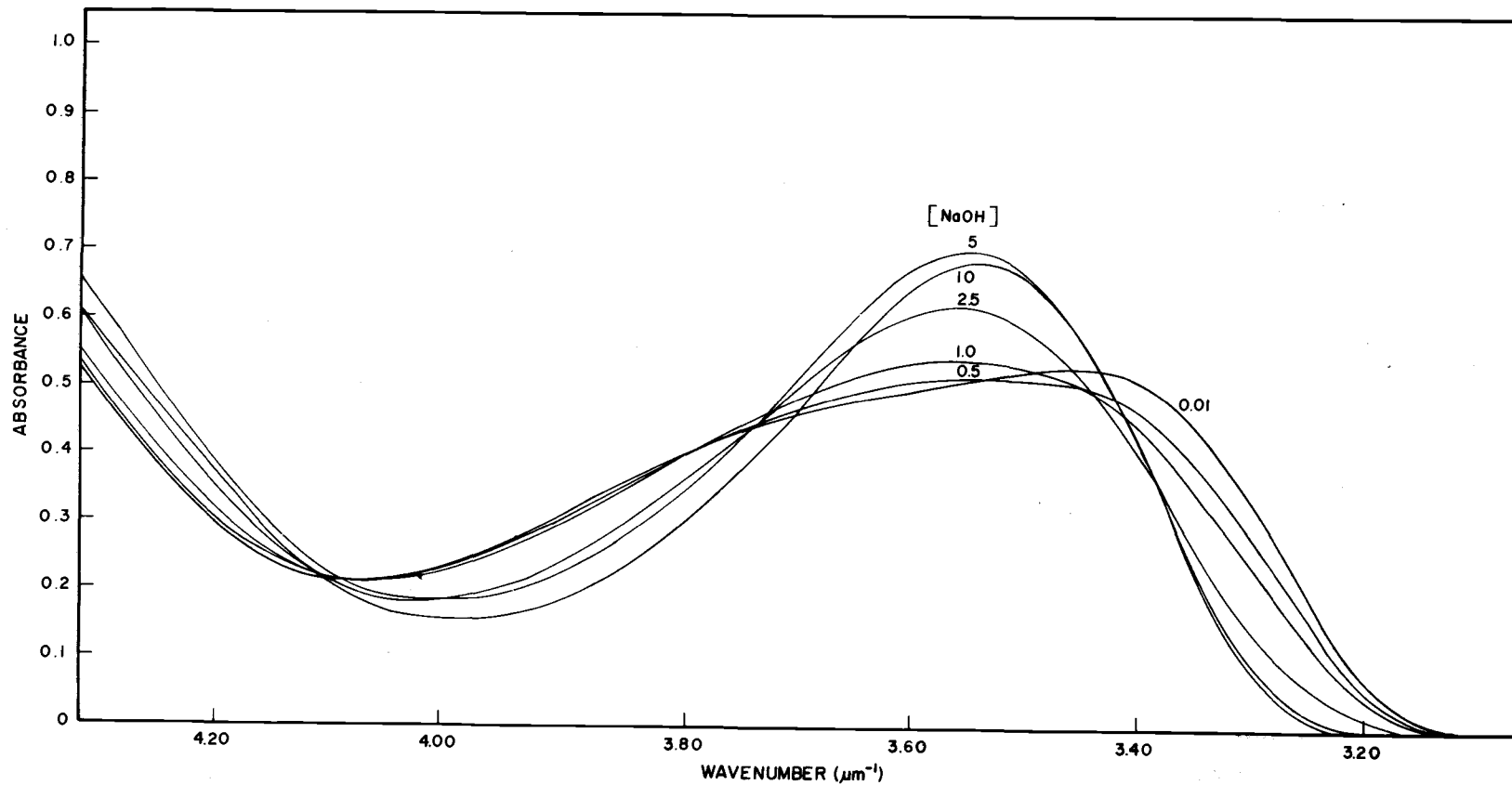


Figure 3.7. Absorption spectra of  $10^{-4}$  M thymine as a function of [NaOH].

the ground state from which the fluorescing species at pH 12 arise (Gill, 1968; Berens and Wierzchowski, 1969)).

- b. The contribution of  $3 \text{ HT}^-$  to the total absorption at pH 12 is its relative absorption spectrum normalized to the red edge of the total spectrum where  $1 \text{ HT}^-$  most likely does not absorb<sup>5</sup>. The difference between the total and  $3 \text{ HT}^-$  is then the  $1 \text{ HT}^-$  absorption spectrum.
- c. The tautomeric equilibrium constant ( $K = \frac{[3 \text{ HT}^-]}{[1 \text{ HT}^-]}$ ) for the reaction  $1 \text{ HT}^- \rightleftharpoons 3 \text{ HT}^-$ , is 1.25. Previous estimates of K range from 1.00 to 1.50 (Wierzchowski et al., 1965) and our value of 1.25 is chosen for convenience.

The two isobestic points apparent in Figure 3.6 imply a two component system at these pH's. However, the existence of three absorbing components (T,  $1 \text{ HT}^-$  and  $3 \text{ HT}^-$ ) is well documented (Wierzchowski et al., 1965). It seems reasonable to assume therefore that a rapid equilibrium between  $1 \text{ HT}^-$  and  $3 \text{ HT}^-$  exists at these pH's, so rapid in fact that the two monoanions respond to changes in pH as one component. Between pH 9 and 12 concentrations were therefore calculated assuming a two component system containing T (pure spectrum = pH 7) and  $1 \text{ HT}^- + 3 \text{ HT}^-$  (pure spectrum = pH 12).

From pH 13 to 10 M NaOH, component concentrations were

---

<sup>5</sup> Eastman (1969) has used a similar type of fit to estimate the absorption spectrum of a fluorescent tautomer of adenine.

calculated as follows. From Beer's Law the total extinction coefficient,  $\epsilon_{\bar{\nu}}^{\text{total}}$ , at pH 12 and energy  $\bar{\nu}$  can be expressed in terms of the extinction coefficients of 1  $\text{HT}^-$  and 3  $\text{HT}^-$  and the tautomeric constant by,

$$\epsilon_{\bar{\nu}}^{\text{total}} = \left(\frac{1}{K+1}\right) \epsilon_{\bar{\nu}}^{(1)} + \left(\frac{K}{K+1}\right) \epsilon_{\bar{\nu}}^{(3)} . \quad (3.1)$$

By fitting the relative absorption spectrum of 3  $\text{HT}^-$  (see assumption (b)) to the total spectrum at pH 12, the magnitude of  $\left(\frac{K}{1+K}\right) \epsilon_{\bar{\nu}}^{(3)}$  is determined. Using assumption (c) and Equation (1.1),  $\epsilon_{\bar{\nu}}^{(3)}$  and  $\epsilon_{\bar{\nu}}^{(1)}$  can then be evaluated.

At any pH > 12 there are at most three species contributing to the total absorption ( $\text{T}^{2-}$ , 1  $\text{HT}^-$ , and 3  $\text{HT}^-$ ) and three simultaneous equations can be set up of the sort,

$$\begin{aligned} A_{\bar{\nu}_1}^{\text{total}} &= [1 \text{HT}^-] \epsilon_{\bar{\nu}_1}^{(1)} + [\text{T}^{2-}] \epsilon_{\bar{\nu}_1}^{(2)} + [3 \text{HT}^-] \epsilon_{\bar{\nu}_1}^{(3)} \\ A_{\bar{\nu}_2}^{\text{total}} &= [1 \text{HT}^-] \epsilon_{\bar{\nu}_2}^{(1)} + [\text{T}^{2-}] \epsilon_{\bar{\nu}_2}^{(2)} + [3 \text{HT}^-] \epsilon_{\bar{\nu}_2}^{(3)} \\ A_{\bar{\nu}_3}^{\text{total}} &= [1 \text{HT}^-] \epsilon_{\bar{\nu}_3}^{(1)} + [\text{T}^{2-}] \epsilon_{\bar{\nu}_3}^{(2)} + [3 \text{HT}^-] \epsilon_{\bar{\nu}_3}^{(3)} \end{aligned} \quad (3.2)$$

where  $A_{\bar{\nu}_n}^{\text{total}}$  is the measured absorbance at energy  $\bar{\nu}_n$ . Since all  $\epsilon_{\bar{\nu}}$ 's are known, the three unknown component concentrations were then evaluated at any pH from Equation (3.2) with the aid of a programmed Hewlett Packard HP-9100-A calculator.

In Figure 3.8 the relative fluorescence intensity at  $2.50 \mu\text{m}^{-1}$  is plotted as a function of pH. Since alkaline thymine has a fluorescence quantum yield about 17 times that of neutral thymine, at all pH's  $> 9$  the emission intensity at  $2.50 \mu\text{m}^{-1}$  is due almost totally to alkaline thymine. The plot therefore monitors relative fluorescence for ionized species of thymine as a function of pH. A similar curve is also shown for neutral thymine by plotting the fluorescence intensity at  $2.94 \mu\text{m}^{-1}$  below pH 9. At pH's above 9 contributions to the fluorescence at  $2.94 \mu\text{m}^{-1}$  due to alkaline species have been subtracted (Values of neutral thymine were unobtainable above pH 9.35 because of the more intense alkaline fluorescence. The dashed line is a reasonable extrapolation.).

$\phi_f$ , excited at  $3.34 \mu\text{m}^{-1}$  as a function of pH, is also shown in Figure 3.8. Even though the emission intensity has decreased by almost 70% at pH 9.6,  $\phi_f$  has remained essentially unchanged. Since at  $3.34 \mu\text{m}^{-1}$  only  $3\text{HT}^-$  absorbs, the decreased emission intensity is consistent with the decrease in concentration of  $3\text{HT}^-$  due to ground state protonation; the invariance of  $\phi_f$  is consistent with emission originating from only  $3\text{HT}^-$  at this excitation energy.

The first and second pK's of thymine, determined from the above spectroscopic data are presented in Table 3.1. For  $\text{pK}_1$ , there is good agreement between different tautomers and with a reported pK of 9.90 (Shugar and Fox, 1952). Estimated  $\text{pK}_2$ 's agree

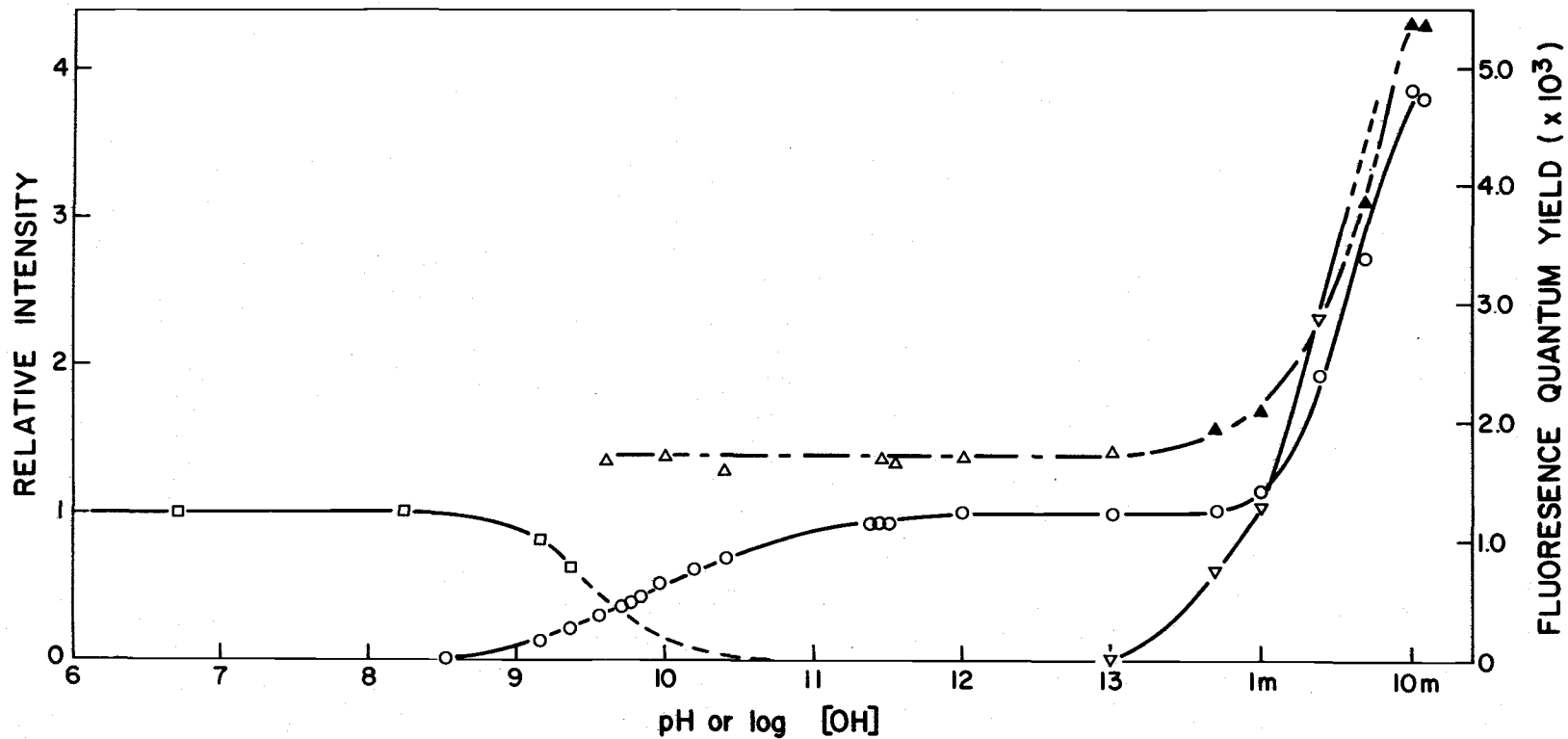


Figure 3. 8. pH effect on some fluorescence properties of thymine: relative fluorescence intensity at  $2.94\mu\text{m}^{-1}$  ( $\square$ — $\square$ ), relative fluorescence intensity at  $2.5\mu\text{m}^{-1}$  ( $\circ$ — $\circ$ ), fluorescence quantum yield ( $\Delta$ — $\Delta$ ) and ( $\blacktriangle$ — $\blacktriangle$ ), fluorescence quantum yield due to  $\text{T}^{2-}$  ( $\nabla$ — $\nabla$ ).

Table 3.1. Ground and excited state pK's of thymine.

Method	Ground State		Excited State <sup>(a)</sup>				
	pK <sub>1</sub>	pK <sub>2</sub>	Method	pK <sub>1</sub> <sup>*</sup>			
	Ionization Process			Ionization Process			
	T → 1 or 3HT <sup>-</sup>	1 or 3HT <sup>-</sup> → T <sup>2-</sup>		T → 1HT <sup>-</sup>	T → 3HT <sup>-</sup>	1HT <sup>-</sup> → T <sup>2-</sup>	3HT <sup>-</sup> → T <sup>2-</sup>
T absorption	9.92	----	eq. (I. 21) <sup>b</sup>	9.71	1.80	9.64	17.43
1 HT <sup>-</sup> absorption	9.92	14.30	eq. (I. 21) <sup>c</sup>	----	1.17	----	16.93
3 HT <sup>-</sup> absorption	9.94	14.14	eq. (I. 21) <sup>d</sup>	----	3.67	----	15.68
T <sup>2-</sup> absorption	----	14.23					

(a) Calculated assuming pK<sub>1</sub> = 9.92, pK<sub>2</sub> = 14.22

(b)  $\Delta \bar{\nu}_{00}$  estimated from the difference in absorption maximum between the appropriate ionized structures.

(c)  $\bar{\nu}_{00}$ 's estimated from the absorption-fluorescence overlap of the appropriate ionized structures.

(d)  $\bar{\nu}_{00}$ 's estimated from the average of absorption and fluorescence maxima.

within experimental error (average = 14.22).  $pK_2$ 's estimated in this manner are only approximate since no attempt was made to hold the ionic strength constant.

## Discussion

### Emission Spectra

Before any other comments it is important to establish whether the structure appearing in our emission spectra compared with the previously reported smooth envelopes at  $300^{\circ}$  K (Berens and Wierzchowski, 1969; Gill, 1968) and at  $77^{\circ}$  K (Longworth, 1966) is genuine or an artifact.

Emission artifacts could arise from either an instrumental signal or from an impurity in the solution. Instrumental artifacts and intrinsic emissions from impurities in the NaOH or water can be eliminated from consideration because the reported spectra include subtraction of a solvent scan of the appropriate NaOH concentration from the original emission scan. Instrumental integrity is further assured since neither the recorded emission from PPO nor any other reported spectra (see Section I) shows a similar structure in the same wave-number region as thymine emission. Fluorescent impurities in thymine itself also seem unlikely since its purity has been established (Section I) and because thymine purchased from three supplies all

gave the same structured emission.

An anomolous emission signal might still arise via an energy transfer process from thymine to a non-abosrbing "impurity" acceptor which then emits a structured fluorescence superimposed on a smooth thymine emission. Such a situation is not probable for three reasons: 1) one would not expect emission arising via energy transfer from thymine to be coincident with thymine fluorecence, but shifted to lower energies, 2) the increase in acceptor concentration in going from pH 12 to 10 M NaOH (assuming NaOH contains the impurity) should give a relative increase in structure which is not observed and 3) the distance between donor and acceptor molecules is much too large for efficient energy transfer in the context of a  $T_S$  for alkaline thymine of  $4 \times 10^{-11}$  sec. (calculated from Equation (L14)).

Comparison of Figures 3.2, 3.3, and 3.4 show a marked change in the absorption of thymine in going from pH 12 to 10 M NaOH. Since excitation spectra closely follow these absorption changes there can be little doubt that the observed emission in all cases is from thymine, particularly in view of the very close correspondence of absorption and excitation spectra at 10 M NaOH.

The polarization of emission shows only small changes across the emission spectra at all NaOH concentrations. This implies that fluorescence must arise from a single electronic transition containing several strong vibrational transitions which account for the structured

spectrum, and confirms the fact that only one fluorescent transition is present. In addition, the observed band separation of  $0.15 \mu\text{m}^{-1}$  corresponds to C=C, C=N, or C=O stretching frequencies in the infrared spectrum and the  $0.25 \mu\text{m}^{-1}$  separation corresponds to C-H or N-H stretching frequencies (Blout and Fields, 1950). It appears therefore that the structured emission is genuine and is an intrinsic property of the excited singlet of ionized thymine.

In view of this, it is necessary to search for some explanation as to the lack of any previously detected structure. Compared to earlier work there is not a significant difference in resolution. Gill (1968) reports an emission bandwidth identical to ours at  $100 \text{ \AA}$  and there is no reason to expect the unreported bandwidths of Berens and Wierzchowski (1969) to be much different, also there is no way of knowing the comparative stray light characteristics of the other instruments. For emission spectra at  $300^\circ \text{K}$ , Gill used a  $10^{-3} \text{ M}$  solution, a factor of 10 greater than us and 50 greater than Berens and Wierzchowski, and therefore solute interactions in the ground or excited state may account for Gill's lack of structure. Uncertainties as to the physical state of alkaline thymine in low temperature glasses may well account for smooth emission at  $77^\circ \text{K}$ . In general, however, the most important difference compared with previous reports is the higher sensitivity of the Turner 210 (coupled with finite absorbance). For their fluorescence spectrophotometer Berens and Wierzchowski report a

sensitivity of  $10^{-9}$  g/ml quinine, which is comparable to the Turner 210 under normal operation, but when coupled with an absorbance of 0.50 the Turner 210 is ~ 10 times more sensitive.

### Emission Polarization

Polarized emission is not commonly observed from non-viscous solutions at room temperature (see Introduction). From a fundamental equation relating singlet lifetimes to polarization (Perrin, 1926),

$$\tau_S = \frac{6V\eta}{RT} \left( \frac{1}{P} - \frac{1}{2} \right), \quad (3.3)$$

it can be calculated that at  $300^\circ$  K a molecule with an aqueous molar volume  $\approx$  benzene ( $83.5 \text{ cm}^3$  (Edward, 1970)) must have a  $\tau_S \leq 2.9 \times 10^{-10}$  sec. to give a measured emission polarization of 0.28. The calculated  $\tau_S$  (Equation 1.14) for thymine at pH 12 is  $4 \times 10^{-11}$  sec. and it is therefore not surprising to observe a polarization at room temperature.

The short calculated lifetime for alkaline thymine also implies that emission may compete with solvent and vibrational relaxation processes from the Franck-Condon excited state. If this is the case, the small downward slope of polarization for each pH (Figures 3.2-3.4) with lower emission energies might be attributed to a small rotational depolarization when fluorescence arises from more relaxed states. In other words, rather than the emission spectrum arising

from only one excited state going to a distribution of ground states when  $\tau_S > 10^{-9}$  sec., emission may arise from a distribution of excited states. Low energy excited states will have depolarized more than the high energy states during the partial relaxation process giving rise to diminished fluorescence polarization at lower energy.

The 20% relative increase of the blue side of the thymine emission compared to the maximum, when going from pH 12 to 10M NaOH, can be interpreted as a blue shift of the average emission energy (although  $\bar{\nu}_{\max}$  is approximately unchanged) and is consistent with the attendant increase in viscosity. The generally higher polarizations in 10 M NaOH (compare Figures 3.2 and 3.4) confirms this deduction since higher energy emissions should be more polarized.

Polarization measurements can indicate the type of transitions involved in fluorescence. From Equation (I.18) if the angle between absorption and emission transition moments  $\beta$  is  $\sim 90^\circ$ , a negative polarization is expected (with a lower limit of -0.33); if  $\beta \sim 0^\circ$  a positive polarization is expected.  $\pi-\pi^*$  transitions normally occur in the plane of an aromatic molecule and  $\beta$  is small, while  $n-\pi^*$  transitions are perpendicular to the molecular plane (Sidman, 1958) and therefore  $\beta$  is large. The positive polarization (0.2-0.3) at all pH's implies  $\pi-\pi^*$  transitions in alkaline thymine, the same type of transitions as in neutral thymine (from solvent shifts in spectra, Section II).

## pH Effects

In order to construct a consistent picture of the excited singlet of ionized thymine, two experimental results must be explained.

- a. The magnitude of  $\phi_f$  between pH 13 and 10 M NaOH in Figure 3.8 are somewhat inconsistent with concentrations in the same pH region (Figure 3.5). The constant value of  $\phi_f$  between pH 12 and 13 is only about 37% of the maximum yield, while  $3\text{HT}^-$  accounts for about 56% of the light absorbed by thymine at these pH's. Also,  $\phi_f$  increases 24% between 5 and 10 M NaOH, while  $\text{T}^{2-}$  increases only 6%. If no other effects existed, the conversion of thymine monoanions to the dianion should result in exactly parallel trends in  $\text{T}^{2-}$  and  $\phi_f$  as a function of pH. Since there appears to be very little structural difference in the emitting species (see below), whether at pH 13 or 10 M NaOH, an explanation must lie in the physical environment of the emitter. In Figure 3.9 the viscosity of NaOH in aqueous solution is plotted as a function of pH. The solution viscosity changes about thirty-fold from pH 13 to 10 M NaOH, and this will markedly effect  $\tau_S$  and  $\phi_f$  (see Equation (3.1)) and Equation (L.19).<sup>6</sup> The observed increase in  $\phi_f$  seems to be therefore

---

<sup>6</sup> Large increases in  $\phi_f$  as a function of viscosity have been observed for adenine (Eastman and Rosa, 1968), in various solvents.

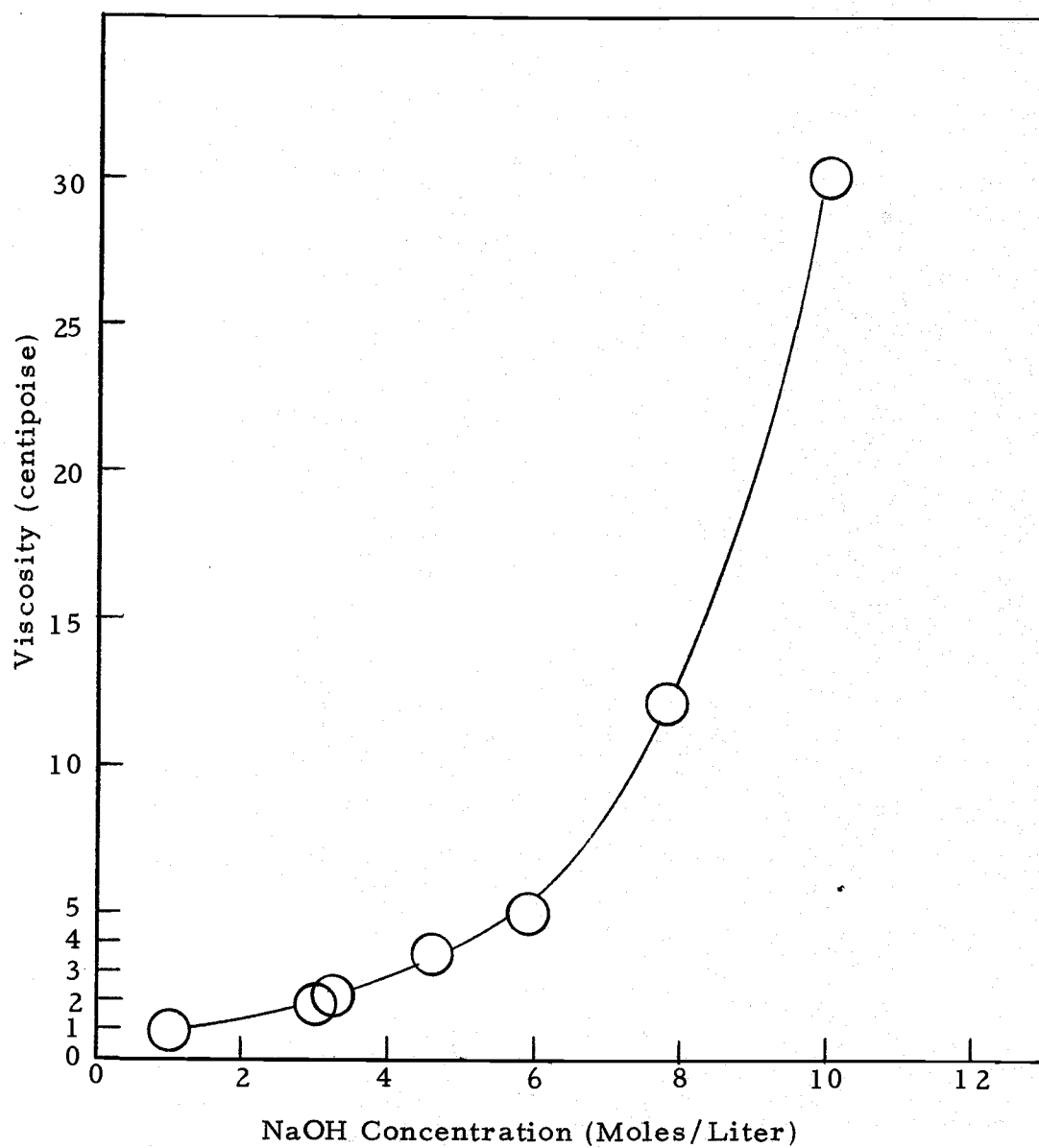


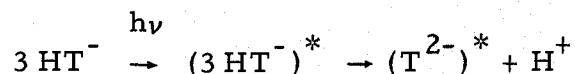
Figure 3.9. Solution viscosity as a function of NaOH concentration (Timmermans, 1960).

a composite of several factors. Quantum yields at NaOH concentrations above  $\sim 3\text{M}$  cannot be adequately analyzed without further experiments and hence values of  $\phi_f$  for  $\text{T}^{2-}$  are not presented above  $3\text{M}$  NaOH (Figure 3.8).

- b. From pH 10 to 13,  $1\text{HT}^-$  and  $3\text{HT}^-$  account for most of the absorbed light at  $\bar{\nu} > 3.54\ \mu\text{m}^{-1}$ ; at  $10\text{M}$  NaOH  $\text{T}^{2-}$  is the absorbing species at all wavenumbers; and between pH 13 and  $10\text{M}$  NaOH all three species absorb (Figure 3.5). The shape of the emission spectra and its polarization, however, are remarkably similar over the entire pH range encompassing a  $10^5$ -fold increase in  $\text{OH}^-$  concentration and a 300% increase in  $\phi_f$ . The three peaks due to vibrational structure at  $2.50$ ,  $2.65$  and  $2.90\ \mu\text{m}^{-1}$  in the emission spectra appear at all pH's and there is little relative change in the intensity of these peaks from pH 10 to  $10\text{M}$  NaOH (The very large change in solvent environment between  $10^{-4}$  and  $10\text{M}$  NaOH has caused only about a 20% relative increase in one vibration.).  $3\text{HT}^-$  is apparently the major emitting species below pH 12, but the very similar emission at  $10\text{M}$  NaOH, where only  $\text{T}^{2-}$  exists in the ground state, requires comment. There must be some very similar characteristics (particularly in electronic distribution) in the excited states of both  $3\text{HT}^-$  and  $\text{T}^{2-}$  to account for the emission

similarities.

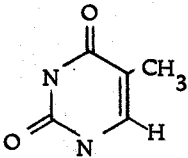
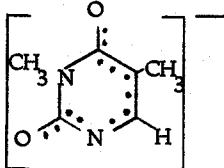
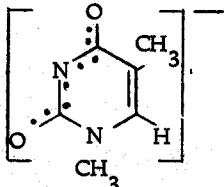
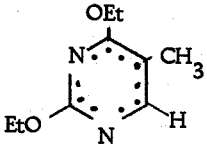
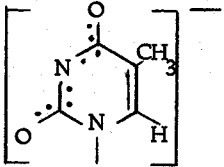
A common interpretation in terms of the acid-base behavior of excited states is that  $3\text{HT}^-$  and  $\text{T}^{2-}$  are indeed identical in the excited state. An excited state deprotonization of  $3\text{HT}^-$ , i. e.



followed by emission from the resultant excited  $\text{T}^{2-}$ , could account for the observed facts. This process requires that  $3\text{HT}^-$  become significantly more acidic in its excited state relative to its ground state. Excited state  $\text{pK}'\text{s}$  calculated from absorption and emission spectra by several methods are shown in Table 3.1.  $3\text{HT}^-$  is in fact considerably more basic in its excited state ( $\text{pK}_2^* \sim 16$ ) and this fact makes the above process unlikely.

A similar electronic distribution does not require totally similar covalent structure. A comparison of the structures of  $1\text{HT}^-$ ,  $3\text{HT}^-$  and  $\text{T}^{2-}$  in Figure 3.1 shows that the #1, 2, 5 and 6 ring positions have complete conjugation for  $3\text{HT}^-$  and  $\text{T}^{2-}$  while  $1\text{HT}^-$  does not. It is tempting therefore to postulate that the transition responsible for fluorescence originates in this part of the ring. This rather simple conclusion can be given added weight by a consideration of the fluorescence of some derivatives of thymine (Table 3.2). In every case a compound with  $\pi$  conjugation spanning the #1, 2, 4, 5 and 6 positions fluoresces ( $\phi_f > 10^{-3}$ ), whereas those without such conjugation

Table 3.2. Room temperature fluorescence of thymine derivatives.

Compound	Structure	$\phi_f$	Reference
Thymine, pH 7		$1 \times 10^{-4}$	Hauswirth and Daniels, 1970
3-methylthymine, pH 12		$> 10^{-3}$	Berens and Wierzchowski, 1969
1-Methylthymine, pH 12		$< 10^{-3}$	Berens and Wierzchowski, 1969
2,4-Diethoxythymine, pH 7		$1.6 \times 10^{-3}$	Hauswirth and Daniels, 1970a
Thymidine, pH 11	 Sugar	$< 10^{-3}$	Longworth <i>et al.</i> , 1966

fluoresce only weakly if at all ( $\phi_f < 10^{-3}$ ).

This conclusion may have important consequences in relation to DNA excited state energy processes and photochemistry if DNA fluorescence is detected and shown to be localized. The similar excited state properties of DNA and neutral and alkaline thymine (see Introduction, this section) might mean that the major fluorescing state in DNA resides in the thymine molecule. In its normal structure thymine is linked on the # 1 position to a ribose-phosphate-ribose backbone with other bases. It is expected to have the neutral diketo structure and a singlet lifetime about like neutral thymine ( $1.5 \times 10^{-12}$  sec., see Section I). Even if a biprotonic exchange with adenine occurs leaving thymine in an 4-enol form,  $\pi$  conjugation cannot span the # 1, 2, 4, 5, and 6 positions and DNA is therefore still expected to have  $\phi_f < 10^{-3}$ . Preliminary investigations confirm these predictions about DNA fluorescence. Although this work has led to a negative conclusion concerning DNA, it may mean by the process of elimination that emission in DNA originates from the #3 position of thymine.

The  $pK^*$  calculations in Table 3.1 predict the possibility of other protic reactions in the excited state. Processes involving  $1 HT^-$  may occur with the indicated  $pK^*$ 's, but since there is no indication from the fluorescence excitation spectrum that this tautomer emits (in addition at  $77^\circ K$  Berens and Wierzchowski find that the

1-methylthymine anion has a  $\phi_{fl}$  less than 30% of 3-methylthymine anion and 20% of  $T^-$ ), there is no way to decide with certainty. The very acidic  $pK_1^*$  for  $(T)^* \rightleftharpoons (3HT^-)^*$  probably does not occur because the fluorescence intensity closely follows ground state  $pK$  changes (Figure 3.8) and no change in fluorescence is observed in 0.5 M  $H_2SO_4$  (Section I).

In summary it appears that the structured emission of alkaline thymine arises from a  $\pi-\pi^*$  transition in #1, 2, 4, 5 and 6 conjugated systems and its short lifetime may mean emission from Franck-Condon excited states. Acid-base reactions in the excited states of either neutral or alkaline thymine, if they occur at all, do not involve the emitting state.

## BIBLIOGRAPHY

- Baba, H. L. Goodman, and P. C. Valenti. 1966. Solvent effects on the fluorescence spectra of diazines. Dipole moments in the  $(n, \pi^*)$  excited states. *Journal of the American Chemical Society* 88:5410-5415.
- Basu, S. 1964. Theory of solvent effects on molecular electronic spectra. *Advances in Quantum Chemistry* 1:145-169.
- Bayliss, W. S. and E. G. McRae. 1954. Solvent effects in organic spectra: dipole forces and the Franck-Condon Principle. *Journal of Physical Chemistry* 58:1002-1006.
- Berens, K. and K. L. Wierzchowski. 1969. Luminescence of tautomeric forms of thymine monoanions. *Photochemistry and Photobiology* 9:433-438.
- Berlman, I. B. and T. A. Walter. 1962. Fluorescence quenching of a scintillation solution of oxygen. *Journal of Chemical Physics* 37:1888-1889.
- Berlman, I. 1965. *Handbook of Fluorescence Spectra of Aromatic Molecules*. New York, Academic Press, 258 p.
- Bersohn, R. and I. Isenberg. 1963. On the phosphorescence of DNA. *Biochemical and Biophysical Research Communications* 13:205-208.
- Beukers, R. , J. Ijlstra, and W. Berends. 1960. The effect of U. V. light on some components of the nucleic acids. VI. The origin of the U. V. sensitivity of DNA. *Recueil Des Travaux Chimiques Des Pays-Bas* 79:101-104.
- Beukers, R. and W. Berends. 1960. Isolation and identification of the irradiation products of thymine. *Biochimica Et Biophysica Acta* 41:550-551.
- Bhaumik, M. L. and R. Hardwick. 1963. Lattice work performed by excited molecules. *Journal of Chemical Physics* 39:1595-1598.
- Birks, J. B. and D. J. Dyson. 1963. The relations between the fluorescence and absorption properties of organic molecules. *Proc. Roy. Soc. (London)* 275:135-148.

- Blackburn, G. M. and R. J. H. Davies. 1965. The structure of thymine photodimer. *Chemical Communications* No. 11:215-216.
- Blout, E. R. and M. Fields. 1950. Absorption spectra. VIII. The infrared spectra of some purines and pyrimidines. *Journal of the American Chemical Society* 72:479-484.
- Börreson, H. C. 1963. On the luminescence properties of some purines and pyrimidines. *Acta Chemica Scandinavica* 17:921-929.
- \_\_\_\_\_. 1965. Effects of cooling on the fluorescence of biological guanine derivatives. *Acta Chemica Scandinavica* 19:2100-2112.
- \_\_\_\_\_. 1967. Fluorescence and tautomerism of protonated and methylated adenine derivatives. *Acta Chemica Scandinavica* 21:2463-2473.
- Brown, I. H. and H. E. Johns. 1968. Photochemistry of uracil. Intersystem crossing and dimerization in aqueous solution. *Photochemistry and Photobiology* 8:273-286.
- Burr, J. G. 1968. Advances in the Photochemistry of Nucleic Acids. in *Advances in Photochemistry* ed. by W. A. Noyes, Jr., G. S. Hammond and J. N. Pitts, Jr. Vol. 6, p. 193-300.
- Callis, P. R., E. J. Rosa and W. T. Simpson. 1964. Search for accidental degeneracy in purines. *Journal of the American Chemical Society* 86:2292-2294.
- Chapman, J. H., T. Förster, G. Kortüm, E. Lippert, W. H. Melhuish, G. Nebbia, and C. A. Parker. 1963. Proposal for standardization of methods of reporting fluorescence emission spectra. *Zeitschrift für Analytische Chemie* 197:431-433.
- Chemical Rubber Company. 1968. *Handbook of Chemistry and Physics* ed. by R. C. Weast. Chemical Rubber Company, Cleveland, Ohio, 49th Edition.
- Collie, J. B. Hasted and D. M. Ritson. 1948. The dielectric properties of water and heavy water. *Physical Society of London, Proceedings* 60:145-160.
- Crown Zellerbach Corporation. 1967. *Dimethyl Sulfoxide Technical Bulletin*. Camas, Washington.

- Daniels, M. and A. Grimison. 1963. Photochemistry of thymine. *Nature* 197:484.
- Daniels, M. and W. Hauswirth. 1970. Oregon State University, Corvallis, Oregon. Submitted to *Science*.
- Dawson, W. R. and M. W. Windsor. 1968. Fluorescence yields of aromatic compounds. *Journal of Physical Chemistry* 72:3251-3260.
- deVoe, H. and I. Tinoco, Jr. 1962. The stability of helical polynucleotides: Base contributions. *Journal of Molecular Biology* 4:500-517.
- Eastman, J. W. 1966. Standardization of fluorescence spectra and the calibration of spectrofluorimeters. *Applied Optics* 5:1125-1132.
- Eastman, J. W. and E. J. Rosa. 1968. The fluorescence of adenine. The effects of solvent and temperature on the quantum yield. *Photochemistry and Photobiology* 7:189-201.
- Eastman, J. W. 1969. The fluorescence tautomerism of adenine. *Berichte der Bunsengesellschaft* 73:407-412.
- Edward, J. T. 1970. Molecular volumes and the Stokes-Einstein Equation. *Journal of Chemical Education* 47: 261-270.
- Einstein, A. 1917. Zur Quantentheorie der Strahlung. *Physikalischer Zeitschrift*. 18:121-128.
- Eisenberg, D. and W. Kauzman. 1969. The structure and properties of water. New York, Oxford Press, 296 p.
- Eisenger, J. and R. G. Shulman. 1966. Triplet excitations in polyadenylic acid. *Proceedings of the National Academy of Sciences* 55:1387-1391.
- Eisenger, J. 1968. The excited states of nucleic acids. *Photochemistry and Photobiology* 7:597-612.
- \_\_\_\_\_. 1968. Excited electronic states of DNA. *Science* 161:1311-1319.

- Eisinger, J., A. A. Lamola, J. W. Longworth and W. B. Gratzer. 1970. Biological molecules in their excited states. *Nature* 226:113-118.
- Ermolaev, V. L. 1963. Energy transfer of organic systems involving the triplet state. III. Rigid solutions and crystals. *Soviet Physics Uspekhi* 80:333-358.
- Evett, J. and I. Isenberg. 1969. DNA-polylysine interaction as studied by polarization of fluorescence. *Annals of the New York Academy of Science* 158:210-222.
- Feofilov, P. P. 1961. The physical basis of polarized emission. tr. by Consultants Bureau, New York, 274 p.
- Fisher, G. J. and H. E. Johns. 1970. Personal communication and in course of publication.
- Fletcher, A. N. 1967. Relative fluorescence quantum yields of quinine sulfate and 2-aminopurine. *Journal of Molecular Spectroscopy* 23:221-224.
- \_\_\_\_\_. 1969. Quinine sulfate as a fluorescence quantum yield standard. *Photochemistry and Photobiology* 9:439-444.
- Förster, T. 1950. Elektrolytische dissoziation energeregter moleküle. *Zeitschrift für Elektrochemie* 54:42-46.
- \_\_\_\_\_. 1951. Fluoreszenz organischer verbindungen. Göttingen, Vandenhoeck und Ruprecht, 312 p.
- Förster, T. and K. Rokos. 1967. A deuterium isotope effect on fluorescence. *Chemical Physics Letters* 1:279-280.
- Galley, W. C. 1968. On the triplet states of polynucleotide-acridine complexes. I. Triplet energy delocalization in the 9-amino-acridine-DNA complex. *Biopolymers* 6:1279-1296.
- Gill, J. E. 1968. The fluorescence excitation spectrum of thymine. Evidence for wavelength dependence of the quantum yield. *Journal of Molecular Spectroscopy* 27:539-542.
- \_\_\_\_\_. 1969. The fluorescence excitation spectrum of quinine bisulfate. *Photochemistry and Photobiology* 9:313-322.

- Gill, J. E. 1970. Fluorescence of 5-methylcytosine. *Photochemistry and Photobiology* 11:259-269.
- Greenstock, C. L., I. H. Brown, J. W. Hunt and H. E. Johns. 1967. Photodimerization of pyrimidine nucleic acid derivatives in aqueous solution and the effect of oxygen. *Biochemical and Biophysical Research Communications* 27:431-436.
- Gueron, M., J. Eisinger, and R. G. Shulman. 1967. Excited states of nucleotides and singlet energy transfer in polynucleotides 47:4077-4091.
- Gueron, M. and R. G. Shulman. 1968. Energy transfer in polynucleotides. *Annual Review of Biochemistry* 37:571-596.
- Haugland, R. P., J. Yguerabide and L. Stryer. 1969. Dependence of the kinetics of singlet-singlet energy transfer on spectral overlap. *Proceedings of the National Academy of Science* 63: 23-30.
- Hauswirth, W. and M. Daniels. 1970a. *Photochemistry and Photobiology*. (In press).
- \_\_\_\_\_. 1970b. Oregon State University, Corvallis, Oregon. (In preparation).
- Hercules, D. M. and L. B. Rogers. 1960. Luminescence spectra of naphthols and naphthalenediols: Low-temperature phenomena. *Journal of Physical Chemistry* 64:397-400.
- Hoffman, T. A. and J. Ladik. 1964. Quantum mechanical considerations of some properties of DNA, in *Advances in Chemical Physics*, ed. J. Dochesne. Interscience, London, Vol. VII, p. 84-158.
- Honnas, P. I. and H. P. Steen. 1970. X-ray and U. V. -induced excitation of adenine, thymine, and the related nucleosides and nucleotides in solution at 77° K. *Photochemistry and Photobiology* 11:67-76.
- Isenberg, I., R. B. Leslie, S. L. Baird, R. Rosenbluth, and R. Bersohn. 1964. Delayed fluorescence in DNA-acridine dye complexes. *Proceedings of the National Academy of Science* 52: 379-387.
- Jackson, G. and G. Porter. 1961. Acidity constants in the triplet state. *Proceedings of the Royal Society of London. Series A* 260:13-30.

- Jaffe, H. H. and H. L. Jones. 1964. Excited state pK values. III. The application of the Hammett Equation. *Journal of Organic Chemistry* 30:964-969.
- Johns, H. E., M. L. Pearson, J. C. LeBlanc and C. W. Helleiner. 1964. The ultraviolet photochemistry of thymidyl-(3'→5')-thymidine. *Journal of Molecular Biology* 9:503-524.
- Johns, H. E. 1969. Photochemical reactions in the nucleic acids. in *Methods in Enzymology* ed. by K. Kuskin, Academic Press, New York, Vol. XVI. p. 253-316.
- Kleinwachter, V., J. Drobnik, and L. Augenstein. 1966. Spectroscopic properties of the lowest-lying excited states of 2-aminopyrimidine, cytosine, uracil and their derivatives. *Photochemistry and Photobiology* 5:579-586.
- \_\_\_\_\_. 1967. Spectroscopic studies of the purines. III. Properties of the purines substituted at the sixth and ninth positions. *Photochemistry and Photobiology* 6:133-146.
- Labhart, H. 1967. *Advances in chemical physics* ed. by I. Prigogine, Interscience, London, vol. XIII. p. 179.
- Lamola, A. A., M. Gueron, T. Yamane, S. Eisinger and R. G. Shulman. 1967. Triplet state of DNA. *Journal of Chemical Physics* 47:2210-2219.
- Lamola, A. A. 1968. Excited state precursors of thymine photodimers. *Photochemistry and Photobiology* 7:619-632.
- Lamola, A. A. and J. Eisinger. 1969. Probes for excited molecules in molecular luminescence. ed. by E. C. Lim, New York, N. Y., W. A. Benjamin. p. 801-812.
- Langelaar, G., G. N. de Vries, and D. Beelaar. 1969. Sensitivity improvements in spectrophospho-fluorimetry. *Journal of Sci. Insts. (J. Phys. E)* 2:149-152.
- Ledger, M. B. and P. Suppan. 1967. Spectroscopic studies of electron distribution. *Spectrochimica Acta* 23:641-653.
- Lewis, G. N. and M. Kasha. 1945. Phosphorescence in fluid media and the reverse process of singlet-triplet absorption. *Journal of the American Chemical Society* 67:994-1003.

- Levschin, W. L. 1927. Die Auslöschung der Fluoreszenz in festen und flüssigen Farbstofflösungen. *Zeitschrift für Physik* 43:230-253.
- Lippert, E. 1957. Spektroskopische Bestimmung des Dipolmomentes aromatischer Verbindung im ersten angeregten Singulettzustand. *Zeitschrift für Elektrochemie* 61:962-975.
- Lippert, E., W. Lüder and F. Moll. 1959. Polarisations- und Relaxations-Effekte in der Temperaturabhängigkeit von Absorptions- und Fluoreszenzspektren aromatischer Verbindungen in polaren Lösungsmitteln. *Spectrochimica Acta* 10:858-869.
- Lipsett, F. R., G. Bechtold, F. O. Blair, F. V. Cairns and D. H. O'Hara. 1970. Apparatus for measurement of luminescence spectra with a digital recording system. *Applied Optics* 9:1312-1318.
- Longworth, J. W., R. O. Rahn, and R. G. Shulman. 1966. Luminescence of pyrimidines, purines, nucleosides and nucleotides at 77° K. The effect of ionization and tautomerization. *Journal of Chemical Physics* 45:2930-2939.
- Longworth, J. W. and F. A. Bovey. 1966. Conformations and Interactions of excited states. *Biopolymers* 4:1115-1129. 1966.
- McRae, E. G. 1957. Theory of solvent effects on molecular electronic spectra. Frequency shifts. *Journal of Physical Chemistry* 61:562-572.
- McGlynn, S. P., F. J. Smith and G. Cilento. 1964. Some aspects of the triplet state. *Photochemistry and Photobiology* 3:269-294.
- Melhuish, W. H. 1961. Quantum efficiencies of fluorescence of organic substances. *Journal of Physical Chemistry* 65:229-235.
- Miles, D. W., R. K. Robins and H. Eyring. 1967. Optical rotatory dispersion, circular dichroism and absorption studies on some naturally occurring ribonucleosides and related derivatives. *Proceedings of the National Academy of Science* 57:1138-1145.
- Miles, D. W., M. J. Robins, R. K. Robins, and H. Eyring. 1969. Circular dichroism of nucleoside derivatives VI. The optically active bands of adenine nucleoside derivatives. *Proceedings of the National Academy of Science* 62:22-29.

- Moore, A. M. and C. H. Thomson. 1955. Ultraviolet irradiation of pyrimidine derivatives. *Science* 122:594-595.
- Morrison, H., A. Feeley and R. Kleopfer. 1968. Solution-phase photo-dimerization of dimethyl thymine. *Chemical Communications* 358-359.
- National Academy of Sciences-National Research Council. 1960. Specifications and criteria for biochemical compounds. Washington, D. C. Publication 719 p. P-18.
- Nnadi, J. C. and S. Y. Wang. 1969. D<sub>2</sub>O solvent effect on photo-product compositions of pyrimidines. *Tetrahedron Letters* No. 27:2211-2213.
- Onsager, L. 1936. Electric moments of molecules in liquids. *Journal of the American Chemical Society* 58:1486-1493.
- Osborne, A. D. and G. Porter. 1965. Diffusion studies in viscous media. *Royal Society of London Proceedings* A284:9-16.
- Parker, C. A. 1968. *Photoluminescence of solutions*. Amsterdam, Elsvier. 544 p.
- Perrin, F. 1926. Polarisation de la lumière de fluorescence. Vie moyenne des molécules dans l'état excité. *Journal de physique et le radium* 7:389-401.
- Pullman, A. 1970. Quantum aspects of heterocyclic compounds in Chemistry and Biochemistry. in the Jerusalem symposia on quantum Chemistry and Biochemistry. ed. by E. D. Bergman and B. Pullman, Jerusalem, vol. II.
- Rentzepis, P. M. 1969. Lasers in Chemistry. *Photochemistry and Photobiology* 8:579-583.
- Robinson, G. W. and R. P. Forsch. 1963. Electronic energy transfer and relaxation. *Journal of Chemical Physics* 38:1187-1203.
- Rorsch, A., R. Beukers, J. Ijlstra and W. Berends. 1959. The effect of U. V. light on some components of the nucleic acids I. uracil, thymine. *Recueil des Travaux Chimiques des Pays-Bas*. 79:423-429.

- Scott, T. G., R. D. Spencer, W. J. Leonard and G. Weber. 1970. Emission properties of NADH. Studies of fluorescence lifetimes and quantum efficiencies of NADH, AcPyADH, and simplified synthetic models. *Journal of American Chemical Society* 92: 687-695.
- Setlow, J. K. 1966. The molecular basis of biological effects of ultraviolet radiation and photoreactivation, in *Current Topics in Radiation Research* ed. by M. Ebert and A. Howard, North-Holland, Amsterdam, vol II. 195-248.
- Setlow, R. B. 1966. Cyclobutane-type pyrimidine dimers in polynucleotides. *Science* 153:379-386.
- Shore, V. G. and A. B. Pardee. 1956. Fluorescence of some proteins, nucleic acids and related compounds. *Archives of Biochemistry and Biophysics* 60:100-107.
- Shugar, D. and J. J. Fox. 1952. Spectrophotometric studies of nucleic acid derivatives and related compounds as a function of pH I. pyrimidines. *Biochimica et Biophysica Acta* 9:199-218.
- Shugar, D. and K. L. Wierzchowski. 1958. Structure and photochemical behavior of nucleic acids and related components. *Journal of Polymer Science* 31:269-279.
- Shulman, R. G. and R. O. Rahn. 1966. Electron spin resonance of the excited triplet states of pyrimidines and purines. *Journal of Chemical Physics* 45:2940-2946.
- Sidman, J. W. 1958. Electronic transitions due to nonbonding electrons. *Chemical Reviews*. 58:639-713.
- Siebold, K. and H. Labhart. 1970. Physikalisch-chemisches Institut der Universität Zurich, Zurich, Switzerland. Personal Communication.
- Smith, K. C. 1964. Photochemistry of the nucleic acids, in *Photo-physiology*, ed. by A. C. Giese, Academic Press, New York, vol. II. 329-388.
- Stewart, R. F. and N. Davidson. 1963. Polarized absorption spectra of purines and pyrimidines. *Journal of Chemical Physics* 39: 255-266.

- Stewart, R. F. and L. H. Jensen. 1964. Crystal structure of 9-methyladenine. *Journal of Chemical Physics* 40:2071-2075.
- Strickler, S. J. and R. A. Berg. 1962. Relationship between absorption intensity and fluorescence lifetime of molecules. *Journal of Chemical Physics* 37:814-822.
- Stryer, L. 1966. Excited state proton transfer reactions. A deuterium isotope effect on fluorescence. *Journal of the American Chemical Society* 88:5108-5712.
- Suppan, P. 1968. Solvent effects on the theory of electronic transitions: Experimental observations and applications to structural problems of excited molecules. *Journal of the Chemical Society (London) A*:3125-3133.
- Taylor, C. A., M. A. El-Bayoumi and M. Kasha. 1969. Excited-state two-proton tautomerism in hydrogen-bonded N-heterocyclic base pairs. *Proceedings of the National Academy of Sciences* 63:253-260.
- Taylor, K. J., T. C. Berg and P. D. Jarman. 1966. A scanning spectrophotometer for low intensity unstable sources. *Journal of Scientific Instrumentation* 42:921-923.
- Timmermans, J. 1960. The physio-chemical constants of binary systems in concentrated solutions. New York, Interscience, vol. 4, p. 247.
- Tsai, S. C. and G. W. Robinson. 1968. Phosphorescence and the true lifetime of triplet states in fluid solutions. *Journal of Chemical Physics* 49:3184-3191.
- Turner, G. K. 1964. An absolute spectrofluorimeter. *Science*. 146:183-190.
- \_\_\_\_\_. 1968. Turner Model 210 "Spectro" Service Manual. Palo Alto, California.
- Udenfriend S., and P. Zaltzman. 1962. Fluorescence characteristics of purines, pyrimidines and their derivatives. *Analytical Biochemistry* 3:49-59.
- Wacker, A. 1963. Molecular mechanisms of radiation effects, in *Progress in Nucleic Acid Research* ed. by J. N. Davidson and W. E. Cohn, Academic Press, New York, vol 1. 369-399.

- Wang, S. Y., M. Apicella, B. R. Stone. 1956. Ultraviolet irradiation of 1,3-dimethyluracil. *Journal of the American Chemical Society* 48:4180.
- Wang, S. Y. 1968. Photochemistry of nucleic acids and related compounds. I. The first step in the ultraviolet irradiation of 1,3-dimethyluracil. *Journal of the American Chemical Society* 80:6196-6198.
- \_\_\_\_\_. 1959. Ultraviolet irradiation of 1,3-dimethylthymine. 184:BA59-BA60.
- \_\_\_\_\_. 1960. Reversible behavior of the ultraviolet irradiated deoxyribonucleic acid and its apurinic acid. *Nature* 188:844-846.
- \_\_\_\_\_. 1961. Photochemical reactions in frozen solutions. *Nature* 190:690-694.
- Ward, D. C., E. Reich and L. Stryer. 1969. Fluorescence studies of the nucleotides and polynucleotides. *Journal of Biological Chemistry* 244:1228-1237.
- Ware, W. R. and B. A. Baldwin. 1963. Absorption intensity and fluorescence lifetime of molecules. *Journal of Chemical Physics* 40:1703-1705.
- Weber, G. 1954. Dependence of the polarization of the fluorescence on the concentration. *Transactions of the Faraday Society* 50:552-560.
- \_\_\_\_\_. 1957. Intramolecular transfer of electronic energy in dihydro diphosphopyridine nucleotides. *Nature* 180:1409.
- Weber, G. and F. W. J. Teal. 1957. Fluorescence excitation spectrum of organic compounds in solution. *Transactions of the Faraday Society* 53:640-645.
- Weber, K. 1931. Über die enge beziehung der fluoreszenz auslöschung zur hemmung photochemischer reaktionen. *Zeitschrift für Physikalische Chemie* 15:18-44. 1931.
- Wehry, E. L. and L. B. Rogers. 1966. In *Fluorescence and Phosphorescence Analysis* ed. by D. M. Hercules, New York, N. Y. Interscience, p. 125-135.

- Wehry, E. L. 1967. Valence-shell expansion in electronically excited states of aromatic sulfur compounds. *Journal of the American Chemical Society* 89:41-45.
- Weller, A. 1952. Quantitative untersuchungen der fluoreszenzwandlung bei naphtholen. *Zeitschrift für Elektrochemie* 56: 662-668.
- \_\_\_\_\_. 1961. Fast reactions of excited molecules, in *Progress in Reaction Kinetics*, ed. by G. Porter. Pergamon, New York, vol. 1. p. 181-214.
- Whillans, D. W., M. A. Herbert, J. W. Hunt and H. E. Johns. 1969. Optical detection of the triplet state of uracil. *Biochemical and Biophysical Research Communications* 36:912-918.
- Whillans, D. W. and H. E. Johns. 1969. Dependence of intersystem crossing on excitation energy in orotic acid. *Photochemistry and Photobiology* 9:323-330.
- Whitten, D. G. and Y. S. Lee. 1970. Reactions of hidden  $n-\pi^*$  excited states in N-heteroaromatics. *Journal of the American Chemical Society* 92:415-416.
- Wierzchowski, K. L., E. Litonska, and D. Shugar. 1965. Infrared and ultraviolet studies on the tautomeric equilibria in aqueous medium between monoanionic species of uracil, thymine, 5-fluorouracil, and other 2,4-diketopyrimidines. *Journal of the American Chemical Society* 87:4621-4629. 1965.
- Wilkinson, F. and J. T. Dubois. 1963. Energy-transfer by spectro-photofluorometric method. *Journal of Chemical Physics* 39: 377-383.

## APPENDICES

## APPENDIX I.

DETERMINATION OF CORRECTED FLUORESCENCE  
EXCITATION AND EMISSION SPECTRA FOR  
SOLUTIONS OF FINITE ABSORBANCE

## Introduction

The determination of true relative fluorescence data (i. e. corrected for instrumental artifacts) in instruments with right-angle geometry requires uniform irradiation through the sample. In a "corrected" instrument an attempt is made to make the instrumental response approximately proportional to the product of the fluorescence quantum yield  $\phi_f$  and the absorbance  $A$ . As consequence of the exponential nature of absorption of low energy photons, the absorbance is only a good approximation to the true absorbed intensity at absorbances  $< 0.02$  (Parker, 1968, p. 222), where only a + 2% error is introduced. At higher absorbances the approximation,

$$A = 1 - \exp(-\epsilon(\bar{\nu})cl) \approx \epsilon(\bar{\nu})cl$$

is increasingly less accurate. For solutes having high quantum yields of emission,  $\phi_f > 10^{-2}$ , this causes no problems since a low absorbance solution will still give a good fluorescence signal. However, for weak emitters various changes in experimental technique are necessary to obtain good signal/noise ratios. Some of the modifications which have been used separately or together increase the absorbed intensity

by a) widening of the slits (the consequent loss of resolution may be tolerated for broad structureless absorption and emission spectra), b) increasing the source lamp e. g. by using 900 w (Longworth and Bovey, 1966), 1600 w (Langelaar et al., 1967), or 6500 (Lipsett et al., 1970) w Xenon lamps in place of the more common 75 or 150 w lamps (attention must be paid to photochemical effects), and c) increasing the absorbance of the solution. Detection systems have been made more sensitive by i) modulation of the exciting beam in conjunction with phase-locked amplification (Longworth and Bovey 1966; Eisinger, 1969)., ii) use of R. C. noise filtration of suitable time-constant, (Eastman, 1966)., iii) reduction of stray light with double monochromators and iv) digitizing of photomultiplier signals together with repetitive scanning and accumulation of spectra in a multichannel analyzer (Taylor et al., 1966; Hauswirth and Daniels, 1970a), a time averaging computer or a digital computer.

In the current work on the room temperature fluorescence of the purine and pyrimidine bases from DNA, a method of using solutions of moderate absorbance ( $A \sim 0.6$ ) in conjunction with M. C. A. data accumulation to detect the weak fluorescence signals has been developed. This has required correction of the data for the high absorbances used. Presented here are the methods of correction<sup>7</sup> together with

---

<sup>7</sup> During the preparation of this thesis a paper by Gill (1970) appeared which contains the only detailed account of corrections we are aware of; they are developed in an entirely independent way.

experimental tests of their validity with previously well-characterized compounds.

## Materials and Methods

### Experimental

2,5-Diphenyloxazole (PPO), scintillation grade, was purchased from Packard Instrument Co. and used without further purification. For fluorescence measurements, it was dissolved in cyclohexane (Hartman-Ledden Co., fluorometric grade) and flushed with nitrogen (National Cylinder Gas Co., pre-purified, less than 8 ppm  $O_2$ ).

Anthracence (James Hinton Co., zone refined) also dissolved in  $N_2$ -flushed cyclohexane was used without further purification. Quinine bisulfate (Malinckrodt, N. F. grade) was recrystallized four times in triply distilled water and measurements taken in 0.1 N  $H_2SO_4$ .

Thymine (Calbiochem, A grade) was dissolved in 10M aqueous NaOH (Hartman-Ledden Co., fluorometric grade) which had been diluted to 0.01 M with triply distilled water.

Fluorescence and absorption data were recorded on a Turner Model 210 spectrofluorometer. All fluorescence excitation and absorption spectra were taken with a 25 Å excitation monochromator bandwidth and with the emission bandwidth 100 Å for excitation and 250 Å for absorption. Emission spectra were taken with a 150 Å

excitation bandwidth and 25 Å emission monochromator bandwidth. Some absorption data for low absorbance solutions were confirmed on a Cary Model 15 spectrophotometer using a 10 cm pathlength cell.

### Correction Procedures

The Turner Model 210, is a constant bandwidth, right-angle optics, energy corrected instrument. Its output is a ratio of the photomultiplier voltage due to fluorescence to that due to a reference lamp when the energy output of the lamp is made equal to the transmitted excitation energy through a bolometer-feedback system (Turner, 1964). The routine operation of the Turner is based on infinitesimal absorbing solutions of moderate fluorescence as detailed by Turner (1964). For solutions of finite absorbance additional considerations are needed as outlined below.

### Emission Spectra

The total transmitted energy at any bandwidth,

$$\int^{\lambda} \frac{dE_t^{\lambda}}{d\lambda} d\lambda$$

can be approximated as the product of the energy transmitted at the excitation wavelength and the fixed excitation bandwidth  $\Delta\lambda$ , and will be abbreviated as  $E\Delta\lambda_{ex}$ . When equal energies from the solution and reference lamp are incident on the bolometer the relationship is

(Turner, 1964),

$$E_r = K_1 E \Delta \lambda_{ex} \quad (\text{A. 1. 1})$$

where  $E_r$  = reference lamp energy

$K_1$  = instrumental constants and fraction of energy detected.

Substituting for  $E$  in terms of the transmitted quantal intensity  $I_t$ ,

$$E \propto \frac{I_t}{\lambda_{ex}} \quad E \Delta \lambda_{ex} \propto \frac{I_o \exp(-A)}{\lambda_{ex}} \Delta \lambda_{ex}$$

so that

$$E_r = K_2 \frac{I_o \exp(-A)}{\lambda_{ex}} \Delta \lambda_{ex} \quad , \quad (\text{A. 1. 2})$$

where  $I_o$  = incident quantal intensity at the excitation wavelength,  $\lambda_{ex}$

$A$  = absorbance at  $\lambda_{ex}$ .

The response of the photomultiplier to the reference beam is then

$$V_R = K_3 f_a(\lambda_{em}) \frac{I_o \exp(-A)}{\lambda_{ex}} \Delta \lambda_{ex} \quad (\text{A. 1. 3})$$

where  $f_a(\lambda_{em})$  = attenuation factor of the wedge-filter cam system,

and is a function of  $\lambda$  emission.

Alternately the photomultiplier also sees the fluorescence defined as

$$\begin{aligned} V_F &= K_4 f_b(\lambda_{em}) \frac{dF}{d\lambda_{em}} \Delta \lambda_{em} \\ &= K_4 f_b(\lambda_{em}) I_o [1 - \exp(-A)] \Delta \lambda_{ex} \frac{d\phi_f}{d\lambda_{ex}} \Delta \lambda_{em} \end{aligned} \quad (\text{A. 1. 4})$$

where  $f_b(\lambda_{em})$  = variation in detector sensitivity as a function of  $\lambda_{em}$

$\frac{dF}{d\lambda_{em}}$  = spectral distribution of fluorescence intensity

$I_0 [1 - \exp(-A)] \Delta\lambda_{ex}$  = absorbed quantal intensity at finite absorbance  $A$  and bandwidth  $\Delta\lambda_{ex}$ .

$\phi_f$  = quantum yield of fluorescence.

Letting  $\theta_e$  denote the ratio-recording pen position,

$$\theta_e = \frac{V_F}{V_R} = K_5 \frac{f_b(\lambda_{em})}{f_a(\lambda_{em})} \lambda_{ex} \frac{[1 - \exp(-A)]}{\exp(-A)} \frac{d\phi_f}{d\lambda_{em}} \Delta\lambda_{em} \quad (A.1.5)$$

When  $f_a(\lambda_{em})$  and  $f_b(\lambda_{em})$  are made proportional through a mechanical drive from the emission monochromator, the resulting fundamental instrumental equation accounting for finite absorbance is,

$$\theta_e = K_6 \lambda_{ex} [\exp(A) - 1] \frac{d\phi_f}{d\lambda_{em}} \Delta\lambda_{em} \quad (A.1.6)$$

Since  $\frac{1 - \exp(-A)}{\exp(-A)} \cong A$  in the low absorbance limit, the fundamental instrumental equation for solutions with absorbances  $< 0.04$  is

$$\theta_0 = K_6 \lambda_{ex} A \frac{d\phi_f}{d\lambda_{em}} \Delta\lambda_{em} \quad (A.1.7)$$

For emission spectra  $\lambda_{ex}$ ,  $A$ , and  $\Delta\lambda_{em}$  are constant and

$$\theta_e^{em} = K_7 [\exp(A) - 1] \frac{d\phi_f}{d\lambda_{em}} \Delta\lambda_{em} = K_7' \frac{d\phi_f}{d\lambda_{em}} \Delta\lambda_{em} \quad (A.1.8)$$

and in the low absorbance limit,

$$\theta_0^{\text{em}} = K_7 A \frac{d\phi_f}{d\lambda_{\text{em}}} \Delta\lambda_{\text{em}} = K_7'' \frac{d\phi_f}{d\lambda_{\text{em}}} \Delta\lambda_{\text{em}}. \quad (\text{A.1.9})$$

The relative emission shape therefore will remain unaltered and corrected at finite absorbances, provided the geometry of emission collecting optics is valid at the absorbance used. (The collecting optics are obviously designed not for a point emitter, but for a large emitter of approximately cell dimensions (Turner, 1968)).

True relative emission spectra have the form,

$$R^{\text{em}} = K \frac{d\phi_f}{d\lambda_{\text{em}}}$$

and therefore from Equation (A.1.8),

$$R^{\text{em}} = \frac{\theta_e^{\text{em}}}{\Delta\lambda_{\text{em}}} = K_7' \frac{d\phi_f}{d\lambda_{\text{em}}}. \quad (\text{A.1.10})$$

In order to report emission spectra in the more meaningful and internationally recommended (Chapman et al., 1963) units of relative quantum yields at constant wavenumber resolution, the conversion is required, (Parker, 1968, p.153)

$$d\bar{\nu} = \frac{d\lambda}{\lambda^2}$$

and from Equation (A.1.10) the reported emission data  $R^{\text{em}}$  are given as,

$$R_{\nu}^{\text{em}} = \frac{\theta_e^{\text{em}}}{\Delta\lambda_{\text{em}}} (\lambda_{\text{em}})^2 = K_7' \frac{d\phi_f}{d\nu_{\text{em}}} \quad (\text{A. 1. 11})$$

### Excitation Spectra

For excitation spectra  $\Delta\lambda_{\text{em}}$  and usually  $\frac{d\phi_f}{\lambda_{\text{em}}}$  are kept constant and the signal at finite absorbance is,

$$\theta_e^{\text{ex}} = K_8 \lambda_{\text{ex}} [\exp(A)-1] ; \quad (\text{A. 1. 12})$$

and in the low absorbance limit,

$$\theta_0^{\text{ex}} = K_8 \lambda_{\text{ex}} A . \quad (\text{A. 1. 13})$$

The true relative excitation spectrum  $R^{\text{ex}}$  is then

$$\frac{\theta_e^{\text{ex}}}{\lambda_{\text{ex}}} = K_8 [\exp(A)-1] , \quad (\text{A. 1. 14})$$

and for the limiting case of infinitesimal absorbance,

$$\frac{\theta_0^{\text{ex}}}{\lambda_{\text{ex}}} = K_8 A . \quad (\text{A. 1. 15})$$

To compare  $\theta_e^{\text{ex}}$  with the absorption spectra the data is reported as,

$$R^{\text{ex}} = \frac{\theta_e^{\text{ex}}}{\lambda_{\text{ex}}} \frac{A}{[\exp(A)-1]} = K_8 A . \quad (\text{A. 1. 16})$$

Having no  $d\lambda$  term, (See Equation (A. 1.5)),  $R^{ex}$  is plotted directly on either a linear wavenumber or wavelength scale.

### Quantum Yields

The quantum yield can be determined as previously (Turner, 1964) by integrating Equation (A. 1. 6) and using this resultant area under the emission curve to calculate the yield relative to a standard:

$$\int_{\lambda_{em}} \theta_e^{em} d\lambda_{em} = K_6 \lambda_{ex} [\exp(A)-1] \Delta\lambda_{em} \int_{\lambda_{em}} \frac{d\phi_f}{d\lambda_{em}} d\lambda_{em} . \quad (A. 1. 17)$$

Letting  $B$  = emission area and  $\phi_f$  the integrated quantum yield,

$$B = K_6 \lambda_{ex} [\exp(A)-1] \Delta\lambda_{em} \phi_f .$$

From Equation (A. 1. 5) it can be seen that the term  $[\exp(A)-1]$  is a simplified form of a ratio of the absorbed and transmitted intensities, and relative to a standard fluorescent compound of quantum yield  $\phi_s$ , the quantum yield of an unknown is,

$$\phi_u = \phi_s \frac{B_u}{B_s} \frac{K_s}{K_u} \frac{\lambda_{ex}^s}{\lambda_{ex}^u} \frac{(\% As / \% Ts)}{(\% Au / \% Tu)} \quad (A. 1. 18)$$

where  $K_s$ ,  $K_u$  = instrumental settings, including  $\Delta\lambda_{em}$ , and  $A' =$  absorption not absorbance  $A$ .

The use of  $\%A_s$  and  $\%A_u$ , the percent absorption at  $\lambda_{ex}$ , gives only a true measure of the ratio of absorbed quanta if both absorption spectra are relatively flat in the vicinity of  $\lambda_{ex}$  or the excitation bandwidths are quite small. To derive an expression of utility for molecules of low  $\phi_f$  the excitation bandwidth must be wide (150 Å in this case) so that maximum quanta are incident. With wide slits a significant energy range of quanta are incident to the solution and the absorption values must be taken on the Turner 210 with the same bandwidths as used for excitation in fluorescence measurements. This is necessary to get an accurate measure of the relative absorbed quanta, particularly for molecules like anthracene where the absorption spectrum varies sharply around  $\lambda_{ex}$  at 357 nm.

Taking  $\phi_{fl}$  for PPO in cyclobutane as 1.00 (Berlman, 1965), Equation (A.1.18) was used to calculate the anthracene quantum yields. For quinine bisulfate and alkaline thymine, an additional factor accounting for the difference of indices of refraction between the solvents water and cyclohexane must be included on the right side of Equation (A.1.18), (Fletcher, 1967),

$$\left(\frac{n_{\text{water}}}{n_{\text{cyclohex.}}}\right)^2 \quad . \quad (A.1.19)$$

In all cases quantum yields were calculated relative to the PPO at the same absorbance which maintains the same emitting geometry (Parker, 1968, p. 263).

## Results

The procedures derived in the previous section were applied to the fluorescent data of substances chosen for the following characteristics:

- a. Highly structured spectra in different wavenumber regions (anthracene and PPO in cyclohexane), and
- b. Well documented unstructured excitation spectrum and emission spectrum in the visible region (quinine bisulfate in 0.1 N  $\text{H}_2\text{SO}_4$ ), or well documented fluorescence excitation spectrum differing from its absorption spectrum (aqueous thymine in 0.01 N NaOH).

For excitation spectra the validity of the corrections was checked by comparing the relative intensities of uncorrected and corrected excitation spectra of solutions of various absorbances (from 0.02 to 0.64) with the absorption intensities at the same wavenumber. "Uncorrected" intensities and spectra refer to data transformed for plotting on a linear energy scale but not corrected for finite absorbance. Relative fluorescence emission intensities are also compared for several concentrations of some species. In order not to obscure possible deviations all fluorescence and absorption data were normalized to 1.00 at the most intense peak in the recorded range (except for quinine excitation which was normalized to 1.00 at  $2.89 \mu\text{m}^{-1}$ ). Where possible,

comparison is also made to previously reported data.

### Excitation and Emission Spectra

Anthracene. For all absorbances, including  $0.64$  at  $2.80 \mu\text{m}^{-1}$ , there is good agreement between corrected relative fluorescence excitation, absorption, and previously reported absorption spectra intensities (Table A.1.1). Since the output of the Turner 210 for excitation is a function of the ratio of absorbed and transmitted quanta (Equations (A.1.5) and (A.1.6)), at finite absorbances highly absorbing bands will cause a disproportionate increase in the excitation of signal (or relatively higher peak to valley ratios in structured spectra). Uncorrected excitation spectra are therefore in progressively worse agreement with absorption as the concentration is increased (Figure A.1.1). Relative emission intensities (Table A.1.2 and Figure A.1.1) are virtually constant for all four concentrations tested, although there is some minor disagreement with Berlman's (1965, p. 123) data (10% maximum discrepancy).

PPO. As with anthracene, the corrected relative excitation intensities at all absorbances agree well with absorption data and previous reports (Table A.1.3). Emission spectra (Figure A.1.2) agree well within the three samples run but are markedly higher than Berlman's data at the first low energy maximum and minimum. This can probably be attributed to significant overlap of absorption and

Table A. 1. 1. Relative absorbance and corrected fluorescence excitation spectrum intensities for several concentrations of anthracene in cyclohexane.

$\bar{\nu}$ ( $\mu\text{m}^{-1}$ )	Spectral Feature	$R_{\bar{\nu}}^{\text{ex}} / R_{2.80}^{\text{ex}}$				$A_{\bar{\nu}} / A_{2.80}$	
		Absorbance at $2.80 \mu\text{m}^{-1}$				this work	Berlman (1965, p. 123) *
		0.02	0.20	0.40	0.68		
3.24	Maximum	.17	.15	.13	.14	.14	.13
3.08	Maximum	.36	.38	.34	.35	.36	.34
3.03	Minimum	.28	.28	.26	.25	.27	.24
2.94	Maximum	.67	.67	.66	.67	.67	.65
2.88	Minimum	.36	.36	.34	.36	.34	.32
2.72	Minimum	.24	.25	.22	.22	.22	.21
2.65	Maximum	.94	.94	.95	.96	.97	.98

\* Data taken from a spectrum

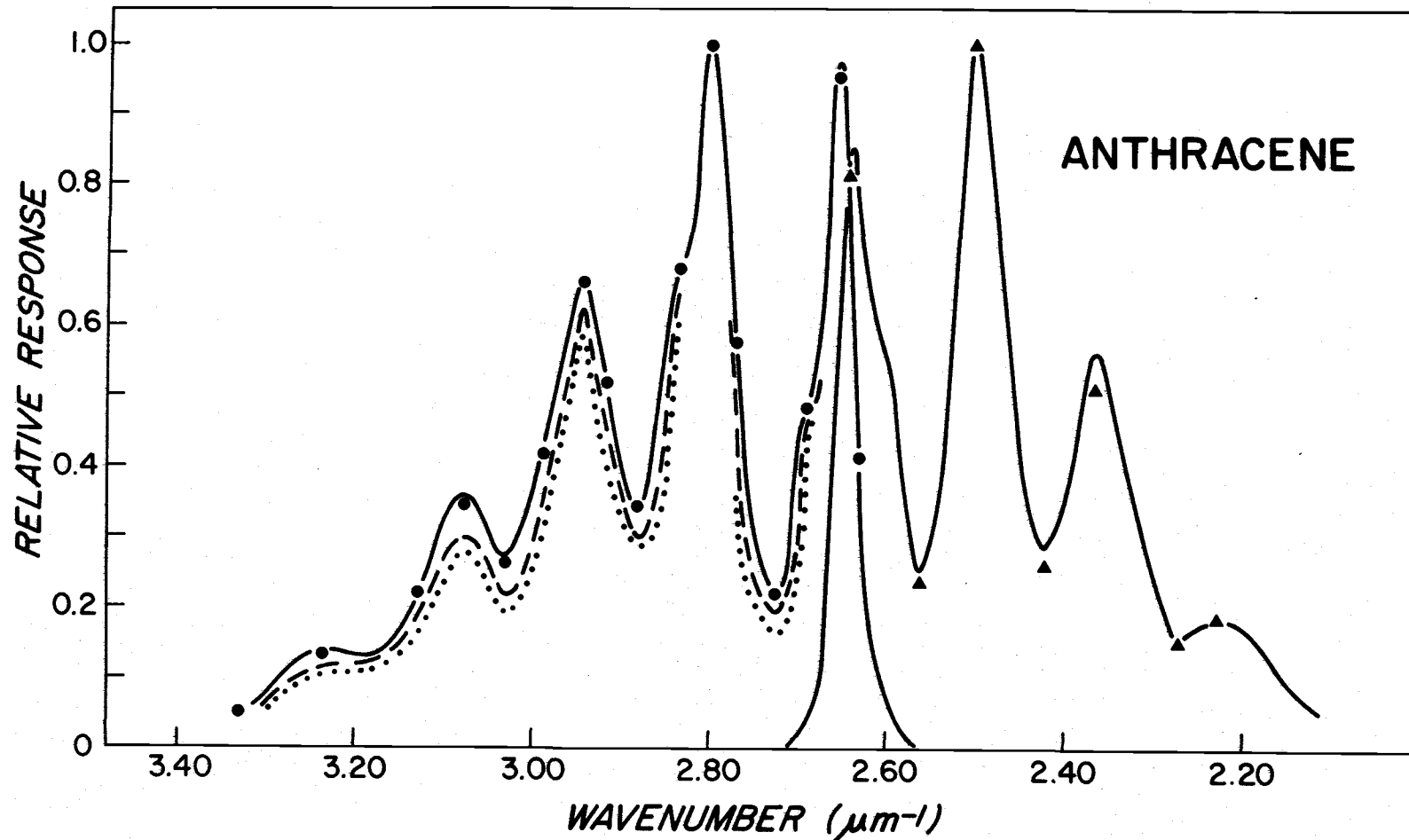


Figure A.1.1. Relative absorption and emission spectra (solid lines) and uncorrected excitation spectra for anthracene in cyclohexane at  $A_{2.80} = 0.40$  (dashed line) and  $A_{2.80} = 0.68$  (dotted line), all normalized to unity at their most intense peak. The solid circles are the excitation values corrected in finite dilution (Equation (A.1.16)). The solid triangles are the results of Berlman (1965).

Table A. 1. 2. Relative fluorescence emission spectrum intensities for several concentrations of anthracene in cyclohexane.

$\bar{\nu}$ ( $\mu\text{m}^{-1}$ )	Spectral Feature	$R_{\bar{\nu}}^{\text{em}} / R_{2.50}^{\text{em}}$			Berlman (1965, p. 123) <sup>+</sup>
		Absorbance at $2.80 \mu\text{m}^{-1}$			
		0.02	0.20	0.40	
2.64	Maximum	.85	*	*	.81
2.56	Minimum	.25	*	*	.23
2.42	Minimum	.28	.28	.27	.25
2.35	Maximum	.56	.56	.55	.50
2.23	Maximum	.18	.18	.18	.16

\* Self absorption lowers the relative emission intensity ratio

<sup>+</sup> Data taken from a spectrum

Table A.1.3. Relative absorbance and corrected excitation spectrum intensities for several concentrations of PPO in cyclohexane.

$\bar{\nu}$ ( $\mu\text{m}^{-1}$ )	$R_{\bar{\nu}}^{\text{ex}}/R_{3.20}^{\text{ex}}$			$A_{\bar{\nu}}/A_{3.20}$	
	Absorbance at $3.20 \mu\text{m}^{-1}$			this work	Gill (1969) <sup>+</sup>
	0.02	0.20	0.40		
3.57	.46	.45	.43	.46	.46
3.45	.72	.69	.67	.72	.72
3.24	.97	.98	.98	.97	.96
3.19	.91	.91	.92	.91	.91
3.15	.93	.93	.94	.93	.94
3.00	.46	.43	.41	.44	.42

<sup>+</sup> Data taken from a spectrum

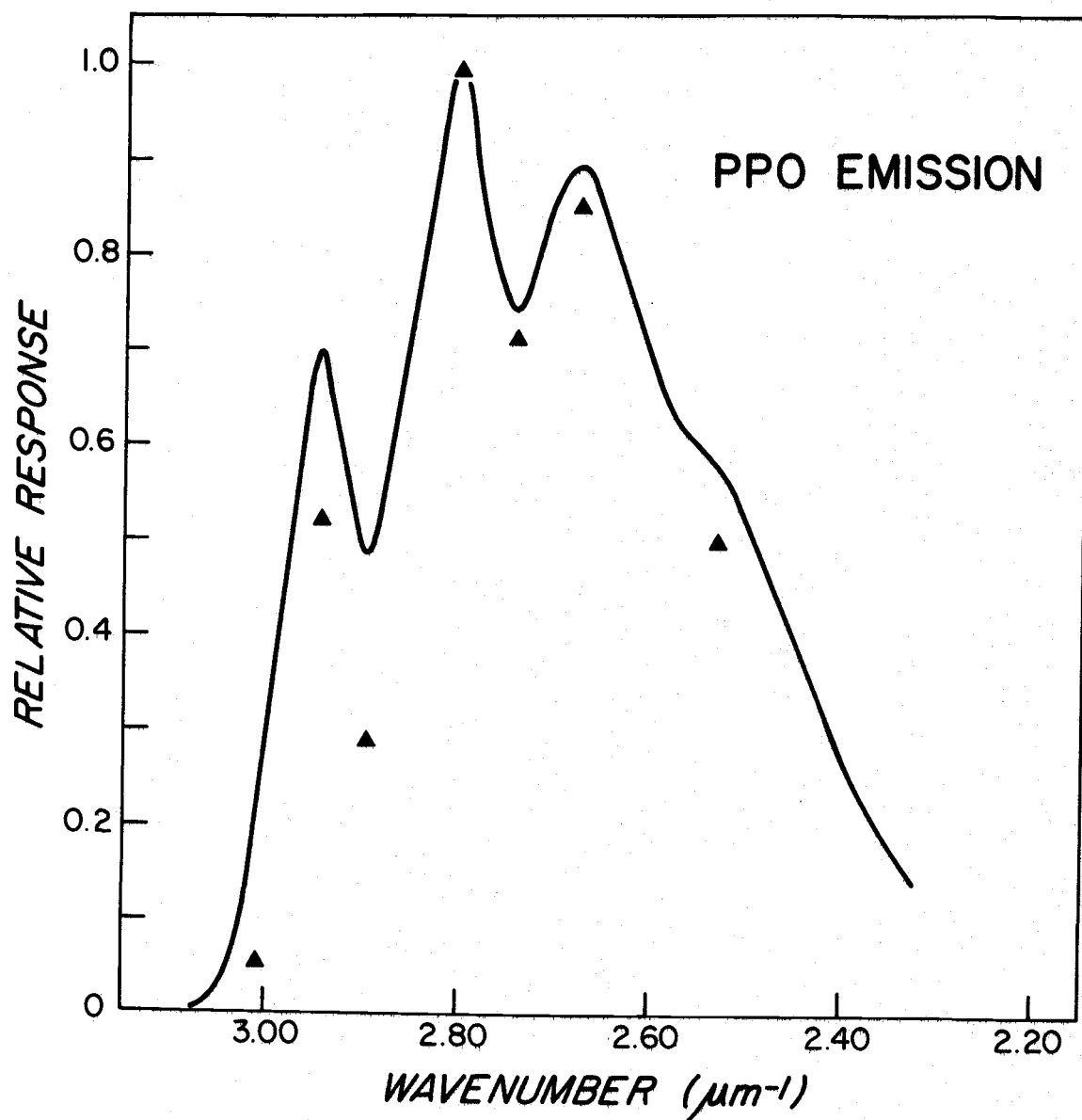


Figure A.1.2. Corrected emission spectrum of PPO in cyclohexane normalized to unity at  $2.80 \mu\text{m}^{-1}$ . The solid triangles are the reported results of Berlman (1965).

emission spectra at  $2.95 \mu\text{m}^{-1}$ , causing errors due to reabsorption at the higher concentrations used in Berlman's front-face-measurements.

Quinine Bisulfate. Fluorescence excitation and absorption spectra agree as expected (Table A. 1. 4) to within 2% for the low absorbance sample ( $A_{2.89} = 0.02$ ) when both spectra are recorded at the same bandwidth resolution and to within 4% of previously reported values. At an absorbance of 0.20 the uncorrected excitation spectrum shows marked disagreement with absorption (Figure A. 1. 3) and at  $4.00 \mu\text{m}^{-1}$ , where the absorbance is 1.06, the deviation is as high as 58%. Application of the corrections for finite absorbance brings all values to agreement within 3%. For the solution with  $A_{2.89} = 0.40$  uncorrected values are again in error (Table A. 1. 3) and correction brings the relative intensity at  $3.16 \mu\text{m}^{-1}$  to within 3% and of  $4.35 \mu\text{m}^{-1}$  to within 17%. This latter value is probably not better because the low output of the xenon source lamp at  $4.35 \mu\text{m}^{-1}$  coupled with an absorbance here of about 0.80 allows only a very small amount of transmitted and fluorescent light to reach the photomultiplier. The very high absorbance at  $4.00 \mu\text{m}^{-1}$  ( $> 2.00$ ) precludes accurate data here.

Alkaline Thymine. Corrected excitation intensities (Table A. 1. 5) agree to within 5% of previous values except at  $3.20 \mu\text{m}^{-1}$  where there is larger disagreement with one reference. Comparison of the fluorescence excitation and absorption spectrum shows the

Table A.1.4. Relative absorbance and corrected fluorescence excitation spectrum intensities for several concentrations of quinine bisulfate in 0.1N H<sub>2</sub>SO<sub>4</sub>.

$\bar{\nu}$ ( $\mu\text{m}^{-1}$ )	$R_{\bar{\nu}}^{\text{ex}}/R_{2.89}^{\text{ex}}$			Gill (1969)	$A_{\bar{\nu}}/A_{2.89}$
	Absorbance at 2.89 $\mu\text{m}^{-1}$				
	0.02	0.20	0.40		
4.35	2.01	1.95	2.34	1.94 <sup>+</sup>	2.05
4.00	5.00	4.93		5.01 <sup>*</sup>	5.03
3.16	.82	.81	.79	.81 <sup>*</sup>	.82

<sup>+</sup> Data taken from a spectrum

<sup>\*</sup> Taken from tabulated data

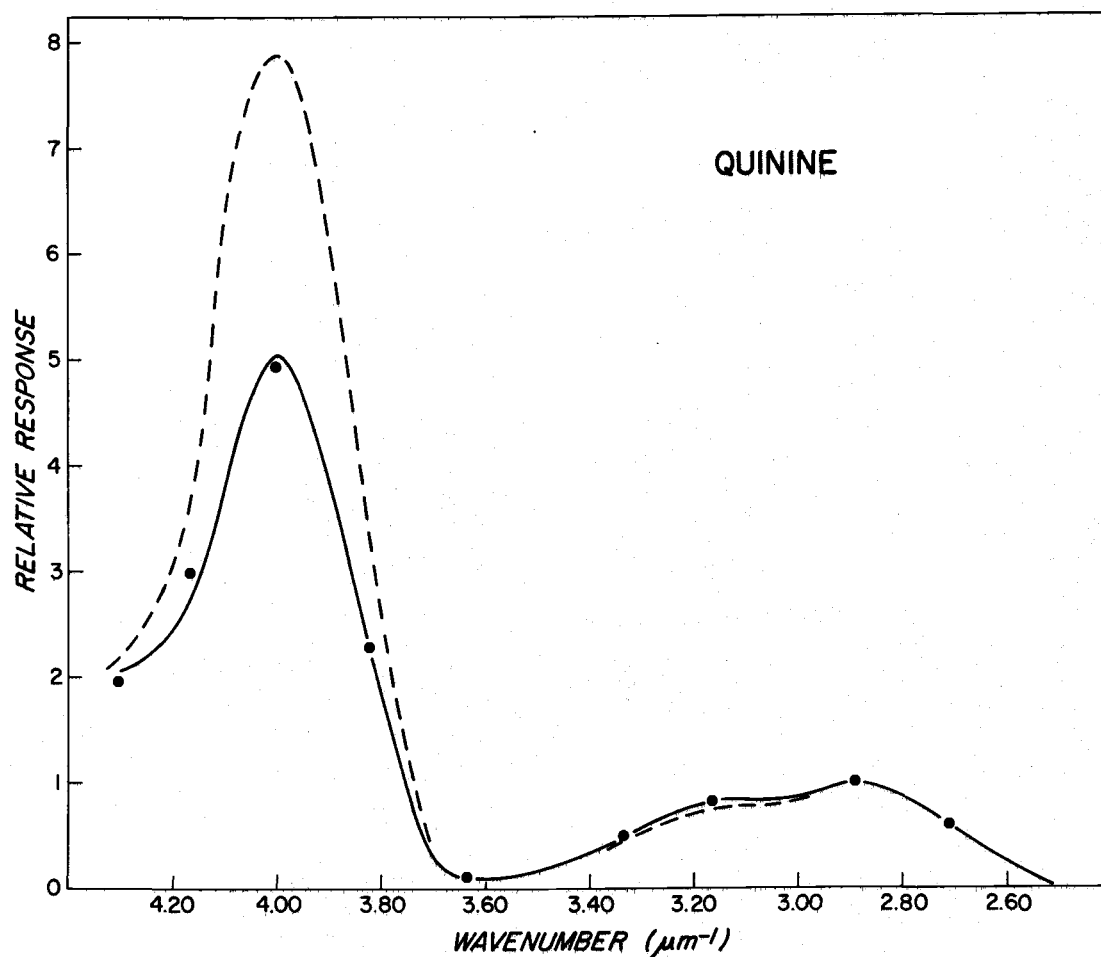


Figure A.1.3. Relative absorption (solid line) and uncorrected fluorescence excitation spectra (dashed line) of quinine (absorbance at  $2.89\mu\text{m}^{-1} = 0.20$ ) in  $0.1\text{N H}_2\text{SO}_4$ , normalized to unity at  $2.89\mu\text{m}^{-1}$ . The solid circles are excitation values corrected to infinite dilution using Equation (A.1.16).

Table A. 1. 5. Relative absorbance and corrected excitation spectrum intensities for  $8 \times 10^{-5}$  M thymine (absorbance at  $3.45 \mu\text{m}^{-1} = 0.44$ ) in 0.01 N NaOH.

$\bar{\nu} (\mu\text{m}^{-1})$	$R_{\bar{\nu}}^{\text{ex}} / R_{\bar{\nu}_{\text{max}}}^{\text{ex}}$			$A_{\bar{\nu}} / A_{3.45}$
	this work	Berens and Wierzchowski (1969)*	Gill (1969)†	
3.80	.23	.23	.26	.76
3.70	.40	.40	.40	.86
3.60	.68	.70	.67	.93
3.50	.91	.92	.90	.98
3.40	1.00	.95	.99	.97
3.30	.70	.70	.72	.60
3.20	.23	.18	.23	.13

\* Data taken from table

† Data taken from a spectrum

usual disagreement in accordance with previous reports (see Section III).

### Quantum Yields

The quantum yields for quinine and anthracene are invariant within 10% over a 34-fold increase in concentration (Table A. 1. 6). Since these yields were calculated relative to PPO at a closely identical absorbance, a true test of Equation (A. 1. 18) must involve a standard at a different absorbance.

The ratio of quantum yields for absorbances of 0. 20 and 0. 40 in Table A. 1. 7 show that uncorrected values (i. e. yields calculated using the factor of  $\frac{A'_s}{A'_u}$  instead of  $(\% A'_s / \% T_s) / (\% A'_u / \% T_u)$  in Equation (A. 1. 18)) are 11 to 23% higher than the expected value of unity and that the corrected values are all within 3%.

Relative quantum yields agree with literature values for anthracene (Berlman, 1965, p. 123) and alkaline thymine (Gill, 1968) but for quinine in 0. 1 N H<sub>2</sub>SO<sub>4</sub>,  $\phi_f$  is ~ 40% higher than the absolute values reported by Dawson and Windsor (1968) and Melhuish (1961). However the most recent value of Scott et al. (1970)  $\phi_f = 0. 70 \pm 0. 02$ , agrees with our yield. The explanation offered is that earlier workers failed to take into account the finite emission area beyond 1. 80  $\mu\text{m}^{-1}$  (550 nm) during their spectral corrections and their quantum yields were therefore low. Since the Turner 210 is a corrected instrument, no after-

Table A.1.6. Fluorescence quantum yields as a function of absorbance at the excitation wave number.

Compound	Fluorescence Quantum Yield					Literature Values
	Absorbance					
	0.02	0.20	0.40	0.44	0.68	
Quinine	0.74	0.73	0.74	----	----	0.50-0.57(a), 0.70(b)
Anthracene	0.35	0.35	0.33	----	0.32	0.36(c)
Thymine (pH 12)	----	----	----	$1.7 \times 10^{-3}$	----	$1.6 \times 10^{-3}$ (d)

(a) Dawson and Windsor (1968); Melhuish (1961)

(b) Scott et al., (1970)

(c) Berlman (1965, p. 123)

(d) Gill (1968)

Table A. 1. 7. Ratio of fluorescence quantum yields for solutions of 0. 40 absorbance to those at 0. 20 absorbance.

$\phi_f(A=0.40)/\phi_f(A=0.20)$		
Compound	Uncorrected	Corrected
PPO	1. 23	0. 97
Quinine	1. 20	0. 98
Anthracene	1. 21	0. 97

the-fact corrections are needed for instrumental response. In this work, a finite emission intensity for quinine bisulfate was noted at  $1.80 \mu\text{m}^{-1}$  and therefore emission spectra were routinely run to  $1.67 \mu\text{m}^{-1}$  (600 nm) (the actual calculated emission area extends slightly past  $1.67 \mu\text{m}^{-1}$  and is estimated by extrapolation of the spectrum slope at this wavenumber; this procedure adds only about 2% of the total area.). Our findings are therefore consistent with Scott's explanation,

In addition, the measured fluorescence lifetime of quinine in  $1 \text{ N H}_2\text{SO}_4$  is  $\tau_s = 19.4 \times 10^{-9}$  sec. (Ware and Baldwin, 1964) and the calculated natural lifetime is  $\tau_0 = 27 \times 10^{-9}$  sec. The theoretically expected fluorescence quantum yield is then  $\tau_s/\tau_0 = 0.72$  in agreement with our value.

#### Discussion

Application of the derived corrections to the observed excitation spectra brings all data into good agreement with the low absorbance excitation spectra, previously reported spectra and, except for alkaline thymine, with the absorption spectra. That the method is successful for all sample absorbances  $\sim 0.40$  (for anthracene to 0.68 and quinine to 1.06 at  $4 \mu\text{m}^{-1}$ ) suggests it is usable up to absorbances between 0.4 and 1.0 and energies  $\sim 4.00 \mu\text{m}^{-1}$ .

Agreement of all reported emission spectra at finite absorbances with those in dilute solution and with previous reports confirms

our conclusions that the relative shape of the emission spectra need no additional correction at higher absorptions. Also the invariance of the calculated quantum yields for anthracene and quinine bisulfate confirm our corrections to the relative emission area.

As indicated, the primary purpose of the corrections derived here is to extend the range of obtaining corrected fluorescence data down to molecules with yields  $< 10^{-3}$ . Successful application to molecules of high quantum yield and alkaline thymine shows the method's validity, but the final test of its usefulness must be detection and correction of fluorescence data from a weak emitter. Section I is ample evidence of its utility.

This method is directly usable for the Turner Model 210 and with slight modification for any instrument with right angle optics of comparable sensitivity. It fills the gap between right angle measurements where low concentrations were of limited use for weak emitters and front face measurements where high concentrations often introduces artifacts due to eximer formation.

## APPENDIX II

SAMPLE CALCULATIONS FOR  
SPECTRAL CORRECTIONSAdenine

The output of the Turner 210 for fluorescence excitation (Figure A. 2. 1) and emission (Figure A. 2. 2) are accumulated as described in Section I. Two scans of each spectrum less two background scans yield Figure A. 2. 3 and Figure A. 2. 4, respectively. Manual tabulation of this data is shown in Table A. 2. 1 under columns  $\theta^{\text{ex}}$  and  $\theta^{\text{em}}$ . These data are handled in successive steps as shown in the columns of Table A. 2. 1. The normalized corrected data for fluorescence excitation  $R^{\text{ex}}$  (Equation A. 1. 16) and emission  $R^{\text{em}}$  (Equation A. 1. 11) and absorption  $R_A$  are then plotted vs. wavenumber and presented in Figure 1. 1.

All other fluorescence spectra taken at finite absorbances are handled in an analogous manner.

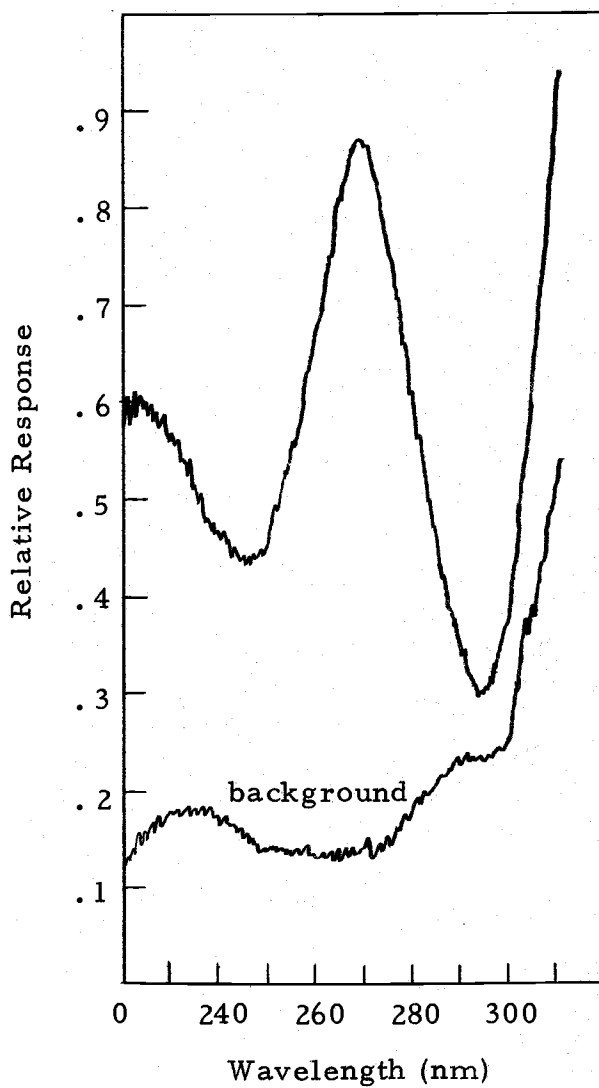


Figure A.2.1. Adenine excitation spectrum, Turner Model 210 output.

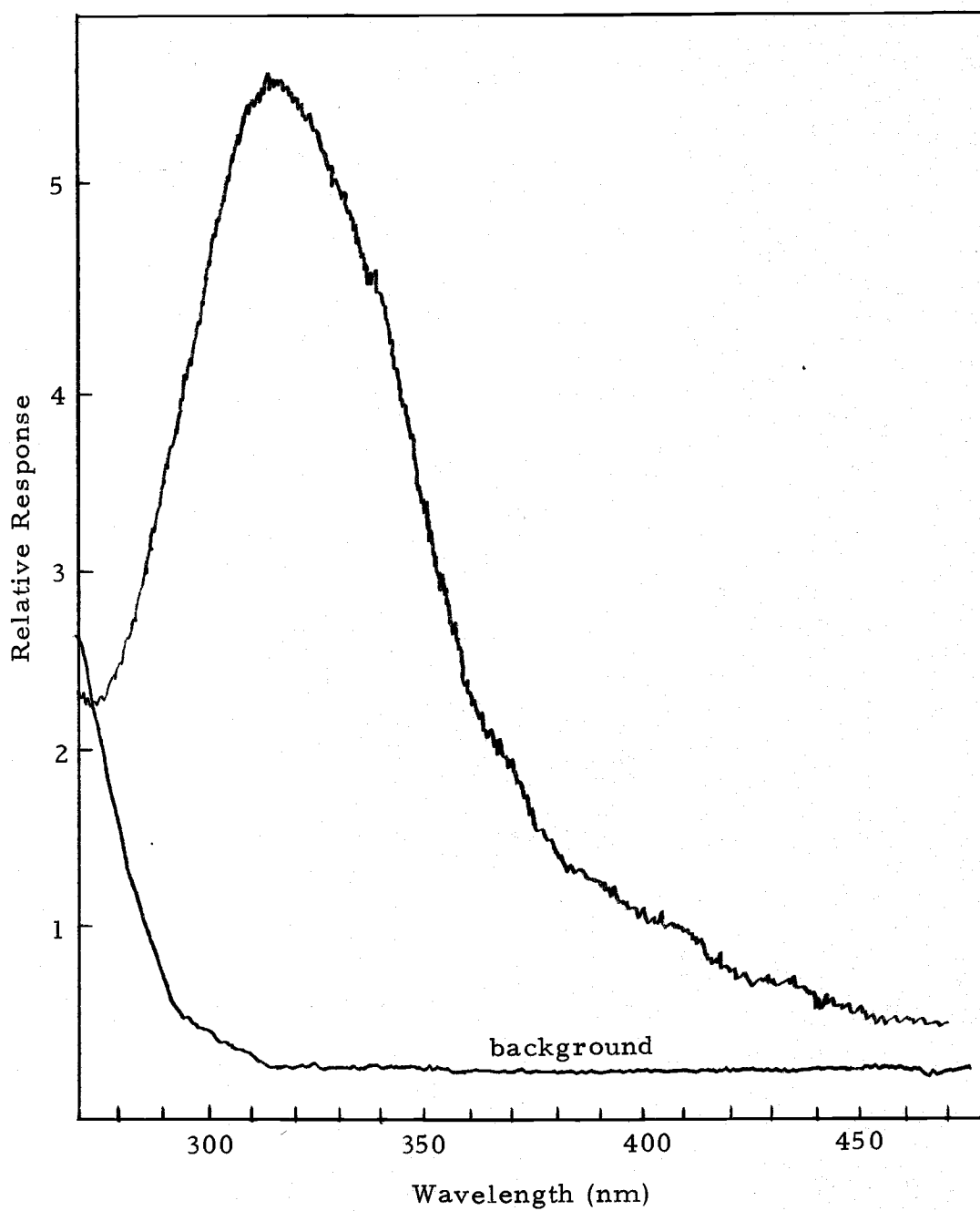


Figure A. 2. 2. Adenine emission, Turner Model 210 output.

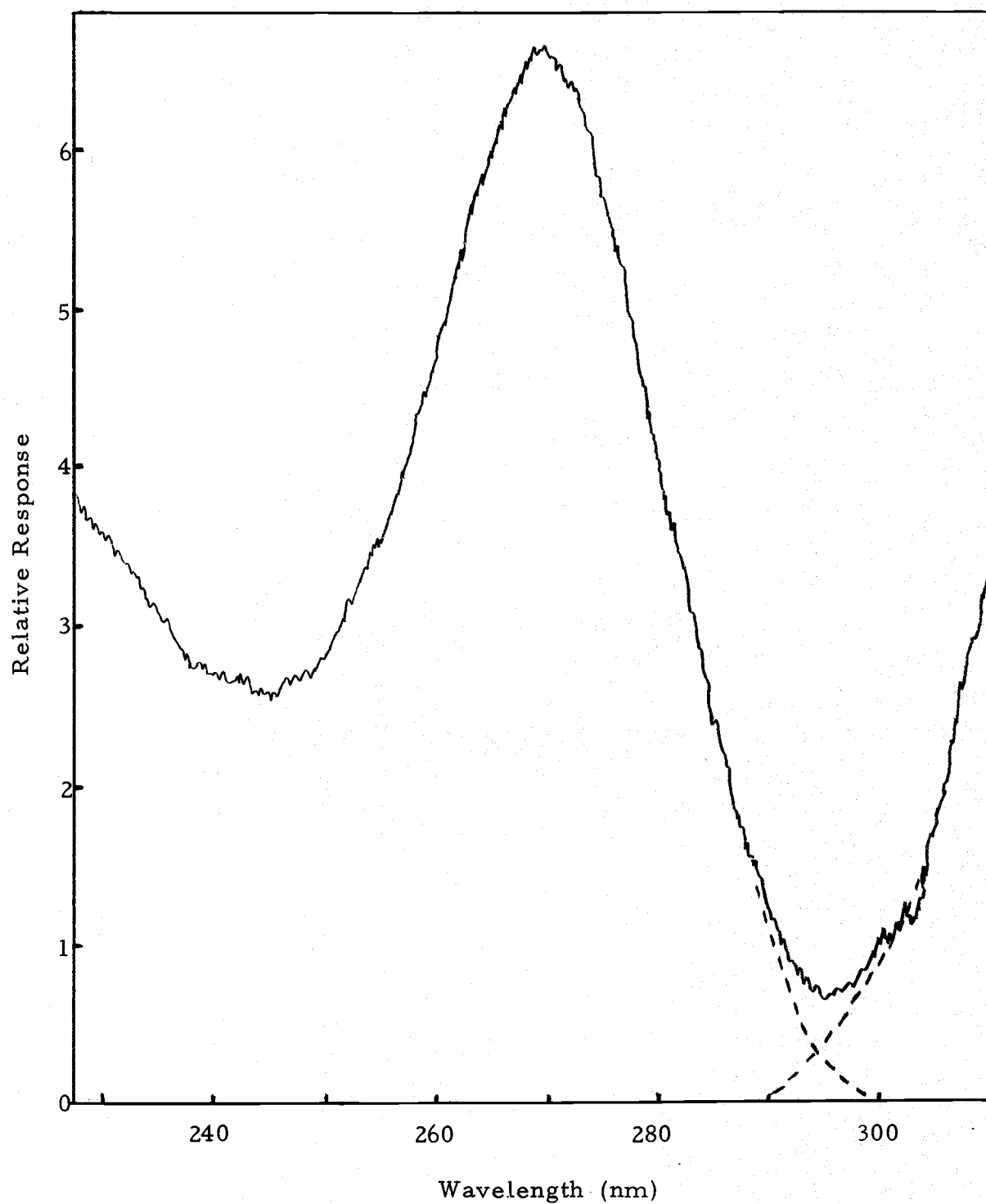


Figure A. 2. 3. Adenine excitation spectrum, multichannel analyser output, 2 scans less 2 background scans

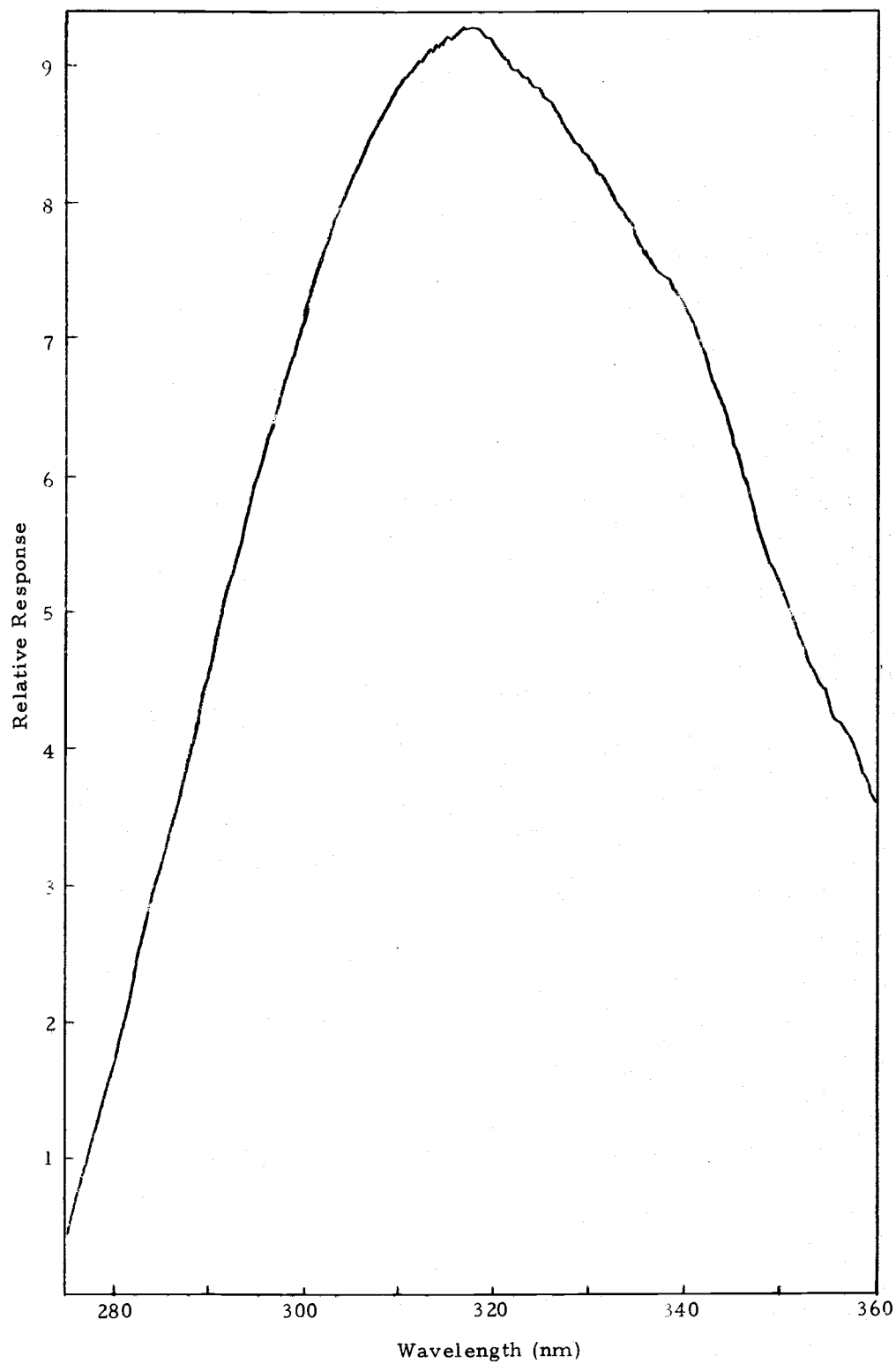


Figure A. 2. 4. Adenine emission spectrum, multichannel analyser output, 2 scans less 2 background scans.

Table A. 2. 1. Data used for calculating adenine fluorescence excitation and emission spectra.

Excitation								Emission				
(nm) $\lambda$	( $\mu\text{m}^{-1}$ ) $\frac{1}{\nu}$	$\theta^{\text{ex}}$	$\frac{\theta^{\text{ex}}}{\lambda}$	A	$\theta_0^{\text{ex}}$	$R^{\text{ex}}$	$R_A$	(nm) $\lambda$	( $\mu\text{m}^{-1}$ ) $\frac{1}{\nu}$	$\theta^{\text{em}}$	$\theta_0^{\text{em}}$	$R^{\text{em}}$
228.5	4.376	360	157	.185	143	769	260	275	3.363	40	30	32
233.5	4.282	305	130	.220	116	624	309	280	3.571	180	141	150
238.5	4.193	265	110	.297	95	511	417	285	3.509	315	256	273
243.5	4.107	235	104	.402	85	457	565	290	3.448	470	395	422
248.5	4.024	280	112	.520	85	457	730	295	3.390	590	513	547
253.5	3.944	355	139	.629	100	538	883	300	3.333	715	644	682
258.5	3.868	465	179	.705	124	667	990	305	3.279	815	758	809
263.5	3.795	538	222	.683	155	833	952	310	3.226	885	850	907
268.5	3.723	662	245	.529	186	1000	743	315	3.175	920	913	982
273.5	3.656	570	207	.307	177	952	431	320	3.125	915	937	1000
278.5	3.590	410	146	.142	136	731	199	325	3.077	375	924	986
283.5	3.527	245	86	.052	84	452	73	330	3.030	870	893	953
288.5	3.466	110	33	.015	38	204	21	335	2.985	772	866	924
293.5	3.406	30						340	2.941	700	809	863
								350	2.857	570	637	680
								360	2.778	355	760	491
								370	2.703	250	383	409
								380	2.632	270	318	339

$\theta^{\text{ex}}$  = relative excitation intensity (uncorrected)

A = absorbance

$\theta_0^{\text{ex}}$  = relative excitation intensity (corrected according to Equation (A. 1.

$R^{\text{ex}}$  =  $\theta_0^{\text{ex}}$  normalized to 1000 at its maximum

$R_A$  = A normalized to 1000 at its maximum

$\theta^{\text{em}}$  = relative emission intensity (uncorrected)

$\theta_0^{\text{em}}$  =  $\lambda^2 \theta^{\text{em}}$

$R^{\text{em}}$  =  $\lambda^2 \theta^{\text{em}}$  normalized to 1000 at its maximum

## APPENDIX III.

## STANDARD FLUORESCENCE SPECTRA

Table A. 3. 1. PPO :  $6 \times 10^{-7}$  M in nitrogen flushed cyclohexane at  $300^{\circ}$  K.

<u>Emission Spectrum</u>			<u>Excitation Spectrum</u>		
Excitation at 313 nm. Excitation bandwidth: 15.0 nm Emission bandwidth: 2.5 nm Scan speed: 0.3 nm/sec			Emission monitored at 357 nm Emission bandwidth 25.0 nm Excitation bandwidth 2.5 nm Scan speed 0.3 nm/sec		
$\lambda$ (nm)	$\bar{\nu}$ ( $\mu\text{m}^{-1}$ )	$R^{\text{em}}$	$\lambda$ (nm)	$\bar{\nu}$ ( $\mu\text{m}^{-1}$ )	$R^{\text{ex}}$
330	3.03	.065	250	4.00	.071
335	2.99	.429	270	3.70	.281
339.5	2.95	.700	280	3.57	.460
342	2.92	.608	290	3.45	.722
345	2.90	.484	295	3.39	.786
350	2.86	.669	303	3.30	1.000
357	2.80	1.000	307	3.26	.966
360	2.78	.861	309	3.24	.971
365	2.74	.741	313	3.19	.913
370	2.70	.853	317	3.15	.934
374	2.67	.896	325	3.08	.638
380	2.63	.778	333	3.00	.460
390	2.56	.617	340	2.94	.223
390	2.53	.569	345	2.90	.018
460	2.50	.518			
410	2.44	.376			
420	2.39	.227			
430	2.33	.137			

Table A. 3. 2. Anthracene:  $5 \times 10^{-6}$  M in nitrogen flushed cyclohexane at 300° K.

<u>Emission Spectrum</u>			<u>Excitation Spectrum</u>		
Excitation at 357.5 nm			Emission monitored at 400 nm		
Excitation bandwidth: 15.0 nm			Emission bandwidth: 25.0 nm		
Emission bandwidth: 2.5 nm			Excitation bandwidth: 2.5 nm		
Scan speed: 0.3 nm/sec			Scan speed: 0.3 nm/sec		
$\lambda$ (nm)	$\bar{\nu}$ ( $\mu\text{m}^{-1}$ )	$R^{\text{em}}$	$\lambda$ (nm)	$\bar{\nu}$ ( $\mu\text{m}^{-1}$ )	$R^{\text{ex}}$
370	2.70	.021	300	3.33	.056
375	2.67	.318	309	3.24	.170
379	2.64	.848	315	3.17	.157
381	2.62	.688	320	3.13	.242
383	2.61	.559	325	3.08	.363
390	2.56	.252	330	3.03	.279
395	2.53	.500	335	2.99	.402
400	2.50	1.000	340	2.94	.670
405	2.47	.670	343	2.92	.564
413	2.42	.283	347	2.88	.359
418	2.39	.395	353	2.83	.684
423	2.36	.560	356	2.81	.881
430	2.33	.361	357.5	2.80	1.000
440	2.27	.131	361	2.77	.625
449	2.23	.182	367	2.72	.242
460	2.17	.095	372	3.69	.469
			375	2.67	.702
			377	2.65	.943
			380	2.63	.484
			385	2.60	.089

Table A. 3. 3. Quinine bisulfate:  $5 \times 10^{-6}$  M in  $0.1 \text{ N H}_2\text{SO}_4$  at  $300^\circ \text{K}$ .

<u>Emission Spectrum</u>			<u>Excitation Spectrum</u>		
Excitation at 346 nm			Emission at 450 nm		
Excitation bandwidth: 15.0 nm			Emission bandwidth 10.0 nm		
Emission bandwidth: 2.5 nm			Excitation bandwidth 10.0 nm		
Scan speed: 0.3 nm/sec			Scan speed: 0.3 nm/sec		
$\lambda$ (nm)	$\bar{\nu}$ ( $\mu\text{m}^{-1}$ )	$R^{\text{em}}$	$\lambda$ (nm)	$\bar{\nu}$ ( $\mu\text{m}^{-1}$ )	$R^{\text{ex}}$
370	2.70	.005	230	4.35	2.01
380	2.63	.012	240	4.17	3.15
400	2.50	.125	250	4.00	5.00
420	2.38	.437	255	3.92	4.08
430	2.33	.642	260	3.85	.220
440	2.27	.817	270	3.70	.240
450	2.22	.934	275	3.64	.160
457	2.19	1.000	290	3.45	.350
460	2.17	.991	300	3.33	.550
470	2.13	.982	316	3.16	.820
480	2.08	.953	325	3.08	.790
500	2.00	.794	335	2.99	.870
520	1.92	.600	346	2.89	1.000
540	1.85	.419	360	2.78	.820
560	1.79	.324	365	2.74	.700
580	1.72	.228			
600	1.67	.164			
620	1.61	.078			
640	1.56	.023			

Table A. 3. 4. Thymine in 0. 01 N NaOH,  $10^{-4}$  M at  $300^{\circ}$  K.

<u>Emission Spectrum</u>			<u>Excitation Spectrum</u>		
Excitation at 292 nm			Emission at 380 nm		
Excitation bandwidth 15. 0 nm			Emission bandwidth 10. 0 nm.		
Emission bandwidth 10. 0 nm			Excitation bandwidth 15. 0 nm		
Scan speed: 0. 3 nm/sec			Scan speed: 0. 3 nm/sec		
$\lambda$ (nm)	$\bar{\nu}$ ( $\mu\text{m}^{-1}$ )	$R^{\text{em}}$	$\lambda$ (nm)	$\bar{\nu}$ ( $\mu\text{m}^{-1}$ )	$R^{\text{ex}}$
320	3. 13	. 096	240	4. 17	. 121
330	3. 03	. 300	250	4. 00	. 115
340	2. 94	. 497	260	3. 85	. 166
345	2. 90	. 570	265	3. 77	. 267
350	2. 86	. 621	270	3. 70	. 399
355	2. 82	. 660	275	3. 64	. 564
360	2. 78	. 699	277. 5	3. 61	. 659
365	2. 74	. 778	280	3. 57	. 732
370	2. 70	. 829	287. 5	3. 54	. 831
375	2. 67	. 859	285	3. 51	. 883
380	2. 62	. 899	287. 5	3. 48	. 928
385	2. 60	. 922	290	3. 45	. 972
390	2. 56	. 930	292. 5	3. 42	1. 000
395	2. 53	. 945	295	3. 39	. 995
400	2. 50	. 996	300	3. 33	. 853
410	2. 44	1. 000	305	3. 28	. 564
420	2. 38	. 933	310	3. 23	. 339
440	2. 27	. 820	320	3. 13	. 071
460	2. 17	. 687			
480	2. 08	. 545			
500	2. 00	. 473			
550	1. 82	. 260			